Interaction Notes

Note 177

March 1974

AN EVALUATION OF COMPUTER PROGRAMS USING INTEGRAL EQUATIONS FOR THE ELECTROMAGNETIC ANALYSIS OF THIN WIRE STRUCTURES*

by

E. K. Miller
R. M. Bevensee
A. J. Poggio
R. Adams
F. J. Deadrick
J. A. Landt

UNIVERSITY OF CALIFORNIA

Lawrence Livermore Laboratory
Livermore, California 94550

ABSTRACT

Various features of widely used computer programs for the electromagnetic analysis of thin wire structures using integral equations in the frequency domain are analyzed. A set of criteria are developed so that a given current distribution can be compared to a reference solution by use of a few simple scalars. Extensive computations are performed for the straight wire, L-wire, and crossed wire configurations with easy evaluation using the selected criteria. Using information regarding accuracy, efficiency, and simplicity, a recommendation is made regarding the "best" program available at this date.

*This work was performed under the auspices of the U.S. Atomic Energy Commission.

I. INTRODUCTION

The widespread usage of integral equation techniques in the evaluation of electromagnetic interactions has led to a variety of numerical techniques and as a result, a large number of different computer programs. As might be expected, some subtle differences in the reduction of a physical structure to a computer model using a given numerical technique for solving the integral equation could lead to significant differences in accuracy and efficiency. It is the purpose of this report to investigate various computer codes which are widely used and to evaluate their performance in solving for the bulk current and charge distributions on several thin wire structures. A recommendation will be made regarding which code (in its present stage of development) should be adopted for use in evaluating current and charge distributions on aircraft-like thin wire structures exposed to an EMP environment.

A preliminary discussion of program philosophy regarding mathematical modeling initiates the technical portion of this report. It is followed by a brief theoretical development of the pertinent integral equations finding widespread use in electromagnetic modeling for conducting wire structures. Also included is a discussion of the method of moments with particular regard paid to choices of weight and basis functions. Brief descriptions of presently operational computer programs follow, hopefully providing the reader sufficient information regarding the fundamental differences in the programs. The area of error analysis relevant to this project is discussed in order to establish those error criteria which find use in the determination of efficiency for the computer programs used in this effort. Finally, using the results of error analyses such as convergence rates, a recommendation will be made regarding that program, or combinations of program segments which can be used in analysis of the class of structures considered herein.

II. PRELIMINARY DISCUSSION

The major initial emphasis in this effort has been the collection of data pertaining to the use of various existing computer programs and algorithms which may be applicable to the general problem of analyzing aircraft-like geometries composed of thin wires in the sense of the thin wire approximation. This approximation necessarily limits the highest frequency for which valid and

reliable computations can be performed for surface current and charge density distributions on wire-like structures. In order to systematize our discussion of the various sources of error which may be encountered in the computer modeling process let us consider the steps involved in developing numerical results for the problem of interest. This will be done in order of increasing approximation (or decreasing model realism) beginning with the rigorous problem statement.

A. The Exact "Model"

An exact numerical model of an aircraft would, if it were possible to develop, include the precise geometrical details of the structure as well as the electrical properties of the air frame and would permit variations in the structure geometry which would normally occur during operation. This might include for example, gear up versus gear down, flaps in various configurations, etc. This of course is a formidable problem in the current state of development of computer modeling in electromagnetics. Rather than considering the object to be a closed perfectly conducting surface as is most often the case treated from a numerical viewpoint, it would be necessary to allow for the real-life effects of apertures, finite conductivity, imperfectly conducting contacts, etc. For obvious reasons, real-life problems are generally idealized to a certain extent as is duscussed in the following approximating steps.

B. The Smooth Closed Surface

It can be argued that for many practical considerations it is permissible to replace the complicated geometry of an actual aircraft by a smooth version which approximates in gross outline the real structure. It may be furthermore anticipated that it is permissible to consider such a model to be perfectly conducting for purposes of grossly evaluating the surface currents and charge density distributions. An approach somewhat similar to this has been taken for the analysis of a Chinook helicopter (Knepp, et al. 1970). The problem as stated, while neglecting local effects due to apertures, etc., and thus simplifying the original problem a considerable degree, is still extremely difficult in terms of its numerical complexity. Straightforward application of conventional integral equation techniques to this particular problem and extending to the upper frequency of the EMP pulse, 100 MHz or so, could require an indeterminate amount of success. It would furthermore be necessary in any event to consider the perturbing localized effects of apertures, imperfect

conductivity, etc. The impracticability of analyzing an aircraft such as a B1 from this viewpoint for the entire EMP spectrum is fairly obvious. For this reason an additional degree of approximation such as the one that follows, is mandatory.

C. Composite Simple Shapes

Putting aside the question of the wavelength-size ratio for the aircraft but considering for the moment only the complexity involved in defining the geometrical model, it is at once apparent that a great degree of simplification could be obtained were the aircraft modeled not as a smooth, accurate version of the real structure but instead represented by a series of simple geometrical shapes. The most obvious model might consist of constant diameter circular or perhaps elliptical, cylinders in the case of the wings, or tapered cylinders to form cones in the aircraft forward area. An approach basically like this has been used to apply the geometrical theory of diffraction to the analysis of aircraft radiation patterns with a considerable degree of success. The computational problem at this point is however still of impressive complexity since the number of the unknowns or the order of the matrix which results from the integral equation reduction will still increase as the surface area of the aircraft in square wavelengths. Thus while an appreciable degree of simplification will have been obtained from using this model from the geometrical viewpoint of structure description, the actual numerical solution may not have been reduced in magnitude to any appreciable degree. This naturally leads us to a further degree of approximation.

D. The Thin Wire Approximation

The least complex model of an aircraft structure is a "stick model" wherein the aircraft is replaced by interconnected circular cylinders. In this model, each cylinder is used to represent portions of the aircraft such as the fuselage, wings, vertical stabilizer, etc. Such a model necessarily loses a great deal of geometrical detail and as a result is most useful for assessing gross effects and not reliable for detailed studies. For instance, a stick model of the B-1 would be quite useful for determining the bulk current on the fuselage at a given cross-sectional plane but would not be useful for determining surface current density at the wing root. Nonetheless, the information available from stick model studies provides a starting point for more detailed analyses.

The thin wire approximation basically involves three assumptions: a) azimuthal currents may be neglected, b) azimuthal variations of the longitudinal current flow may be neglected, and c) the rigorous kernel may be replaced by the so-called thin

wire kernel to permit the surface integration to be reduced to a line integration along the axis of the wire. As a fourth assumption we might mention that the current flow at the end of the wire is usually taken to be zero regardless of the wire diameter. In order that the thin wire approximation be acceptably accurate it is necessary for two conditions to be met: first, and most obvious, is the fact that the wire diameter must be small relative to the shortest wavelength involved. Generally speaking the maximum wire diameter that can be considered within the context of the thin wire approximation is on the order of 0.2 wavelengths. A second condition concerns the length (L) - to-diameter (D) aspect ratio of the wire. Unless some special treatment is employed it is usually necessary that the L/D ratio of the cylindrical structure or wire exceed 10 or 20 for the problem to be suited to a thin wire treatment. This basically is due to the effect of the end cap on the thin wire fields. For wires with large L/D ratios, the end cap has a negligible effect on the overall solution. However, when L/D becomes small the fields produced by current and charge on the end cap may be of significant influence and therefore require attention if a valid numerical solution is to be obtained (Taylor and Crow, 1971).

It may be appreciated that the thin wire approximation incorporates a great deal of idealization in terms of the computer model which has replaced the actual problem of interest. However, the thin wire approximation has at the same time enjoyed a considerable degree of success in application to many practicable problems including not only those which are obviously suited to this approach (for example wire antennas and scatterers), but for the analysis of extended surface objects in frequency ranges where their maximum transverse dimension is small relative to the wavelength. Furthermore, the thin wire approximation has been employed to develop numerical models of surface structures whose dimensions are not suited to a direct thin wire model by the development of numerical wire meshes or grid models of such structures. The thin wire approximation thus has the potential for providing a numerical approach which is considerably broader in scope than would be at first expected from the assumptions inherent in its development.

The basic approach taken here for determining aircraft EMP surface current and charge density distributions is to work backwards in the direction of an increasingly rigorous computer model from the thin wire approximation discussed above. We see this as involving essentially the following steps: a) identification of the thin wire computational algorithm which may be used with confidence in the low frequency EMP regime; b) determining whether simple corrections, modifications, or extensions of the basic thin wire formulation will permit it to be extended

significantly in frequency coverage. These extensions might involve for example, the end cap correction already mentioned, surface integrations in place of the thin wire kernel, and the possibility of using thin wire model for the still higher frequencies by employing the wire mesh concept; and c) identification of likely approaches for the frequency range where the basic stick model thin wire approximation of the aircraft will no longer work. For other than wire meshes this might involve a surface approach based on either the electric or magnetic field integral equations. In the still higher frequency regime where surface integral equations may be inappropriate because of computational inefficiencies or inaccuracies, entirely different approaches such as those based on physical or geometrical optics may be necessary. As mentioned above, our attention to-date has been focused primarily on step 1, the thin wire model,and in particular the thin wire stick model by which we mean a thin wire computation without wire gridding.

A wide variety of computer programs and algorithms have been developed for the analysis of wire structures. These programs exhibit a diversity of formulations and numerical treatments which differ not only in the integral equation types but also in the current basis functions and boundary condition matching employed for the integral equation solution. A survey of current approaches and organizations responsible for their development follows in the next section.

III. THEORETICAL DEVELOPMENT

In order to facilitate ensuing discussions concerning integral equations for thin wire structures, it is advantageous to pursue an abbreviated derivation of the pertinent formulations. Questions concerning validity of each specific equation, the existence or uniqueness of solutions, and various features of the limiting process which reduces the integral representations to integral equations are necessarily glossed over. Rather, the integral representations will herein be derived and the reduction to integral equations will be performed without considering some of these delicate questions. The resulting integral equations which are among the most widely used, will be specialized to thin wire structures by introducing several approximations leading to the thin wire kernel.

A. Integral Representations

A popular starting point for the derivation of various integral equations for the currents on perfectly conducting bodies is the definition for the electric field in terms of potentials. This expression, valid for a solenoidal magnetic field, ($\nabla \cdot H = 0$) is given by (with exp ($i\omega t$) time convention, $i = \sqrt{-1}$)

$$\bar{E} = -i\omega\mu\bar{A} - \nabla\phi \tag{1}$$

where $\bar{A}$ is the magnetic vector potential and ϕ the scalar potential due to a volume current density $\bar{J}_v$. A gauge condition for these potentials of the form

$$\nabla\cdot\bar{A} = -i\omega\varepsilon\phi \tag{2}$$

allows $\bar{A}$ to be written as the solution of

$$\nabla^2\bar{A} + k^2\bar{A} = -\bar{J}_v \tag{3}$$

that is,

$$\bar{A}(\bar{r}) = \frac{1}{4\pi}\int_{V_s} d^3r'\ \bar{J}_v(\bar{r}')\ G(\bar{r},\bar{r}')\ , \tag{4}$$

$$G(r,r') = \frac{\exp(-ik|\bar{r}-\bar{r}'|)}{|\bar{r}-\bar{r}'|}$$

Using equation (2) and Maxwell's equation for the divergence of $\bar{E}$,

$$\nabla\cdot\bar{E} = \rho/\varepsilon \tag{5}$$

one arrives at the integral expression for the scalar potential

$$\phi = \frac{1}{4\pi\varepsilon}\int_{V_s} d^3r'\rho_v(\bar{r}')\ G(\bar{r},\bar{r}') \tag{6}$$

where the charge density $\rho(\bar{r})$ can be related to the current density through the continuity relation

$$\rho_v(\bar{r}) = -\frac{1}{j\omega} \nabla\cdot\bar{J}_v \tag{7}$$

From the above equations, one can obtain some of the widely used integral expressions for the electric field due to arbitrary electric source distributions contained within a region of space V_s. The first of these arises by using equations (1), (4), and (6), viz.,

$$\bar{E}(\bar{r}) = -\frac{j\omega\mu}{4\pi} \int_{V_s} d^3r'\ \bar{J}_v(\bar{r}')\ G(\bar{r},\bar{r}')$$

$$-\frac{1}{4\pi\varepsilon} \nabla \int_{V_s} d^3r'\ \rho_v(\bar{r}')\ G(\bar{r},\bar{r}') \tag{8}$$

Note that the continuity relation allows this representation to be written solely in terms of the current density $\bar{J}(\bar{r})$. A second form arises by using (1), (2), and (4), viz.,

$$\bar{E}(\bar{r}) = \frac{1}{4\pi j\omega\varepsilon}\ (\nabla\nabla\cdot + k^2) \int_{V_s} d^3r'\ \bar{J}_v(\bar{r}')\ G(\bar{r},\bar{r}') \tag{9}$$

For $\bar{r} \neq \bar{r}'$ ($\bar{r}\varepsilon V_s$), the order of integration and vector differentiation can be interchanged. The subsequent use of the vector relation

$$\nabla\nabla\cdot[\bar{J}_v(\bar{r}')\ G(\bar{r},\bar{r}')] = \nabla[\bar{J}_v(\bar{r}')\cdot\nabla\ G(\bar{r},\bar{r}')]$$

$$= (\bar{J}_v(\bar{r}')\cdot\nabla)\nabla\ G(\bar{r},\bar{r}')$$

leads to

$$\bar{E}(\bar{r}) = \frac{1}{4\pi i\omega\varepsilon} \int_{V_s} d^3r' \{(\bar{J}_v(\bar{r}')\cdot\nabla)\nabla G(\bar{r},\bar{r}') + k^2 \bar{J}_v(\bar{r}') G(\bar{r},\bar{r}')\} \tag{10}$$

or, in dyadic notation,

$$\bar{E}(\bar{r}) = \frac{1}{4\pi i\omega\varepsilon} \int_{V_s} d^3r' \bar{J}_v(\bar{r}')\cdot[\nabla\nabla + k^2 \bar{\bar{I}}] G(\bar{r},\bar{r}') \tag{11}$$

with $\bar{\bar{I}}$ the unit dyadic and the term $[\nabla\nabla + k^2\bar{\bar{I}}]G$ often referred to as a form of Green's dyadic.

For electric current sources constrained to a surface S which may be considered to be the boundary of V_s, the integral representations are simply modified in that volume densities are replaced by surface densities and the integrals are carried out over the surface S. The most widely used integral representations for the electric field due to electric sources over a surface S are therefore

$$\bar{E}(\bar{r}) = -\frac{i\omega\mu}{4\pi} \int_S d^2r' \bar{J}(\bar{r}')G(\bar{r},\bar{r}') + \frac{1}{4\pi i\omega\varepsilon} \nabla \int_S d^2r' \nabla'\cdot\bar{J}(\bar{r}') G(\bar{r},\bar{r}') \tag{12}$$

$$\bar{E}(\bar{r}) = \frac{1}{4\pi i\omega\varepsilon} \left(\nabla\nabla\cdot + k^2\right) \int_S d^2r' \; \bar{J}(\bar{r}') \; G(\bar{r},\bar{r}') \tag{13}$$

$$\bar{E}(\bar{r}) = \frac{1}{4\pi i\omega\varepsilon} \int_S d^2r' \; \bar{J}(\bar{r}') \cdot \left[\nabla\nabla + k^2\bar{\bar{I}}\right] G(\bar{r},\bar{r}') \tag{14}$$

B. Integral Equations

The general boundary value problem of determining the current distribution on a perfect electric conducting surface due to an impressed excitation can be approached using an integral equation. The boundary condition on the surface of the conducting body can be stated as

$$\hat{n}(\bar{r}) \times \bar{E}_t(\bar{r}) = 0 \quad ; \quad \bar{r} \in S \tag{15}$$

with the $\hat{n}(\bar{r})$ the outwardly pointing normal to S and $\bar{E}_t(\bar{r})$ the total electric field at the surface. Since the total electric field is the linear super-position of the impressed (incident) field $\bar{E}^{inc}(\bar{r})$ and the scattered field $\bar{E}_s(\bar{r})$, the boundary condition requires that

$$\hat{n}(\bar{r}) \times \bar{E}^{inc}(\bar{r}) = - \hat{n}(\bar{r}) \times \bar{E}_s(\bar{r}) \quad ; \quad \bar{r} \in S \quad . \tag{16}$$

The scattered field is due to distributions of electric current and charge over S and as such can be represented by equations (12) through (14). Note that the condition $\nabla\cdot\bar{H} = 0$ required for the validity of (12) through (14) is satisfied in the absence of magnetic currents or charges. The procedure of taking the observation point $\bar{r}$ to the surface S must be performed delicately and the integrals in (12) through (14) should be interpreted in a principal value sense. The integral or integrodifferential equations, as the case might be, are therefore

$$\hat{n} \times \bar{E}^{inc}(\bar{r}) = \hat{n} \times \{\frac{i\omega\mu}{4\pi} \int_S d^2r' \; \bar{J}(\bar{r}) \; G(\bar{r},\bar{r}') - \frac{1}{4\pi i\omega\varepsilon} \nabla \int_S d^2r' \; \nabla'\cdot\bar{J}(\bar{r}') \; G(\bar{r},\bar{r}')\} \tag{17}$$

$$\hat{n} \times \bar{E}^{inc}(\bar{r}) = -\hat{n} \times \{\frac{1}{4\pi i\omega\varepsilon} (\nabla\nabla\cdot + k^2) \int_S d^2r' \; \bar{J}(\bar{r}') \; G(\bar{r},\bar{r}')\} \tag{18}$$

$$\hat{n} \times \bar{E}^{inc}(\bar{r}) = -\hat{n} \times \frac{1}{4\pi i\omega\varepsilon} \int_S d^2r' \; \bar{J}(\bar{r}')\cdot\{\nabla\nabla + k^2\bar{\bar{I}}\} \; G(\bar{r},\bar{r}') \tag{19}$$

with $\bar{r} \in S$ and a suitable interpretation having been taken of the limiting procedure as $\bar{r}$ approaches S.

C. Thin Wire Integral Equations

For conducting bodies composed of thin wires, i.e., structures comprised of interconnected conducting cylinders whose radii a_i are small in terms of wavelength ($a_i/\lambda < 1$), several approximations regarding the behavior of current and charge densities can be made. It can be assumed that

1. Azimuthal or circumferential currents produce negligible effects when determining the net axial current on the wires.

2. The induced electric sources on the surface can be located on the axis of the wires thus giving rise to a filamentary source representation.

3. The boundary condition on the electric field can be enforced on the surface of the conductor.

Note that it is equally valid to allow the current to flow on the tube representing the conductor surface and to enforce the boundary condition on the axis (Taylor and Wilton, 1972)

Using $\hat{s}(\bar{r})$ to denote a unit vector tangent to the conductor and parallel to its axis at the observation point $\bar{r}$ and $\hat{s}'(\bar{r})$ to denote the axially aligned unit vector at the source point, the boundary condition and current density become

$$\hat{s}(\bar{r}) \cdot \bar{E}_t(\bar{r}) = 0 \quad ; \quad r \in S \tag{20}$$

$$\bar{J}(\bar{r}') = \hat{s}' \frac{I(\bar{r}')}{2\pi a} \tag{21}$$

Because of the assumption of the locations of the source and observation points, the distance variable $|\bar{r}-\bar{r}'|$ in $G(\bar{r},\bar{r}')$ is approximated by a distance R which can never be zero since it is the distance from a point on the axis of the wire to a point on the surface and as such is never less than the radius a. For example, the distance R for a z aligned straight wire is $R = \sqrt{(z-z')^2 + a^2}$.

With s and s' denoting the axial coordinates at the observation and source points and $C(\bar{r})$ denoting the range of integration over the wires, equations (17) through (19) become

$$\hat{s} \cdot \bar{E}^{inc}(s) = \frac{i\omega\mu}{4\pi} \int_{C(\bar{r})} ds' \, \hat{s} \cdot \hat{s}' \, I(s') \frac{e^{-ikR}}{R} - \frac{1}{4\pi i\omega\varepsilon} \frac{\partial}{\partial s} \int_{C(\bar{r})} ds' \frac{\partial I(s')}{\partial s'} \frac{e^{-ikR}}{R} \tag{22}$$

$$\hat{s}\cdot\bar{E}^{inc}(s) = -\frac{1}{4\pi i\omega\varepsilon}\left(\frac{\partial}{\partial s}\nabla\cdot+k^2\hat{s}\cdot\right)\int_{C(\bar{r})} ds'\hat{s}'I(s')\frac{e^{-ikR}}{R} \tag{23}$$

$$\hat{s}\cdot E^{inc}(s) = -\frac{1}{4\pi i\omega\varepsilon}\int_{C(\bar{r})} ds'\ I(s')\{-\frac{\partial}{\partial s}\frac{\partial}{\partial s'} + k^2\hat{s}\cdot\hat{s}'\}\frac{e^{-ikR}}{R} \tag{24}$$

with $R = |\bar{r}(s) - \bar{r}(s')|$ and $s \in C(\bar{r})$ in all cases.

The integral equations which have been developed differ only in their specific forms and can be transformed one into the other with relative ease. In particular, since the approximate forms in (22) through (24) have bounded integrands, they can be shown to be identical by simple mathematical manipulation such as interchanges of differentiation and integration. This is not to say however that the ease with which each one is solved is similar. In fact, equation (23) is generally cast into a somewhat different form by first solving the differential equation. The result, referred to as the magnetic vector potential integral equation, can be written for thin wire conductors of arbitrary configuration as (Mei, 1965)

$$\int_{C(\bar{r})} ds'\ I(s')\ \{G(s,s')\ \hat{s}\cdot\hat{s} + \frac{1}{2}\int_{C(\bar{r})} d\xi\theta(\xi-s)\ [\frac{\partial G(\xi,s')}{\partial\xi}\ (\xi\cdot s') + \frac{\partial G(\xi,s')}{\partial\xi}$$

$$+ G(\xi,s')\ \frac{\partial(\hat{\xi}\cdot\hat{s}')}{\partial\xi}]\ e^{-ik|s-\xi|}\} = Ae^{-iks} + Be^{iks} + \frac{1}{2i\eta_0}\int_{C(\bar{r})} ds'\ s'\cdot\bar{E}^{inc}(s')$$

$$e^{-ik|s-s'|} \tag{25}$$

where $\theta(\xi-s) = 1$ for $\xi \geq s$ and zero elsewhere.

Hallen's integral equation for straight wires follows from (25) with the introduction of $s=s'$, i.e.,

$$\int_{C(\bar{r})} ds'\, I(s')\, G(s,s') = Ae^{-iks} + Be^{iks} + \frac{1}{2Z_o} \int_{C(\bar{r})} ds'\, \hat{s}\cdot\bar{E}^{inc}(s')\, e^{-ik|s-s'|} \tag{26}$$

$$s \in C(\bar{r})$$

In the following discussions, equation (22) will be referred to as the Potential integrodifferential equation, equation (24) will be referred to as Pocklington's integral equation, while equation (25) will be referred to as the magnetic vector potential integral equation.

D. Numerical Solution Methods

The basic method used in attempts to solve the aforementioned integral equations is the "method of moments". Only a brief discussion of this method is presented at this point since it is assumed that the reader already has a degree of familiarity. For those who do not, Prof. Harrington's book "Field Computation by Moment Methods", Macmillan Company, New York (1968), serves as an excellent introduction.

Denoting any linear operator equation as

$$Lf = g \tag{27}$$

with L a linear operator (e.g., integral, differential, integro-differential), f an unknown response, and g a known forcing or excitation function. The method of moments, in effect, projects the space of g onto another space and enforces the equality between the projections. Concisely then, taking the inner product of (27) with a suitable set of independent weight functions $\{w_m\}$ which define the projection space, one obtains an equation for the equality of projections,

$$\langle w_m, Lf\rangle = \langle w_m, g\rangle \qquad m = 1(1)M\ . \tag{28}$$

It may be necessary for an arbitrary f to expand that function in a set of basis functions $\{f_n\}$, i.e.,

$$f = \sum_{1}^{N} \alpha_n f_n \tag{29}$$

so that (28) becomes

$$\sum_{n=1}^{N} \alpha_n \langle w_m, Lf_n \rangle = \langle w_m, g \rangle \quad m = 1(1)M \quad . \tag{30}$$

Equation (30) can be written in matrix notation as

$$[W][A] = [G] \tag{31}$$

where $W_{mn} = \langle w_m, Lf_n \rangle$

$A_n = \alpha_n$

$G_m = \langle w_m, g \rangle$

so that the solution is simply

$$[A] = [W]^{-1}[G] \tag{32}$$

The numerical solution methods reported upon here will all be based upon a formulation leading to a matrix equation of the form of (31). The differences will be the specific nature of L, and the choices of $\{f_n\}$ and $\{w_m\}$.

The weight functions which are most widely used fall into one of two classes. The first class leads to a collocation solution by choosing

$$w_m = \delta(\bar{x} - \bar{x}_m) \qquad m = 1(1)M \tag{33}$$

that is, the weight function leads to a sampling of the operator equation at a discrete set of points $\{\bar{x}_m\}$. The other class of weight functions lead to a Galerkin type formulation, i.e., with

$$w_m = f_m \quad m = 1(1)M \tag{34}$$

one converts (30) into

$$\sum_{n=1}^{N} \alpha_n \langle f_m, Lf_n \rangle = \langle f_m, g \rangle \qquad m = 1(1)M \tag{35}$$

In the following discussions, each of these classes will appear in the numerical solution techniques.

The basis functions used in the description of the unknown are quite important in determining the ultimate efficiency of a numerical technique. For the purposes of this report, attention will be focused only on the subsectional basis function expansions, i.e., the use of specific functions f_m over subintervals of the domain of the operator L. Complete domain representations are excluded since they may be impractical for complicated structures (Miller and Deadrick, 1973). For instance, if the operation range of L is divided into m portions Δ_i, i = 1(1)M, then one can consider f to be approximated over each Δ_i by one element of the set $\{f_m\}$, namely f_i or by some finite combination over Δ_i. More detailed explanations concerning the moment method and its ramifications are found in Harrington (1968), Mittra (1973), and Fenlon (1969).

A modified version of Fenlon's (1969) tabulation of typical pairs of functions is given in Table 1.

Method	n^{th} term of $\overline{A}$	Weight Function
1. Galerkin	$a_n \overline{f}_n(\overline{r})$	$\overline{f}_m(\overline{r})$
2. General Collocation	$a_n \overline{f}_n(\overline{r})$	$\delta(\overline{r}-\overline{r}_m)$
3. Delta Point Matching	$a_n\, \delta(\overline{r}-\overline{r}_n)$	$\delta(\overline{r}-\overline{r}_m)$
4. Subsectional Collocation	$U(\overline{r}_n) \sum_{p=1}^{P} a_{np} \overline{f}_p(\overline{r})$	$\delta(\overline{r}-\overline{r}_m)$

Table I.
Representative Pairs of Functions in the Method of Moments

IV. SURVEY OF APPLICABLE COMPUTER PROGRAMS

In this section, the basic numerical modeling schemes used in various computer programs will be briefly discussed. The program will be classified as to which equation is used in the formulation and comments relating to specific features will be included. Each computer program will be identified as to its originator.

The computer program list below is by no means exhaustive. It contains programs generated at organizations where there is continuing developmental work in the extension and applicability of the programs. The list of the users of computer methods in the analysis of electromagnetic interactions with wire structures would be very large and quite redundant since successful algorithms find wide usage. The culling of the list of a nucleus leads to most useful overview. Organizations where work is currently known to be in progress on such computer programs (with the names of specific individuals who have aided in this effort) include

1) AFWL, (M. Harrison)
2) Arens Electromagnetics, Inc. (V. Arens)
3) Boeing Aircraft Corporation (W. Curtis)
4) Dikewood Corporation (F. Tesche)
5) MB Associates (G. J. Burke)
6) Mission Research Corporation
7) Mississippi State University (C. D. Taylor)
8) North American Rockwell Corporation (J. Yang)
9) Ohio State University ElectroScience Laboratory (J. Richmond)
10) Sandia Corporation
11) Syracuse University (R. Harrington, B. Strait)
12) TRW, Inc. (W. Imbriale)
13) Technology for Communications International (TCI)
14) University of California, Berkeley (K. K. Mei)
15) University of Mississippi (C. Butler)

These organizations have been contacted with regard to their present state of development, numerical results for certain problems for use in comparisons, and the possibility of obtaining a copy of their program for use at LLL in detailed comparisons.

A. The Potential Integrodifferential Equation

The potential integrodifferential equation has been used in computer programs developed at Syracuse University (Chao and Strait, 1970). This formulation is also being used at present by Boeing (1973). Both codes model curved wires by a continuous collection of straight wire sections, i.e., a piecewise linear approximation to arcs of a curve.

1) Galerkin's Method, Triangle Bases, Triangle Weights (Syracuse U.)

The basis functions in the most widely used program from Syracuse University are triangular with overlapping portions thereby giving rise to a piecewise linear approximation of the current distribution (Chao and Strait, 1970). Galerkin's

method is used in the solution procedure with the weight functions ($\bar{w}_m$) axially directed triangles.

Upon applying the method of moments procedure outlined above, there is found

$$\int_{C(r)} ds\ \hat{s}\cdot\bar{E}^{inc}(s)\ w_m(s) = -\frac{1}{4\pi i\omega\varepsilon}\int_{C(r)} ds \int_{C(r)} ds'\ [k^2\hat{s}\cdot\hat{s}'\ I(s')w_m(s) - \frac{\partial w_m(s)}{\partial s}\frac{\partial I(s')}{\partial s'}]\frac{e^{-ikR}}{R} \tag{36}$$

The triangular expansion function is shown in Figure 1a where the first subscript on the P refers to the wire number and the second to the segment number. For purposes of integration, the triangle is approximated by the pulse functions shown with Q's referring to the centers of these pulses. The required derivative of the current is evaluated at the centers of each of the four pulses representing the triangle thereby avoiding points of indeterminancy of the derivative. The testing (weight) function for the Galerkin procedure is also a triangular function.

An intersection of M wires is handled by overlapping M-1 half-triangles of the M connected wires with one of the other wires. A three wire junction and its model is shown in Figure 2. The overlapping portions are one-half triangle width in length and actually occupy the same region of space. Details of this method are discussed in Logan (1973) and in Appendix A.

2) Collocation, Pulse Bases, Delta Weights (Boeing)

The basis function for the current in the Boeing computer program are pulses, i.e.,

$$I = \sum_{n=1}^{N} I_n \bar{f}_n \tag{37}$$

where $\bar{f}_n$ is an axially directed pulse function of unit amplitude on the nth segment and zero elsewhere. The derivative of current as required by equation (22) is determined by a finite difference scheme applied to the pulses giving rise to the expression

$$\nabla\cdot\bar{I} = \sum_{n=1}^{N} I_n g_n \tag{38}$$

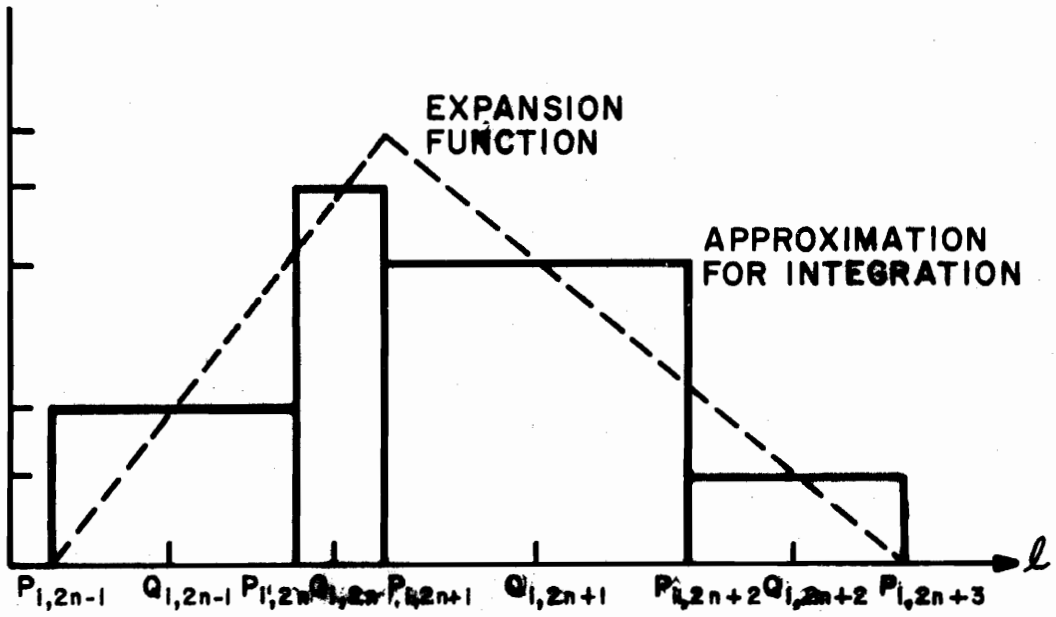

FIGURE 1.

EXPANSION FUNCTIONS (SYRACUSE UNIVERSITY)

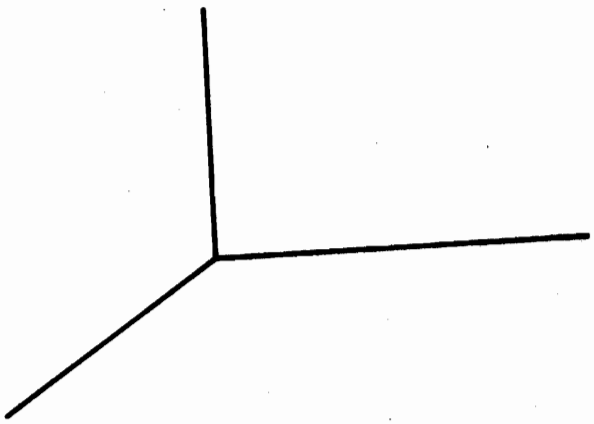

ACTUAL CONFIGURATION

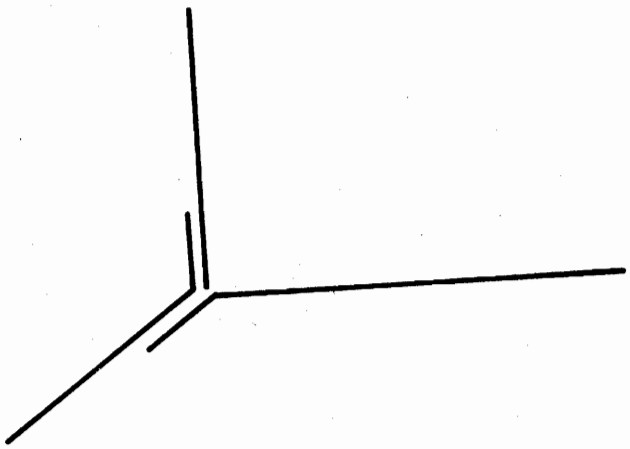

MODEL

FIGURE 2

Junction Treatment (Syracuse University)

An example is shown in Figure 3. The required derivative of the scalar potential is performed numerically by a finite difference approximation. This method for approximating the integral equation is basically that reported on in Harrington (1968).

Junctions in the Boeing program are treated using a charge redistribution technique. For example, if M wires of differing radii intersect at a point, one determines $\nabla \cdot I$ by first noting that the continuity relation, when integrated over the region whose outer limits are defined by the sample points along each arm nearest the intersection, yields

$$i\omega q_{total} = \sum_{i=1}^{M} I_i \tag{39}$$

with the I_i inwardly directed.

Furthermore, the average surface charge density in the vicinity of the intersection is given by

$$\langle \rho_s \rangle = \frac{1}{i\omega} \frac{\sum_{i=1}^{M} I_i}{2\pi \sum_{i=1}^{M} a_i \Delta \ell_i / 2} \tag{40}$$

where $\Delta \ell_i$ and a_i are the length of the i^{th} intersecting segment and its radius, respectively. The derivative of the current on the jth wire is then

$$\nabla \cdot \bar{I}|_j = -a_j \frac{\sum_{i=1}^{M} I_i}{\frac{1}{2} \sum_{i=1}^{M} a_i \Delta \ell_i} \tag{41}$$

with the derivative taken toward the junction. For a further discussion of inherent errors in this method, see Appendix A.

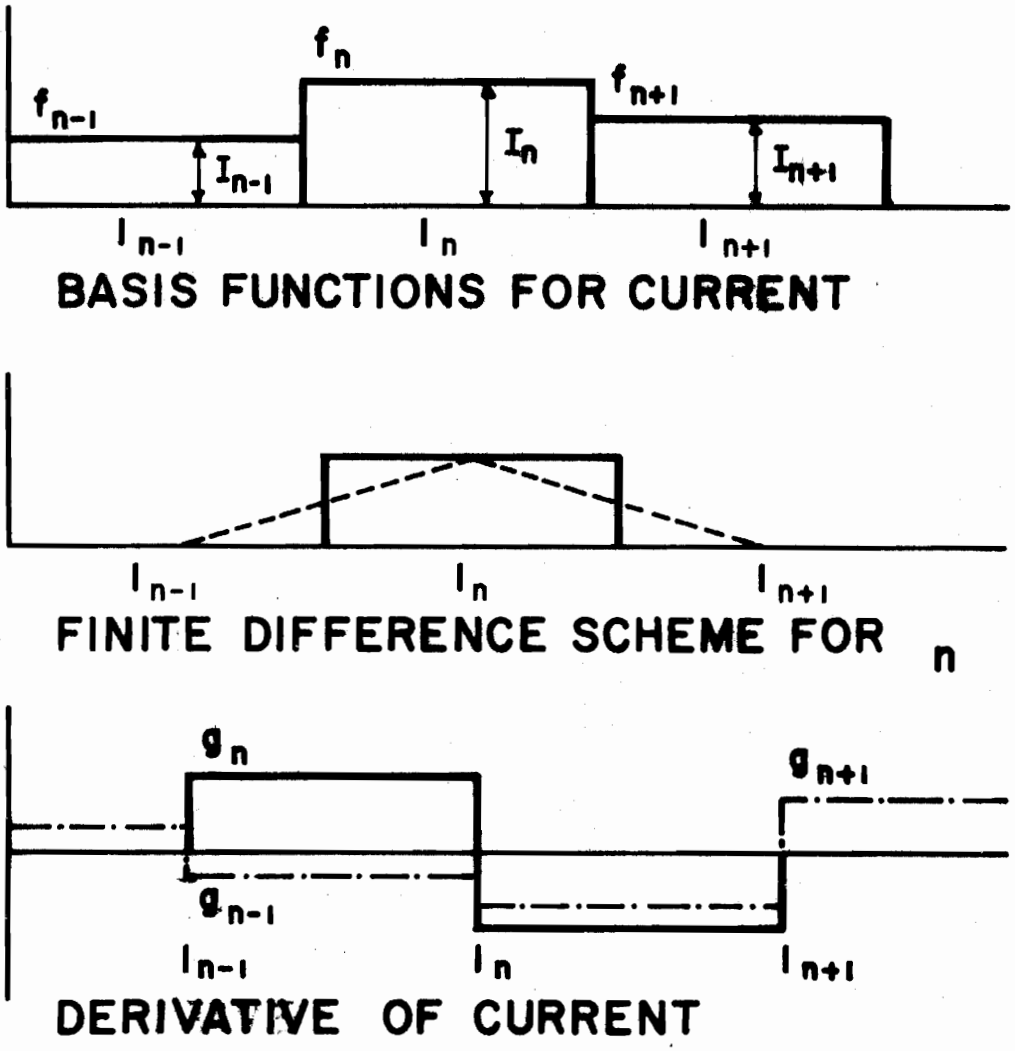

FIGURE 3

BASIS FUNCTIONS (BOEING)

B. Pocklington's Integral Equation

Computer programs using Pocklington's integral equation for the current distributions on wire structures have been developed by, among others, MB Associates, TCI, and Ohio State University. All programs approximate a curved wire by a collection of straight wire sections.

1) Collocation, Sinusoidal Interpolation Basis, Delta Weights, (MB Associates, TCI, and Arens Applied Electromagnetics (AE))

The above programs each make use of sinusoidal interpolation basis functions, i.e.,

$$I(s) = A_i + B_i \cos k(s-s_i) + C_i \sin k(s-s_i)$$

over the interval $s_i - \frac{\Delta}{2} < s \leq s_i + \frac{\Delta}{2}$. The constants A_i, B_i, and C_i are determined by matching the currents at the center of the ith segment as well as at the (i-1)th and (i+1)th in the MBA program and by matching current at the center of the segment as well as current and slope at the ends in the TCI and AE programs. In each of these programs an N segment structure gives rise to set of N unknown constants from which the current distribution can be constructed. The weight functions used in each program are a set of Dirac delta functions thereby leading to an enforcement of the integral equation at a specific set of points on the structure. The number of sample points and number of segments are chosen equal. The functional form of the equation is

$$\hat{s}\cdot\bar{E}^{inc}(s)\big|_{s=s_m} = -\frac{1}{4\pi i\omega\varepsilon}\int_L ds'\, I(s')\left(\frac{\partial}{\partial s}\frac{\partial}{\partial s'} + k^2\hat{s}\cdot\hat{s}'\right)\frac{e^{-ikR}}{R}\Big|_{s=s_m} \qquad (42)$$

$$m = 1(1)N$$

The integrations required to fill the matrix [Z] in the matrix representation can be very time consuming. However for a segment aligned along the z axis in a cylindrical coordinate system, the radial component of electric field can be evaluated analytically for the constant, sine and cosine variations while the z component of electric field can be evaluated analytically for the sine and cosine variation. Hence only one of the six integrals need by evaluated numerically - a distinct advantage in minimizing computer time.

The integration which cannot be performed analytically in the MBA program is done by using an adaptive scheme, namely, Romberg Variable Interval Width Integration (Miller, 1970). In the TCI and AE programs, this same integration is performed by either using a series expansion containing a zeroeth order Hankel function, trigonometric terms and sine and cosine integrals (when the radial distance from the source segment is much less than the total distance) or by Simpson's rule integration (when the radial distance is not much less than the total distance).

Multiple-wire junctions are treated in the MBA program by extrapolating the current on a segment at the junction to the average value of the currents at the centers of the other segments at the junction. This is repeated for each segment and in an approximate sense represents the satisfaction of Kirchoff's condition at the junction. (See Appendix A).

In the TCI program, the multiple wire junction is treated by assuming the wires at the junction are small-angle cones and that a spherical wave representation which includes only the TEM mode and the 1st order spherical TM wave is sufficient (Andreasen, 1968). This representation is used in determining the junction current for each wire thereby allowing the sinusoidal interpolation scheme to be used near the junction while not interpolating across it (See App. A) This technique is presently being used in the AE program.

2) Galerkin's Method, Piecewise Sinusoidal Bases, Piecewise Sinusoidal Weights (Ohio State University (OSU))

The OSU program for thin wire structures is based on the reaction matching concept due to Richmond (1969) which he has, for piecewise sinusoidal basis and weight functions, referred to as the sinusoidal reaction technique. This technique can be shown to be equivalent to Galerkin's method (Thiele, 1970). The functional of interest is

$$\langle \bar{p} \cdot \bar{E}^{inc} \rangle = - \langle I \cdot \bar{E} \rangle$$

where $\langle\ \rangle$ is the line integral over the axis, $\bar{p}$ is the test element, $\bar{E}^{inc}$ the exciting field, I the current on the wire, and $\bar{E}$ the field due to the test element $\bar{p}$. The actual form of the equation solved is

$$\langle \bar{w}_m \cdot \bar{E}^{inc} \rangle = - \frac{1}{4\pi i\omega\varepsilon} \langle I(s')\hat{s}' \cdot \int_L ds\ \bar{w}_m \cdot \bar{\bar{I}} G \rangle \qquad (43)$$

where we have set $\bar{p} = \bar{w}_m$, i.e., the set of test functions is equal to the set of weight functions. In the OSU program the weight functions and the basis functions for the expansion of the current are both overlapping sinusoids and give rise to a piecewise sinusoidal representation of the current. It should be noted that a simple interchange of order of integration in the right hand side of the above equation yields the Galerkin's form of the moment of Pocklington's integral equation.

By virtue of the use of sinusoidal testing functions, the integral

$$\bar{g} = \int_L ds\ \bar{w}_m(s) \cdot \bar{\bar{\Gamma}} G \tag{44}$$

can be performed analytically. In the OSU program the integral

$$\langle I(s')\hat{s}' \cdot g(s') \rangle \tag{45}$$

is evaluated by numerical integration when appropriate, or from closed-form expressions in terms of exponential integrands (Richmond, 1973).

Junctions of M intersecting wires are handled by overlapping M - 1 V dipoles supporting the sinusoidal basis functions in the immediate vicinity of the junction. The technique is implicitly identical to that used in the SYR program. (See Appendix A).

C. Hallen's Integral Equation

Moment method solutions to Hallen's integral equation have been applied to straight wire antennas and arrays of these elements (Mei, 1965), to straight wire structures with simple junctions (crossed dipoles) (Taylor and Crow, 1971), and to the conical spiral antenna (Yeh and Mei, 1967). This particular integral equation has not been used extensively for arbitrary structures due to the complexity of the integrand (see equation (25)). At present, it does not appear that computer programs using this equation are available for the electromagnetic analysis of arbitrary wire configurations.

The University of California program developed by K. K. Mei and students uses collocation with sinusoidal interpolation. The program has been applied to straight wires, arrays, loops, and the conical spiral. There is no known junction treatment capability.

The University of Mississippi and Mississippi State University have computer programs based on Hallen's Integral equation. The programs are based on collocation and are still in a developmental stage. A technique involving the maintenance of scalar potential continuity

allows multiple-wire junctions to be treated (Crow and Shumpert, 1972, Logan, 1973).

V. OVERVIEW

Table II is a tabulation of the known operational, wire configuration computer programs which are in use. Also included in the list is the Lawrence Livermore Laboratory (LLL) program which is a modified version of the MBA program that includes several options to the user. The Hallen formulation programs are indicated for information only since they are not as yet generalized for arbitrary configuration.

VI. ERROR ANALYSIS

Two questions of paramount importance face the user of a computer modeling program in connection with the accuracy of the results which it produces: 1) to what degree is the computed result numerically convergent relative to an "exact" numerical reference; and 2) how closely in agreement are the numerical reference and the actual physical result of interest.

The implications of these two questions are obvious. In any numerical application of the computer model, we must know that not only has our calculation employed enough samples to meet some acceptable error criterion in the numerical sense but that the computed result is also meaningful in a physical sense. The latter does not necessarily follow from the former.

An "exact" numerical solution, if possible to obtain, would mean only that an approximate numerical representation for the problem of interest has been obtained in the limit of vanishing numerical error. But the approximations inherent in the formulation which precedes the development of a numerical algorithm limit the ultimate correlation which can be expected between the actual physical results and the exact numerical solution. We can characterize the latter as being due to a physical modeling error (E_P) in contrast with the numerical modeling error (E_N) of the calculation itself. Note that a necessary, but not sufficient, condition for minimizing E_P is the minimization of E_N. We consider each of these errors in more detail below.

A. The Numerical Modeling Error E_N

There are a variety of ways to quantitatively define E_N for a given problem depending upon the particular physical observable of greatest interest. Almost invariably, whatever the specific method of definition, the standard of comparison against which the result in question is to be measured will be a solution obtained using the maximum feasible number of sample points or unknowns (M) in the calculation. Let us denote this reference answer by A_M with A_N similarly denoting the answer obtained using N unknowns, where $M > N$.

For a scalar measures of the solution accuracy such as provided by the backscatter field amplitude, or the input admittance of an antenna, a simple error definition is then

Table II

Computer Programs/Thin Wire Structures

Organization	Integral Equation Type	Moment Method Soltn Scheme	Weight Functions	Basis Functions	Junction Treatment	Present Restrictions on Complexity
Syracuse Univ.	Potential	Galerkin	Overlapping triangles	Overlapping triangles (piecewise linear)	Overlapping bases, weights	
Ohio State U.	Pocklington	Galerkin (reaction)	Overlapping sinusoids	Overlapping sinusoids (piecewise sinusoidal)	Overlapping bases, weights	
MB Associates	Pocklington	Collocation	deltas	Sinusoidal Inter. (current match)	Extrapolation	
Boeing	Potential	Collocation	deltas	Pulse	Charge Redistribution	
TCI, Arens	Pocklington	Collocation	deltas	Sinusoidal Inter. (current, slope match)	Spherical wave expansion	
U of CA, Berk. (Mei)	Hallen's	Collocation	deltas	Sinusoidal Inter	None	
Univ. of Miss. } Miss. State	Hallen's	Collocation	deltas	Pulses	Scalar Potential Continuity	Simple Structures
LLL	Pocklington	Collocation	deltas	Sinusoidal Inter. a) current match b) current slope match Piecewise sinusoidal pulse	Extrapolation	
North American	Pocklington	Collocation	deltas	Pulses	N.A.	
TRW	Pocklington	Galerkin	Overlapping sinusoids	Overlapping sinusoids	Non-overlapping sines	

$$\varepsilon_s \equiv \left| \frac{A_M - A_N}{A_M} \right| \quad . \tag{46}$$

This particular method for assessing solution accuracy has been employed for radar cross-section computations (Miller, Burke, and Selden, 1971). For antenna applications, the more usual approach has been simply to plot A_N versus N to graphically demonstrate the rate of numerical convergence (Pearson and Butler, 1973; Strait, Sakar and Kuo, 1973; Thiele, 1973). In either case, the problem of error calculation is relatively straight-forward because of the scalar solution measure.

When on the other hand, a vector or scalar function is to be employed for the accuracy check, for example, the current or charge distributions on the structure, the boundary conditions on the total field, or the entire bistatic far-field, then the above definition must be generalized.

Since power flow and energy density, relevant physical quantities, are products of two observables, a mean-square error definition appears both physically and mathematically meaningful. We thus define a general vector error of the form

$$\varepsilon_V \equiv \left\{ \frac{\mathrm{Re} \int (\bar{A}_M - \bar{A}_N) \Delta (\bar{B}_M - \bar{B}_N)^* \nabla ds}{\mathrm{Re} \int \bar{A}_M \Delta \bar{B}_M^* \nabla ds} \right\}^{1/2} \tag{47}^*$$

where Δ and ∇ designate appropriate vector (or scalar) operations and ds is a surface or line integral. If A and B are the electric and magnetic fields, respectively, then Δ and ∇ are vector cross and dot products. Some particular, useful forms ε_V might take are

1. The far-field Poynting vector for the error field

$$\varepsilon_{VF1} = \left\{ \mathrm{Re} \int_{4\pi} \frac{(\bar{E}_M - \bar{E}_N) \times (\bar{H}_M - \bar{H}_N)^* \cdot \hat{r} \, d\Omega}{\mathrm{Re} \int_{4\pi} \bar{E}_M \times \bar{H}_M^* \cdot \hat{r} \, d\Omega} \right\}^{1/2} \tag{48}$$

*Note that a correlation function approach might also be used, i.e.,

$$\int \bar{A}_M \bar{A}_N^* (s - \lambda) ds$$

2. The far-field Poynting vector error

$$\varepsilon_{VF2} = \left\{ \frac{\mathrm{Re} \int_{4\pi} (E_M \times H_M^* - E_N \times H_N^*) \cdot \hat{r} \, d\Omega}{\mathrm{Re} \int_{4\pi} (E_M \times H_M^*) \cdot \hat{r} \, d\Omega} \right\}^{1/2} \tag{49}$$

3. Current distribution

$$\varepsilon_{VI} = \left\{ \frac{\int_L (\bar{I}_M - \bar{I}_N) \cdot (\bar{I}_M - \bar{I}_N)^* \, d\ell}{\int_L \bar{I}_M \cdot I_M^* \, d\ell} \right\}^{1/2} \tag{50}$$

4. Surface tangential electric field

$$\varepsilon_{VE} = \left\{ \frac{\int_L [(\bar{E}^{inc} + \bar{E}_N) \cdot \hat{\ell} (\bar{E}^{inc} + \bar{E}_N)^* \cdot \hat{\ell}] \, d\ell}{\int_L (\bar{E}^{inc} \cdot \hat{\ell})(\bar{E}^{inc} \cdot \hat{\ell})^* \, d\ell} \right\}^{1/2} \tag{51}$$

where $\hat{\ell}$ is a unit tangent vector and we use $\bar{E}^{inc}$ rather than $\bar{E}_M$ since the exciting field is known exactly.

5. Normal Poynting vector at surface

$$\varepsilon_{VS} = \left\{ \frac{\mathrm{Re} \int (\bar{E}^{inc} + \bar{E}_N) \cdot (\overline{I_N}^*) \, d\ell}{\mathrm{Re} \int \bar{E}^{inc} \cdot \bar{I}_M^* \, d\ell} \right\}^{1/2} \tag{52}$$

Of the various ε_V given above, version 4 (ε_{VE}) is perhaps the most convincing because it directly demonstrates how well the boundary conditions on the tangential field are satisfied. It suffers however from the severe disadvantage that many near field calculations would be required for its evaluation. This can make its routine application very expensive in terms of computer time, although it should be noted that no numerical reference as such is required. The same disadvantage holds for version 5(ε_{VS}).

In terms of a near field check on the solution convergence, there remains then only version 3, that for the current distribution. This form is fairly straightforward to evaluate, and does provide a quantitive estimate for the solution accuracy of a near field observable (the current). For EMP applications, this should be more meaningful than would a test of the far-field convergence as given by version 1, since it is generally accepted that the far-field solution is more accurate than the current from which it is obtained. It would be interesting to test this by comparing ε_{VF} and ε_{VI} as a function of N. It should be noted that an error criterion based on charge would also be very useful. In this report, attention will however be concentrated on currents.

If ε_{VI} is then to be selected as the error measure, rather than ε_{VE}, some consideration regarding its interpretaion is needed since ε_{VI} itself cannot directly demonstrate the solution accuracy insofar as matching the boundary conditions are concerned. Any implication concerning the latter must necessarily be inferred. Observe however, that the field values which appear in ε_{VE} are of course computed from integrals of the currents. It is reasonable to expect that, as the current solution converges, integrals of the current will also converge, though not necessarily to the same number of places. It is this expectation upon which our use of ε_{VI} as an indicator of the overall solution accuracy is based. Evaluation of ε_{VE} for comparison with ε_{VI} as a function of N for a test case or two would be useful.

Let us turn now to the numerical calculation of ε_{VI}. As written in (50), this would require a piecewise integration of current products (in the numerator) whose bases are referred to different sets of reference points (segment centers) along the structure. For convenience, and with little loss of generality, we rewrite (50) as

$$\varepsilon_{VI} = \left\{ \frac{\sum_{i=1}^{M} (I_M(\ell_i) - I_{Ni})(I_M(\ell_i) - I_{Ni})^*}{\sum_{i=1}^{N} I_M(\ell_i)\, I_M^*(\ell_i)} \right\}^{1/2} \tag{53}$$

where $I_M(\ell_i)$ denotes the value of $\bar{I}_M$ at the center of segment i (of coordinate ℓ_i) and I_{Ni} is by definition the corresponding sample value of $\bar{I}_N$ on segment i. Note that in general $I_M(\ell_i)$ will require interpolation between two sampled values of $\bar{I}_M$.

Besides defining the numerical convergence error as above, it is also useful to define some measure of the solution which will serve in comparing answers obtained from two different methods. Following the ideas already discussed, it appears natural to use for this purpose

$$\tilde{I}_N \equiv \frac{1}{L} \int_L \bar{I}_N \cdot \bar{I}_N^* d\ell \tag{54}$$

Upon approximating the integral by a segment oriented sum we obtain

$$\tilde{I}_N = \left(\frac{1}{N} \sum_{i=1}^{N} I_{Ni} I_{Ni}^* \right)^{1/2} \tag{55}$$

Values of $\tilde{I}_N$ as a function of N obtained from different programs should be adequate to show the relative agreement which exists between the various numerical and formulational procedures. We could of course also compare these different methods more directly as in equation (53), but that doesn't appear to offer any real advantage over using $\tilde{I}_N$.

B. The Physical Modeling Error, E_P

Little purpose is served by any computation no matter how numerically convergent, and thus accurate appearing, it might be if the computer model does not truly represent the physical problem of interest. We must ultimately be concerned with validating computer results through their degree of correlation with experimental measurement. While alternative analytic and numerical methods may prove useful to a limited extent for checking a given calculation, we can not have the confidence we would like in the numerical approach until measured results actually demonstrate its validity. Of source, the measurement itself is subject to an experimental uncertainty (measurement error E_M), so its use as a standard of comparison is not without its own difficulty.

This brings up a number of interesting questions, of which two are: 1) how can we rectify discrepancies between experiment and calculation when they are significant; and 2) in view of question (1) what numerical solution accuracy should we seek in the calculation? A reasonable answer to (2) would appear to be that as a general rule the computer model should be such as to make $E_N \ll E_P$, for then at least any experimental-numerical difference which occurs will not be due to

a removable calculation error. Thus, while check calculation errors as small as the 10^{-4} value shown in the next section may at first look numerically excessive, such values are important to establish the trend of E_N well below the actual E_N value which might normally be sought.

In order to answer question (1), we must first observe that no better agreement could be expected between measured and computed data than $\sqrt{E_N^2 + E_P^2} \sim E_P$ with no experimental error whatsoever. But any measurement, no matter how carefully performed, will of course result in $E_M > 0$. A discrepancy $\sim \sqrt{E_P^2 + E_M^2}$ must then be anticipated. Since a possible purpose of an experiment is to validate the computation, and to thus estimate E_P, clearly information concerning E_M is pre-requisite to accomplishing this.

Experiments designed to determine the overall value of E_M and its separate sources must thus be considered. It may be possible to do this by taking into account the individual contributions of the various error sources. Somewhat more convincing would be measurements of the observable in question (e.g., surface current) for test cases where E_P can, in principle at least, be made zero. One example would be the plane wave response of a perfectly conducting sphere, whose solution is known as exactly as any real EM problem.

The sphere is routinely used to calibrate radar scattering samples. Both pulse and/or CW measurements of the surface currents over the parameter range of interest could be used to experimentally evaluate E_M.

Provided that E_M can be reduced to acceptably small values, the experimental arrangement can then be used to measure the actual geometries of concern. Suppose that the observable in question has the measured and calculated distributions (in frequency, time, space, etc.) denoted by $\bar{F}_M$ and $\bar{F}_C$, respectively. Let us propose that their discrepancy D be defined in the same way as used for E_N above, by,

$$D(\ell) \equiv \left\{ \frac{\int_R [\bar{F}_M(s) - \bar{F}_C(s - \ell)] \cdot [\bar{F}_M(s) - F_C(s - \ell)]^* ds}{\int_R \bar{F}_M \cdot \bar{F}_M^* \, ds} \right\}^{1/2} \tag{56}$$

with R the range of the variable s. The variable ℓ permits the measured and computed data to be shifted in s for the best match to be obtained, and thus takes into account the frequency, angle and time shifts which often occur between experiment and theory.

Many other forms might also be considered for quantitatively comparing $\bar{F}_M$ and $\bar{F}_C$. Rather than the integral form above, we might employ a differential form

$$\left\{ \frac{\mathrm{Re}\,[\bar{F}_M(s) - \bar{F}_C(s - \ell)]\cdot[\bar{F}_M(s) - \bar{F}_C(s - \ell)]^*}{\frac{1}{R}\int_R \bar{F}_M\cdot\bar{F}_M^*\,ds} \right\}^{1/2} \quad (57)$$

which weights the local difference by the measured mean squared value. If the same approach is used to quantitatively estimate E_M for the rigorous (e.g., sphere) calibration case, then $D_{min} - E_M$ will provide a measure of Ep.

The above discussion is by no means complete in terms of assessing the quality of computed and/or measured data. We have provided an expression to be used below for testing both the numerical error of a calculation and comparing answers obtained from different methods. An expression for comparing computed and measured data has also been given, but no calculations have been performed with it. However the latter is accomplished, it is vitally important to have an adequate quantitative understanding of measurement errors if such a comparison is to ultimately prove meaningful.

VII. NUMERICAL RESULTS

Numerical results will be presented in this section in order that the various techniques described earlier can be compared. This comparison will lead to an objective judgment regarding the "best" program for use in assessing the vulnerability of aircraft structures to EMP.

A. Test Program

1) Test Philosophy

Among the techniques for which computer programs have either been written by LLL or obtained from the originator and are presently operational are:

a. Collocation, sinusoidal interpolation, Pocklington (BRACT)
b. Galerkin, piecewise linear, Potential (SYR)
c. Galerkin, piecewise sinusoidal, Pocklington (OSU)
d. Collocation, pulses, Potential (Boeing) ++
e. Collocation, piecewise sinusoidal, Hallen (AFWL)

†Note this form might be used to compare two different numerical results as well.
++This program is an LLL reconstitution of the program in use at Boeing.

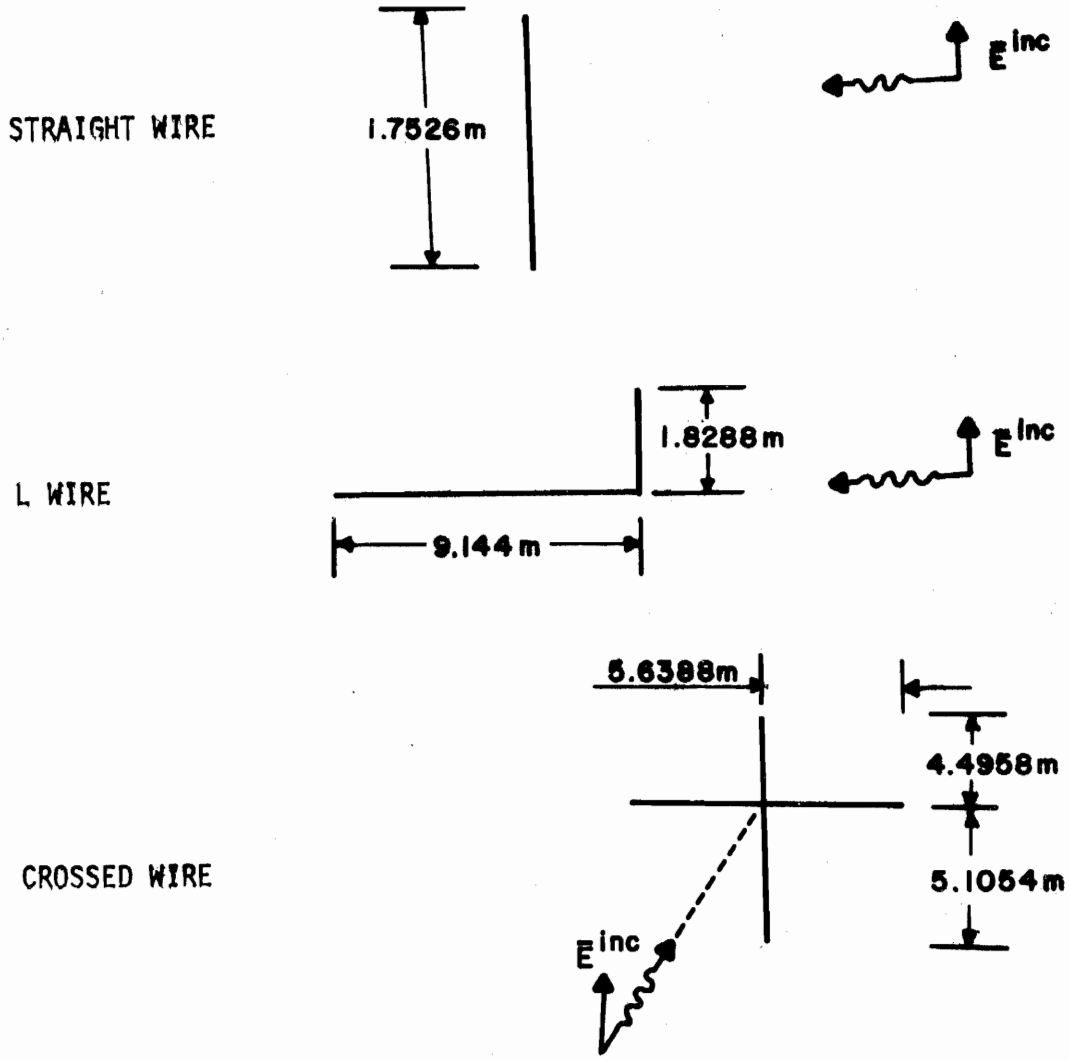

FIGURE 4. WIRE CONFIGURATION

In addition, LLL has generated modifications of BRACT to allow the testing of various schemes for program improvement. These include:

f. Collocation, sinusoidal interpolation with edge matching, Pocklington (MK3C).
g. Collocation, piecewise sinusoid, Pocklington.
h. Collocation, sine and constant, Pocklington.
i. Collocation, pulses, Pocklington.

In order to perform the evaluation of the different computer codes, three test structures were chosen for which the computer programs were to evaluate the current distribution for time harmonic excitation. These structures, composed of straight wire portions and shown in Figure 4, are capable of testing various features and codes. The straight wire, the simplest structure for EM interaction problems, tests the fundamental capabilities of the computer programs. A failure to adequately perform the calculations required for a simple straight wire can only lead to a dismissal of a given program since this function is fundamental to computations for more complicated structures. The next structure in level of difficulty is the L-wire. This structure tests the computer program's ability to model interactions between orthogonal wires and its ability to represent current distributions of possibly different character on the distinct portions of the structure. Finally, a test is performed to evaluate each program's ability to represent the interaction involved when the structure includes an intersection of more than two wires. A crossed wire structure is used for this purpose. The test structures have been chosen with the increasing level of difficulty described above in order to allow the isolation and identification of shortcomings and strong points of each program. It is possible and perhaps likely that a combination of portions of the tested programs will be assembled in order to yield a "best" code.

2) Test Outline

The test structures of Figure 4 have fixed dimensions given in terms of meters. The excitation frequency is constant at 10 MHz with the direction of incidence and polarization shown. Different tests are conducted by keeping the wire diameter and excitation constant and applying multipliers (X) to wire lengths. For example, for the straight wire of radius 1.905×10^{-4}m at broadside incidence, parallel polarization and 10 MHz, computer generated solutions would be obtained for L - 1.7526m (1X), 3.5052m (2X), 8.763m (5X), 15.6972m (10X), etc., with the dimension multiplier in parenthesis. For each case, i.e., a given class of structure (straight, L, or crossed) and multiplier, each computer program is used to generate solutions for the induced current distribution with the number of current samples a variable. These distributions are stored for later processing to obtain the scalar parameters used in establishing convergence criteria.

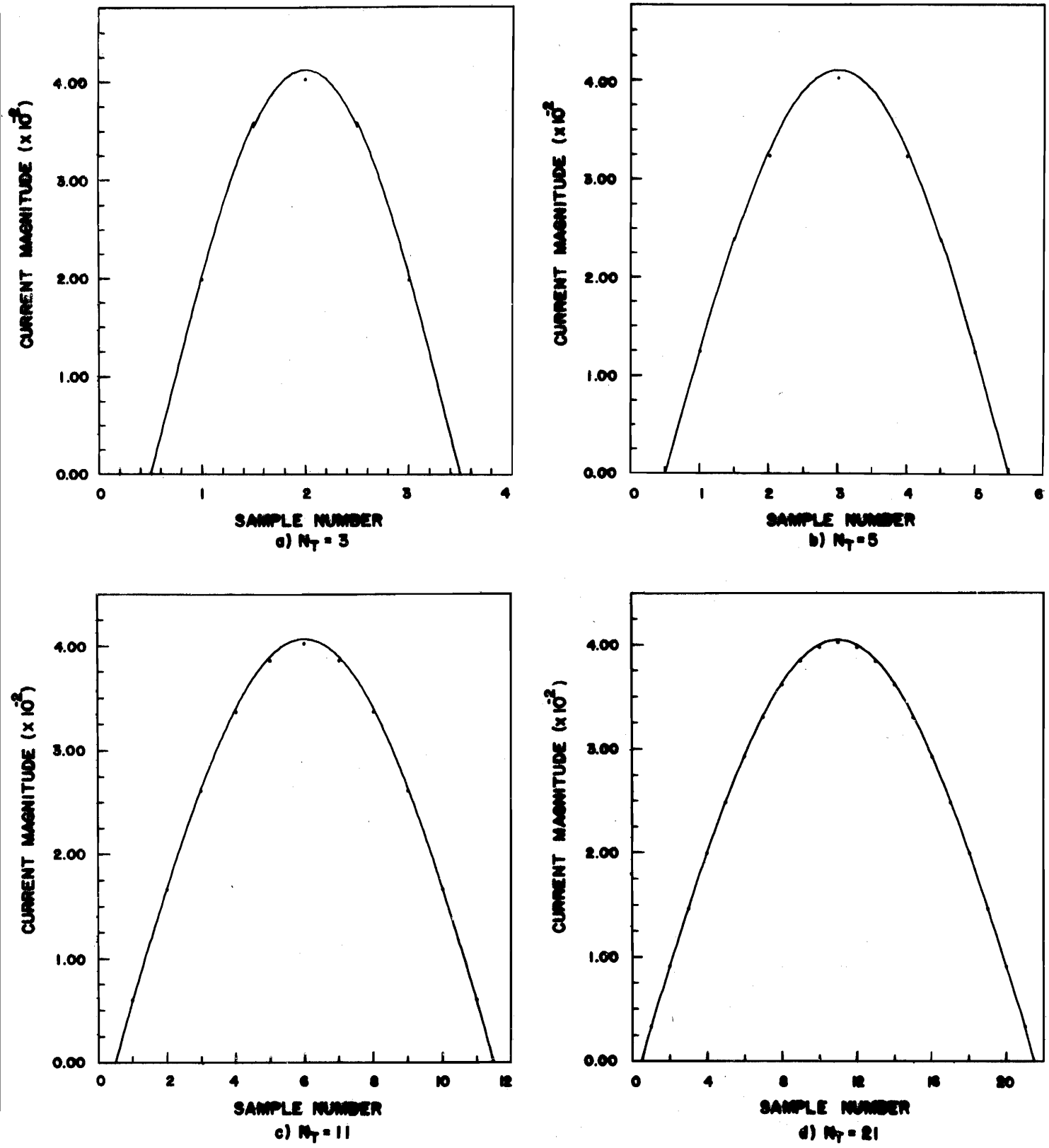

Figure 5: Current Magnitude vs. Sample Number for a Straight Wire with a 10X Multiplier. The Number of Segments or Unknowns is a Parameter.

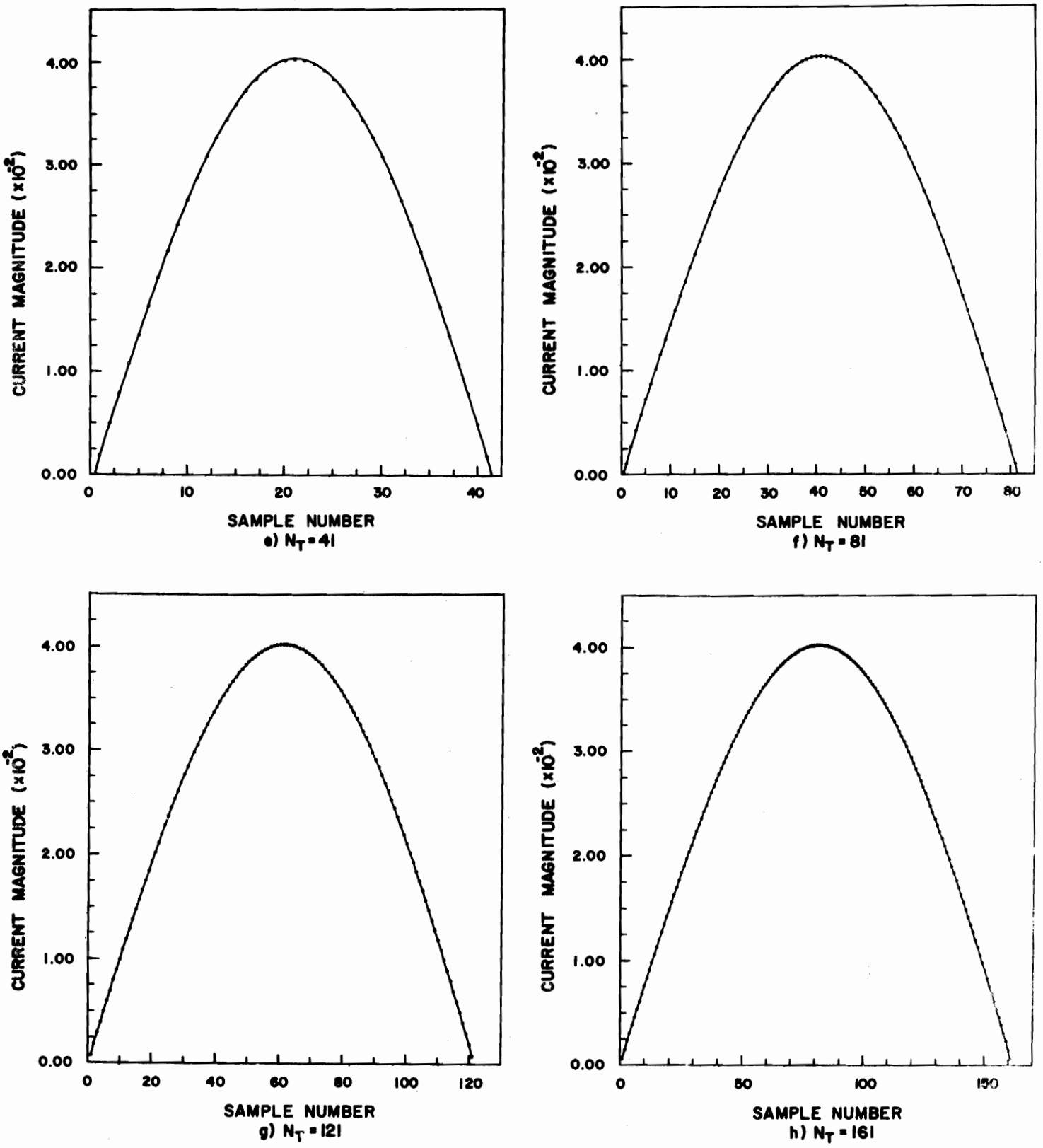

Figure 5: (continued) Current Magnitude vs. Sample Number for a Straight Wire with a 10X Multiplier. The Number of Segments or Unknowns is a Parameter.

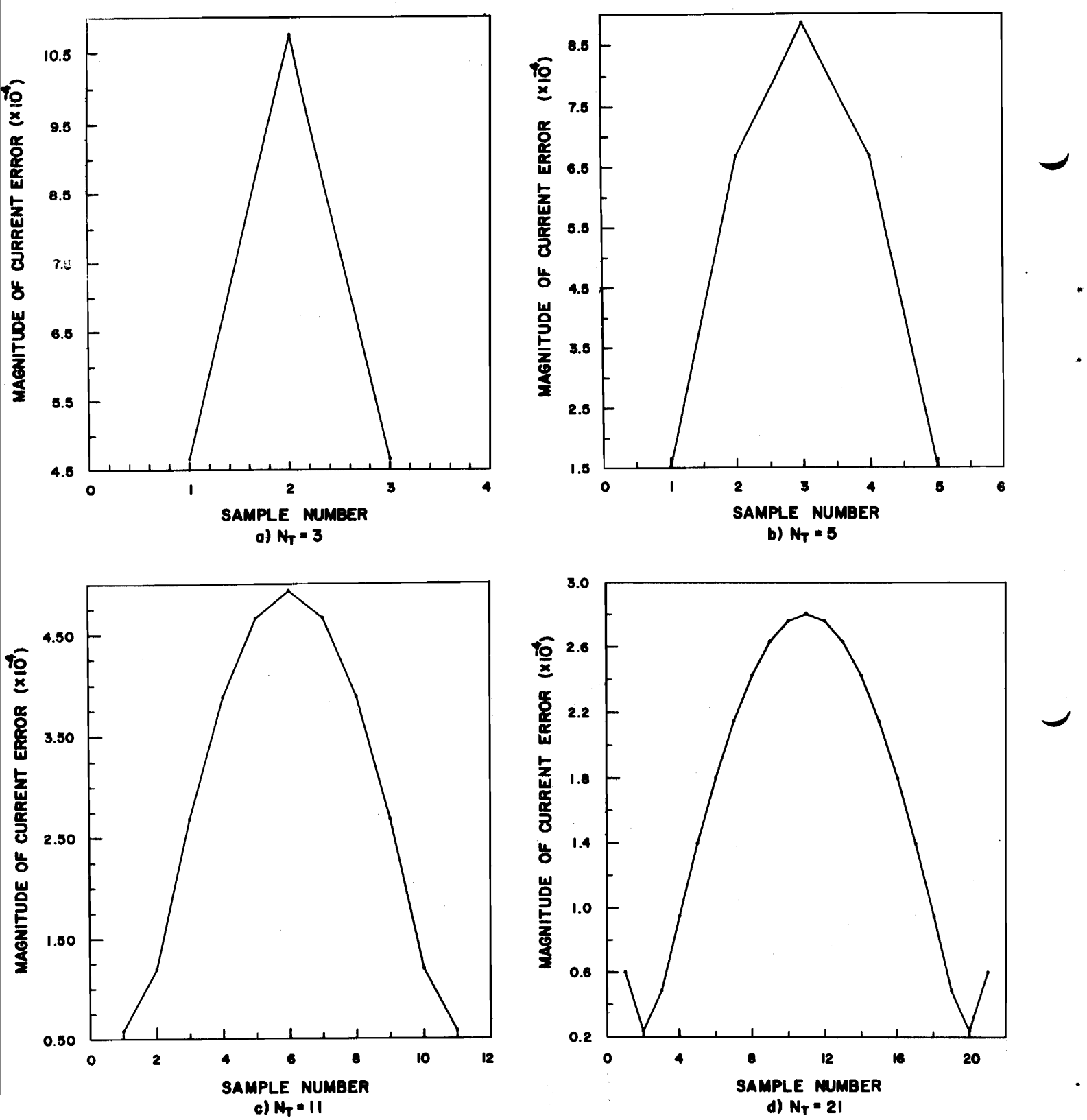

Figure 6: Magnitude of Current Error vs. Sample Number for a Straight Wire with a 10X Multiplier. The Number of Segments or Unknowns is a Parameter.

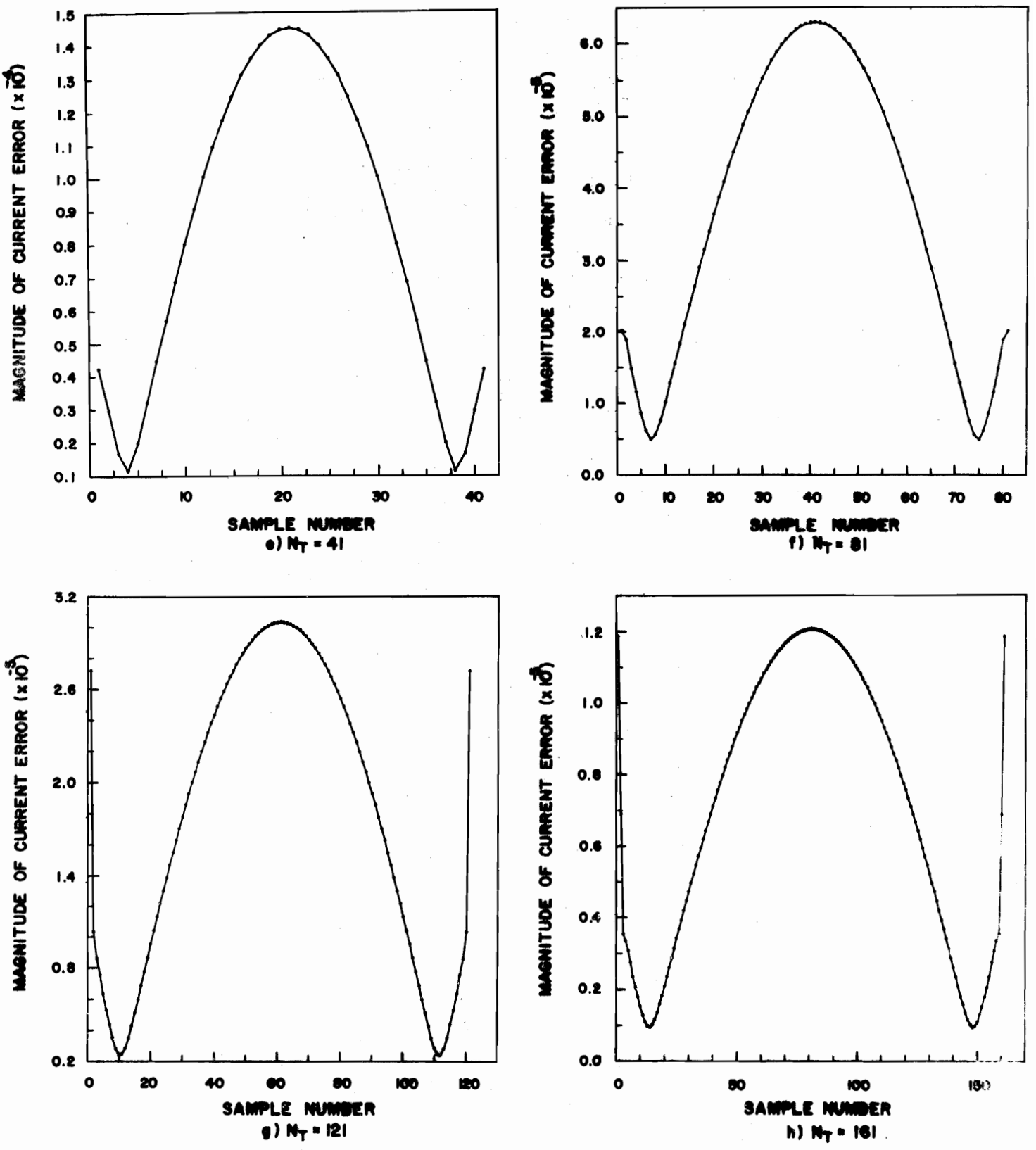

Figure 6: (continued) Magnitude of Current Error vs. Sample Number for a Straight Wire with a 10X Multiplier. The Number of Segments or Unknowns is a Parameter.

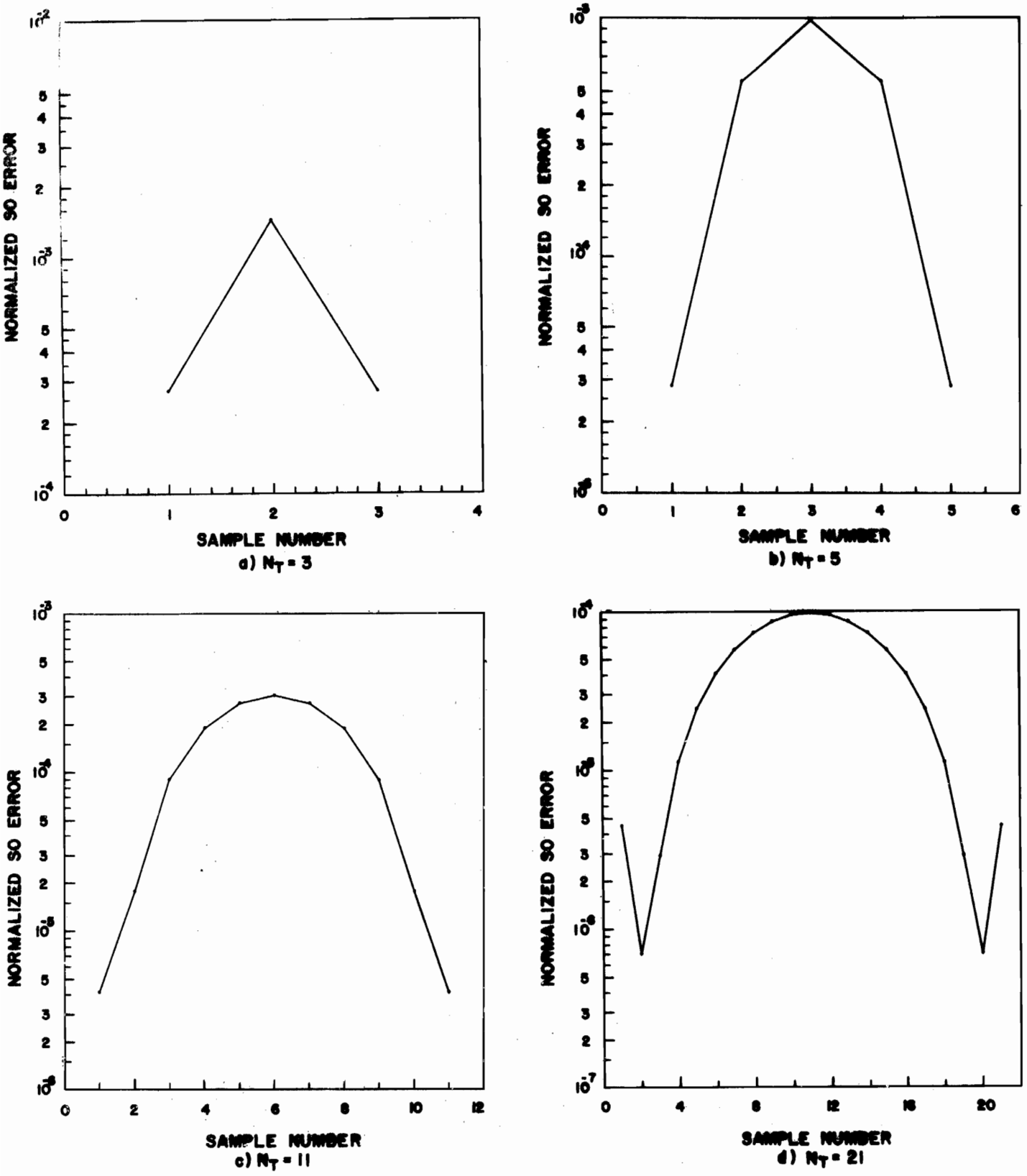

Figure 7: Normalized Square Error vs. Sample Number for a Straight Wire with a 10X Multiplier. The Number of Segments or Unknowns is a Parameter.

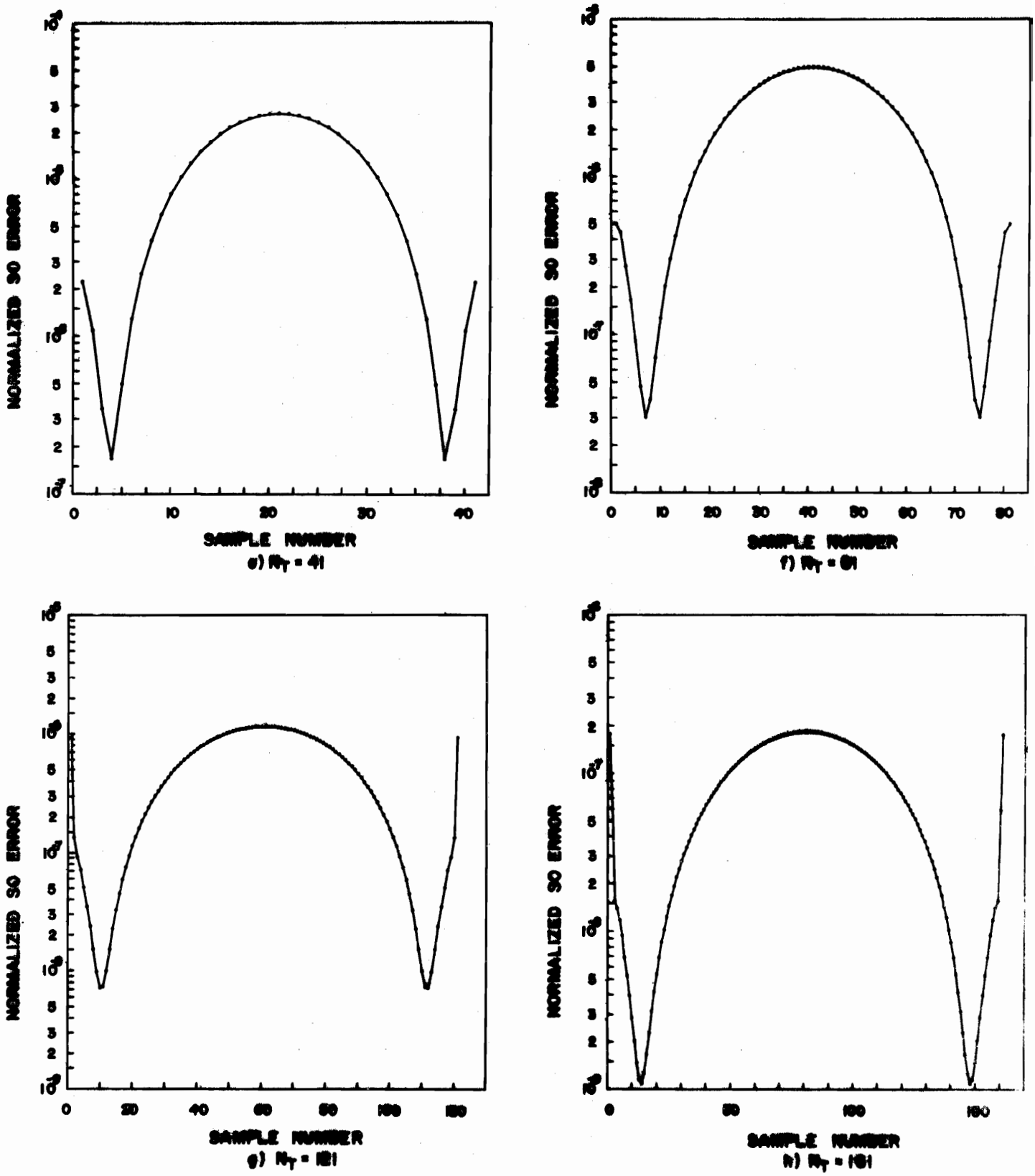

Figure 7: (continued) Normalized Square Error vs. Sample Number for a Straight Wire with a 10X Multiplier. The Number of Segments or Unknowns is a Parameter.

B. Available Evaluation Data

During a typical test run source data, i.e., the data that is the direct numerical result of the computation (the current distribution), is generated. One finds that the amount of source data generated is overwhelming and even when presented in a visual format makes program evaluation difficult. The following two subsections detail the difficulties involved and will describe the use of summary data.

1) Typical Source Data

As an example of the source data available, a set of current magnitude curves for a single structure (straight wire at 10X) generated by BRACT are presented in Figures 5 through 12. The curves for a given number of test segments N_T are generated by using the computed values of $|I|$ at each sample point and subsequently interpolating between these points using the sinusoidal interpolation scheme. Since the interpolation scheme is segment oriented (valid over only a given segment) and since the scheme as used in BRACT does not enforce current continuity between different segments, discontinuities at segment to segment junctions are possible as seen clearly in Figure 5. The X's on the curves represent the current magnitudes as obtained using 201 segments but with the current magnitude evaluated at the sample points pertaining to a given N_T. Hence, regardless of N_R, the number of X's on a curve will always equal N_T and their locations will always coincide with the sample points for that value of N_T. The solution obtained with $N_R = 201$ is referred to as the reference solution.

It should be kept in mind that the curves in Figure 5 represent only one structure, one multiplier, and one program. The proliferation of data can be easily appreciated. In addition to this source data, other data regarding difference between the computed current distribution for a given number of test segments (N_T) and the reference distribution are generated. For example, the magnitude of current error with I_R the reference current distribution and I_T the test current distribution on a sample point-by-sample point basis, i.e.,

$$\varepsilon_i = |I_{Ri} - I_{Ti}| \qquad i = 1(1)N_T \tag{58}$$

for the same case as above, is shown in Figure 6. For this error measure as well as for all those following, the value of the reference solution current is interpolated using a piecewise linear approximation (except BRACT) to provide a value at each test point. The error involved in using a piecewise linear approximation in the reference solution when a reference sample point does not coincide with a test sample point is very small due to the extreme denseness of sampling points in the reference solution.

Figure 7 is representative of the normalized square error on a point-by-point basis, and is the ratio of the magnitude of current error to the root mean square reference current, i.e.,

$$\varepsilon_s = \frac{|I_{Ri} - I_{Ti}|}{\left\{\frac{1}{N_R}\sum_{j=1}^{N_R} |I_{Rj}|^2\right\}^{1/2}} \qquad i = 1(1)N_T \tag{59}$$

Without doubt, the reader can appreciate that the evaluation of this volume of data can, when multiplied by the required number of cases and programs, be a monumental task. Rather than proceed in this manner, an auxiliary set of summary data is generated.

The method for generating the plotted data for BRACT has already been described. For OSU, the current magnitudes for the test case are the current values at segment centers and are evaluated by using the computed current values at junctions and applying the piecewise sinusoidal interpolation scheme of that program. These values are consistent with the program interpolation scheme. The test case curves are then generated by connecting the points with straight lines. Again, this latter operation has no bearing on subsequent error analyses since only values directly obtained in the program are used. In the SYR program source data the curves shown exhibit the actual behavior of the current magnitude as generated by connecting the points with straight lines. Again, this latter operation has no bearing on subsequent error analyses since only values directly obtained in the program are used. In the SYR program source data the curves shown exhibit the actual behavior of the current magnitude as generated and used internally by the computer program since the interpolation scheme in that program is piecewise linear. For the data due to programs using pulses, the test case data is plotted using the pulses interpolation scheme.

2) Typical Summary Data

In order to alleviate the data proliferation, summary data is generated for each structure. These data take the form of

RMS Current: $$I_{RMS} = \left(\frac{1}{N_T}\sum_{i=1}^{N_T} |I_{Ti}|^2\right)^{1/2} \tag{60}$$

RMS Current Error: $$\varepsilon_{RMS} = \left(\frac{1}{N_T}\sum_{i=1}^{N_T} |I_{Ri} - I_{Ti}|^2\right)^{1/2} \tag{61}$$

Normalized RMS Error:

$$(\varepsilon_s)_{RMS} = \left(\frac{N_R}{N_T} \frac{\sum_{i=1}^{N_T} |I_{Ri} - I_{Ti}|^2}{\sum_{i=1}^{N_R} |I_{Ri}|^2} \right)^{1/2} \qquad (62)$$

Examples of summary curves for the data exhibited in the previous section are included in Figures 8 through 10.

From the RMS current plot one can assess the rapidity with which a solution technique leads to a stable solution. One would desire each curve to approach a constant as quickly as possible thereby indicating that the solution has stabilized. A comparison of several programs using the RMS current as a criterion would allow a judgment to be made as to the efficiency of the programs with respect to the number of segments needed to achieve stability in the solution. It must be kept in mind that the different programs being tested will not necessarily be converging to the same RMS current value although the differences are expected to be quite small. The "correct" value, to which all should converge if they were exact, is not a known quantity for the cases considered here and absolute judgment concerning error cannot be made.

The RMS of current error plot in Figure 9 conveys information regarding the difference between the reference and test solutions. It is not used as widely as the normalized RMS current error since it does not use a normalization. However, normalized RMS error can be confidently used to evaluate programs insofar as normalized errors are concerned and provides as well information regarding rate of convergence to the reference value. Since both the RMS error and normalized RMS error must approach zero as N_T approaches N_R, the curves in Figures 9 and 10 have inflection points within the range plotted. The information relating to rate of convergence and error level especially for values of N_T less than the inflection point is nonetheless useful and important. In fact, the RMS current and normalized RMS current error are the two most important curves used in this evaluation. This is not to say that the other data generated are not used. For example, should it be noted that a particular program exhibits a low rate of convergence or a high normalized error for a given structure, the source data can be studied to provide reasons for this poor performance. This procedure will arise in the forthcoming evaluation and its usefulness will then be appreciated.

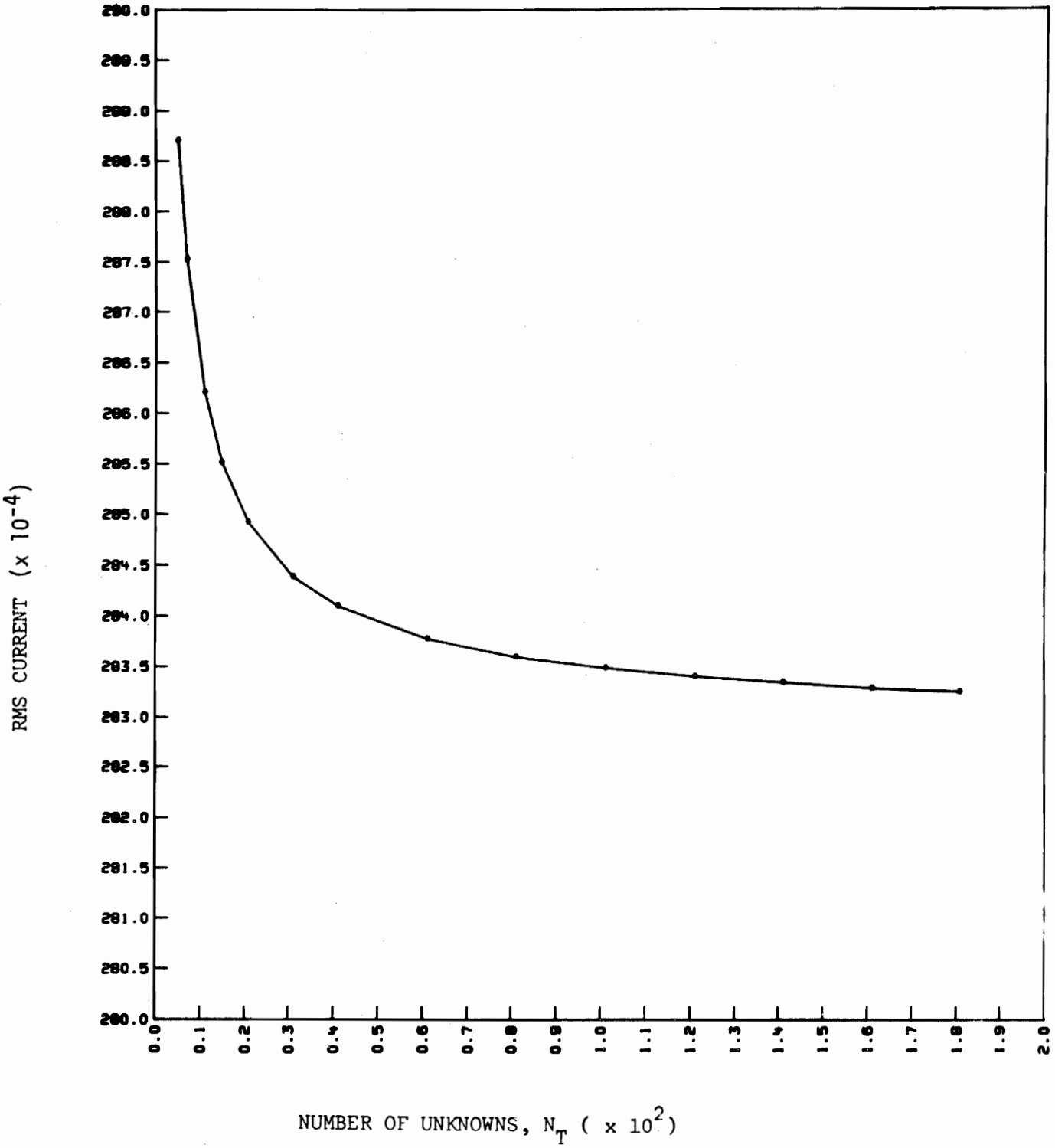

FIGURE 8. RMS CURRENT vs N_T FOR A STRAIGHT WIRE WITH 10X MULTIPLIER.

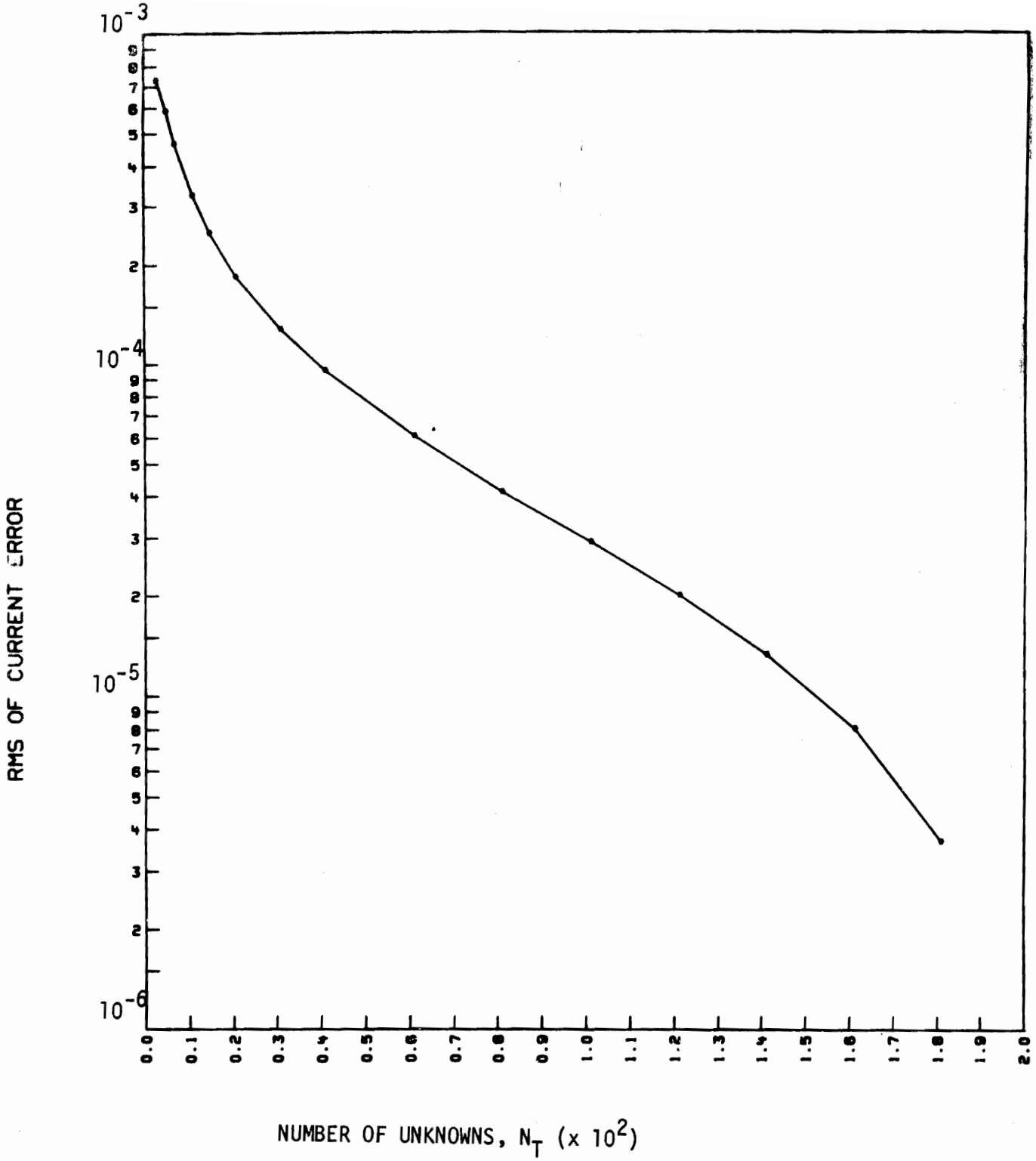

FIGURE 9. RMS ERROR IN CURRENT vs. N_T FOR STRAIGHT WIRE WITH 10X MULTIPLIER

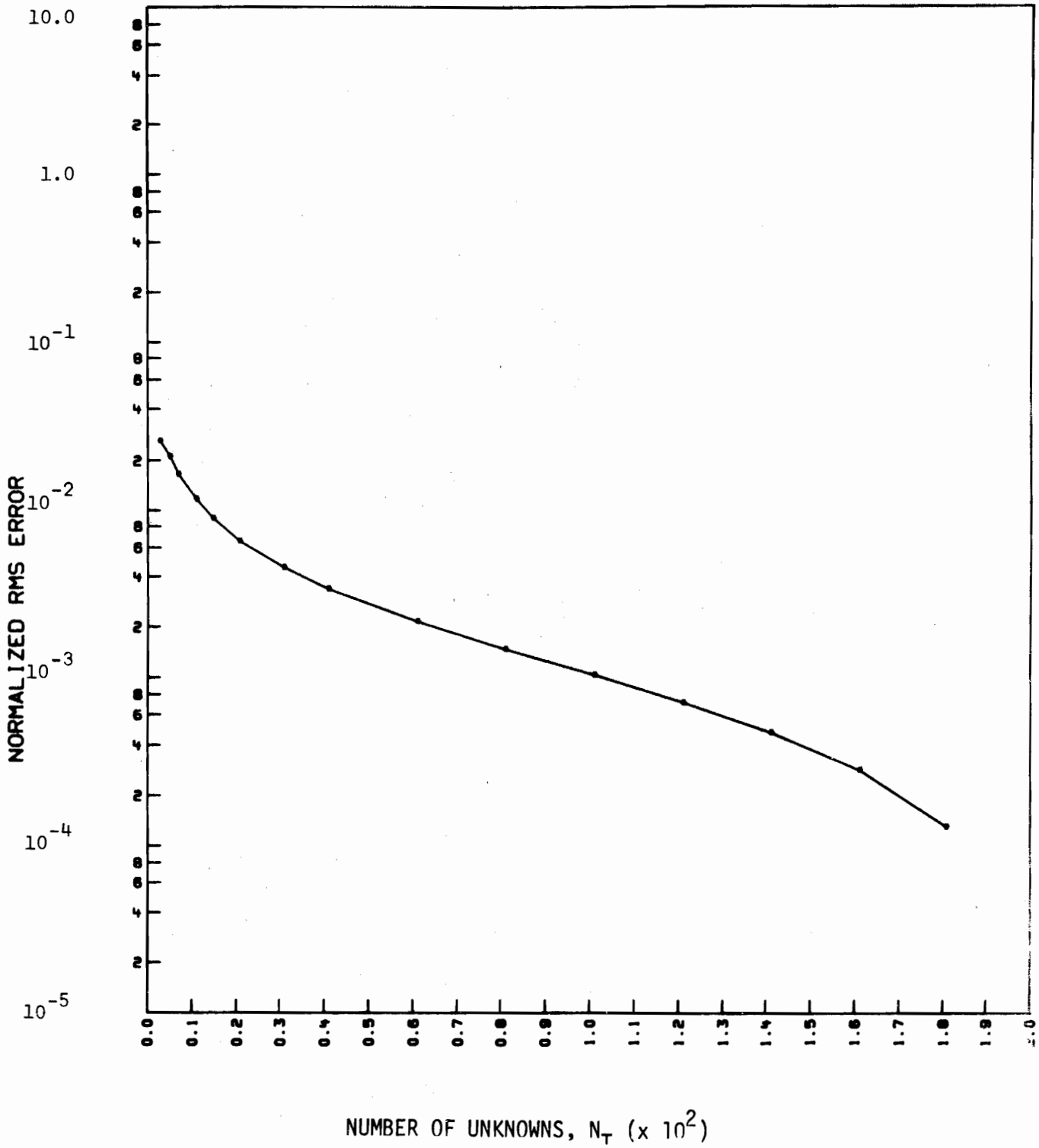

FIGURE 10. NORMALIZED RMS ERROR vs N_T FOR A STRAIGHT WIRE WITH 10X MULTIPLIER

3. Program Evaluation

a) Straight Wire Analysis

As mentioned previously, the ability of a program to accurately compute the current distribution on a straight wire is fundamental. The first evaluation is therefore associated with the straight wire. Judgments pertaining to convergence characteristics will be made using summary data and reasons for any deficiencies will be extracted from source data, if possible. The analysis is begun using the plots of root mean square current (I_{RMS}) and the normalized root mean square error ($(\varepsilon_s)_{RMS}$) versus the number of test segments (N_T) for different multipliers as shown in Figures 11 through 18.

The results for the 1X case (total wire length 0.58λ) shown in Figures 11 and 12 exhibit:

a) the similarity in convergence rates for BRACT (collocation, sinusoidal interpolation, Pocklington), OSU (Galerkin, piecewise sinsuoidal, Pocklington), SYR (Galerkin, piecewise linear, Potential).

b) the deficiency for collocation with pulse basis functions in Pocklington's integral equation as seen in I_{RMS} and $(\varepsilon_S)_{RMS}$.

c) the relatively slow convergence of the Boeing program (collocation, pulses, Potential)

d) the spread in the values of I_{RMS} for large values of N_T as computed using BRACT, OSU, and SYR is about 4% to 5%.

The figures highlight the difficulties associated with pulse basis function. Both the Boeing program and the Pulses program suffer from slow convergence rates as might be expected when one uses a staircase approximation to a smooth curve. The advantage enjoyed by the Boeing program over the Pulse program is attributed to the integral equation formulation used in each program. It is expected that the pulse basis functions, while relatively adequate when used in conjunction with integrals having well behaved kernels (Potential, Hallen's), do not suffice when used with a kernel having a theoretically non-integrable singularity. For example, the Potential integral equation has a kernel exhibiting a r^{-1} singularity while the Pocklington integral equation has a kernel exhibiting a r^{-3} singularity - a possible source of difficulty. On the basis of these observations, the Pulse program using collocation and Pocklington's integral equation is discarded at this point in the program evaluations.

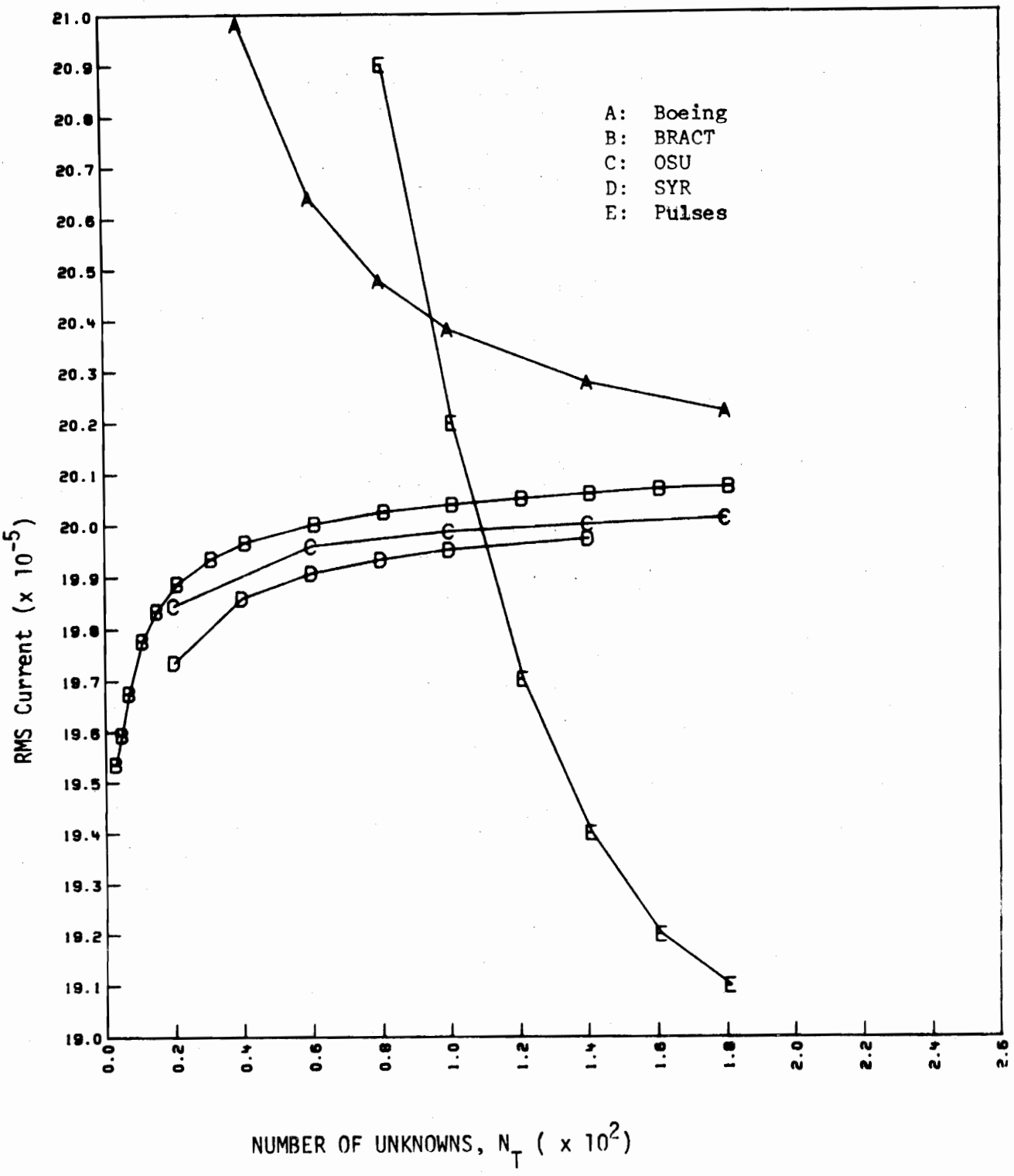

FIGURE 11: RMS CURRENT vs. N_T FOR A STRAIGHT WIRE WITH 1X MULTIPLIER COMPUTED USING DIFFERENT PROGRAMS.

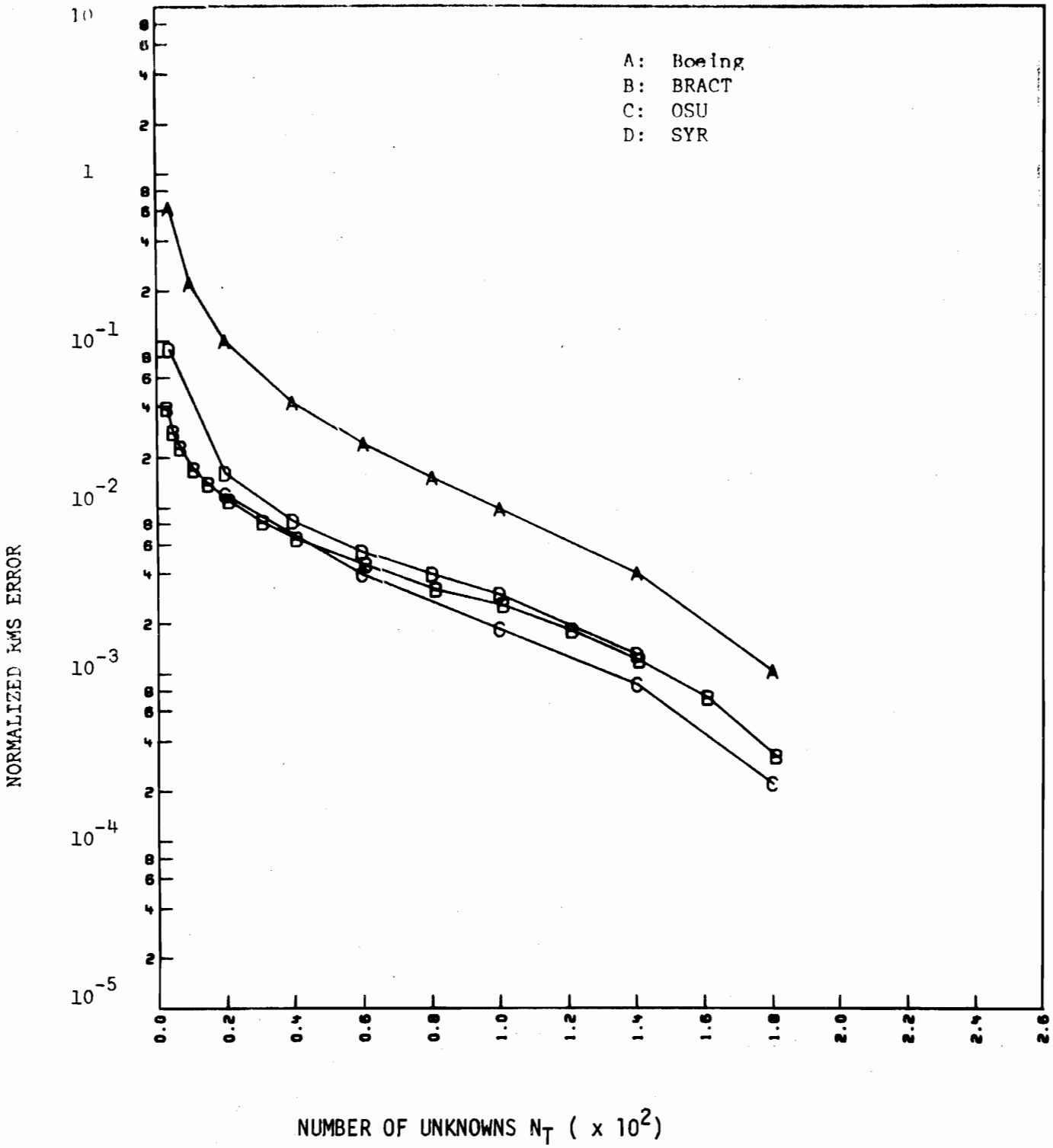

FIGURE 12: NORMALIZED RMS ERROR vs. N_T FOR A STRAIGHT WIRE WITH 1X MULTIPLIER RESULTING FROM DIFFERENT PROGRAMS.

For the 10X multiplier (total wire length 0.58λ), the observations made using Figures 13 and 14 are similar to those for 1X. The spread in values of I_{RMS} at large values of N_T for all but the Boeing program is in the 5% range. Limited data are presented in Figure 13 for the LLL program called GIANT which is similar to BRACT but used matching of current amplitude and slope at segment ends (as in the TCI program). It seems that GIANT converges faster than the other programs but time limitations are precluding a detailed study of GIANT at this time. The somewhat severe deficiency in the Boeing program insofar as the convergence rate is concerned is clearly evident in Figure 14.

It is not until one encounters long straight wires that the clear cut differences between BRACT, OSU, and SYR become apparent. For the 100X multiplier in Figures 15 and 16 (total wire length ~5.8λ), it is noted that BRACT converges quite rapidly to a stable solution while OSU and SYR converge at a slower rate. A deficiency in the Boeing program again is noted. Both I_{RMS} and $(\varepsilon_s)_{RMS}$ support these assertions. The spread in values of I_{RMS} for BRACT, OSU, and SYR for large values of N_T is only 6%. On the basis of the poor convergence characteristics of the Boeing program it is excluded from further detailed consideration even though its relative simplicity made it a desirable program in view of anticipated changes required for high frequency coverage. A portion of the Boeing program, namely the wire junction treatment, should be retained for possible use in other programs.

For the 200X multiplier (wire length about 11.6λ) results shown in Figures 17 and 18 the shortcoming of the SYR program becomes apparent. The convergence rate is quite poor and investigations to determine the reasons lead to the conclusion that the piecewise linear approximation is incapable of approximating a current distribution similar to a standing wave without a large number of sample points. Figure 19a is a plot of current distribution on a 200X straight wire computed using SYR with N_T = 201 and N_R = 350 while by comparison, the similar OSU results for N_T = 200 and N_R = 400 is shown in Figure 19b. Clearly, the sinusoidal representation is more efficient than a piecewise linear representation for standing wave distributions. A similar deficiency of the SYR program for 100X was also noted. For these reasons, Galerkin's method with piecewise linear interpolation and the Potential integral equation is eliminated from further consideration for structures of arbitrary length though this technique is still adequate for lengths no more than a few wavelengths.

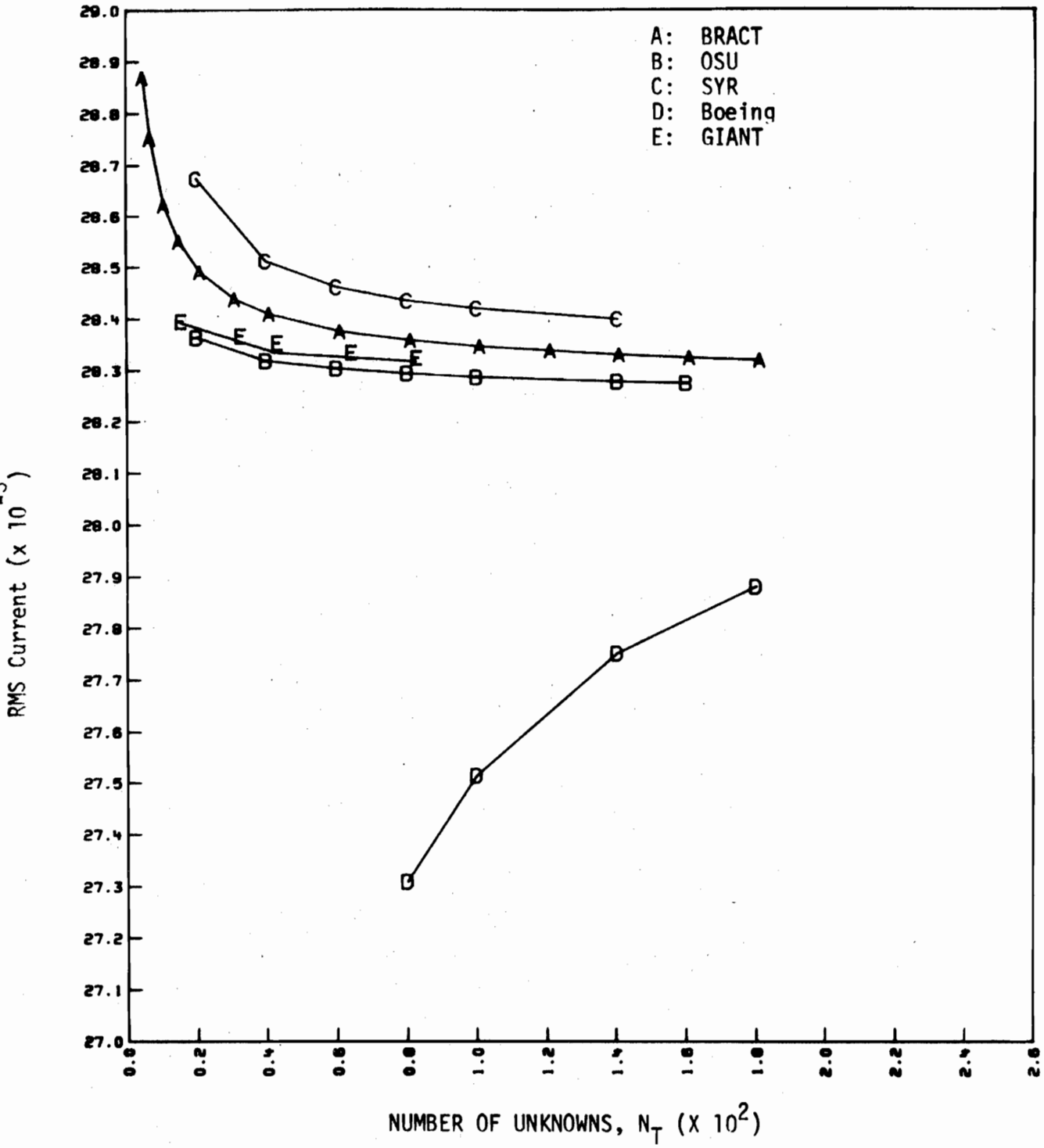

FIGURE 13 RMS CURRENT vs N_T FOR A STRAIGHT WIRE WITH 10X MULTIPLIER COMPUTED USING DIFFERENT PROGRAMS

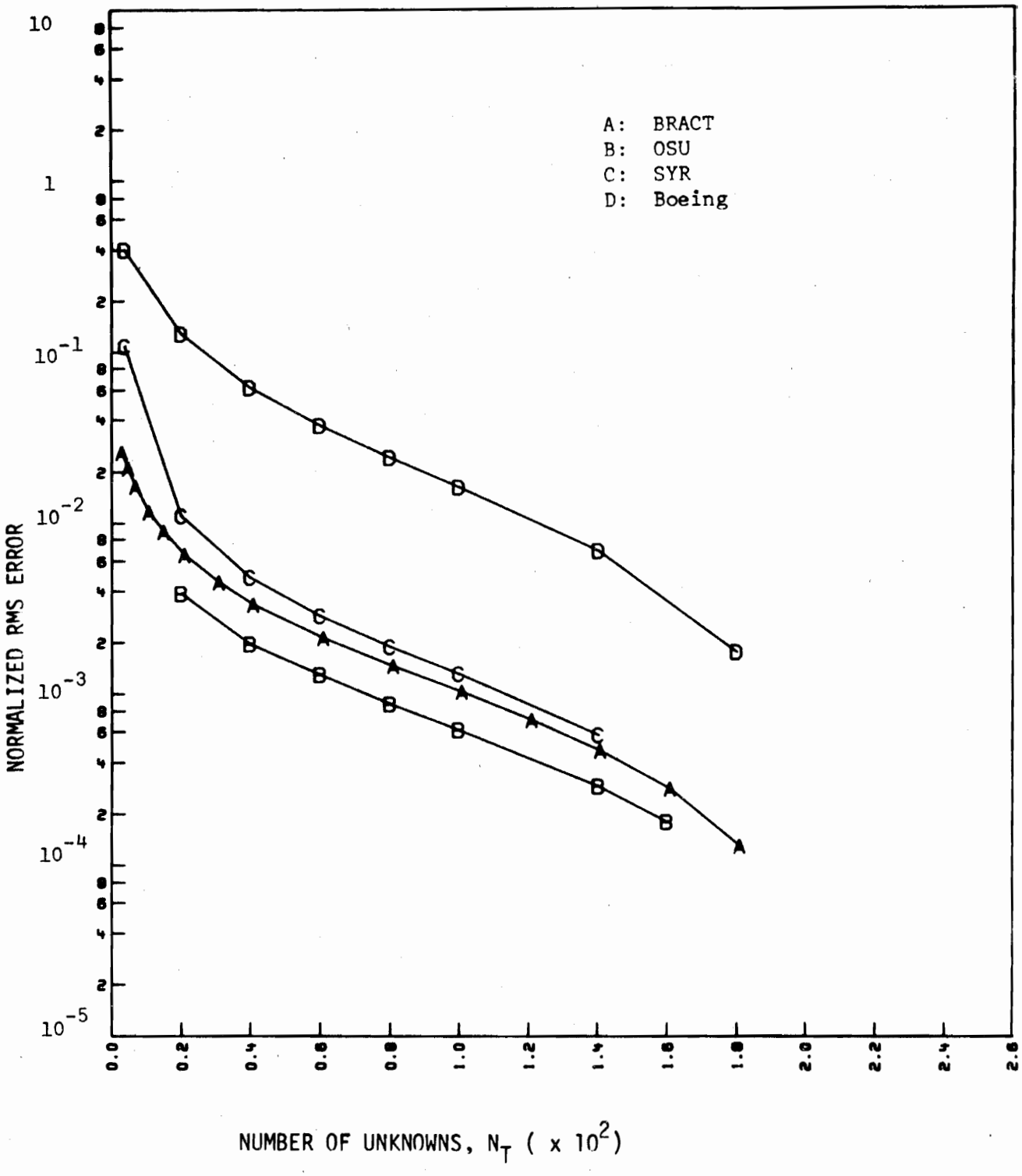

FIGURE 14. NORMALIZED RMS ERROR vs. N_T FOR A STRAIGHT WIRE WITH 10X MULTIPLIER RESULTING FROM DIFFERENT PROGRAMS.

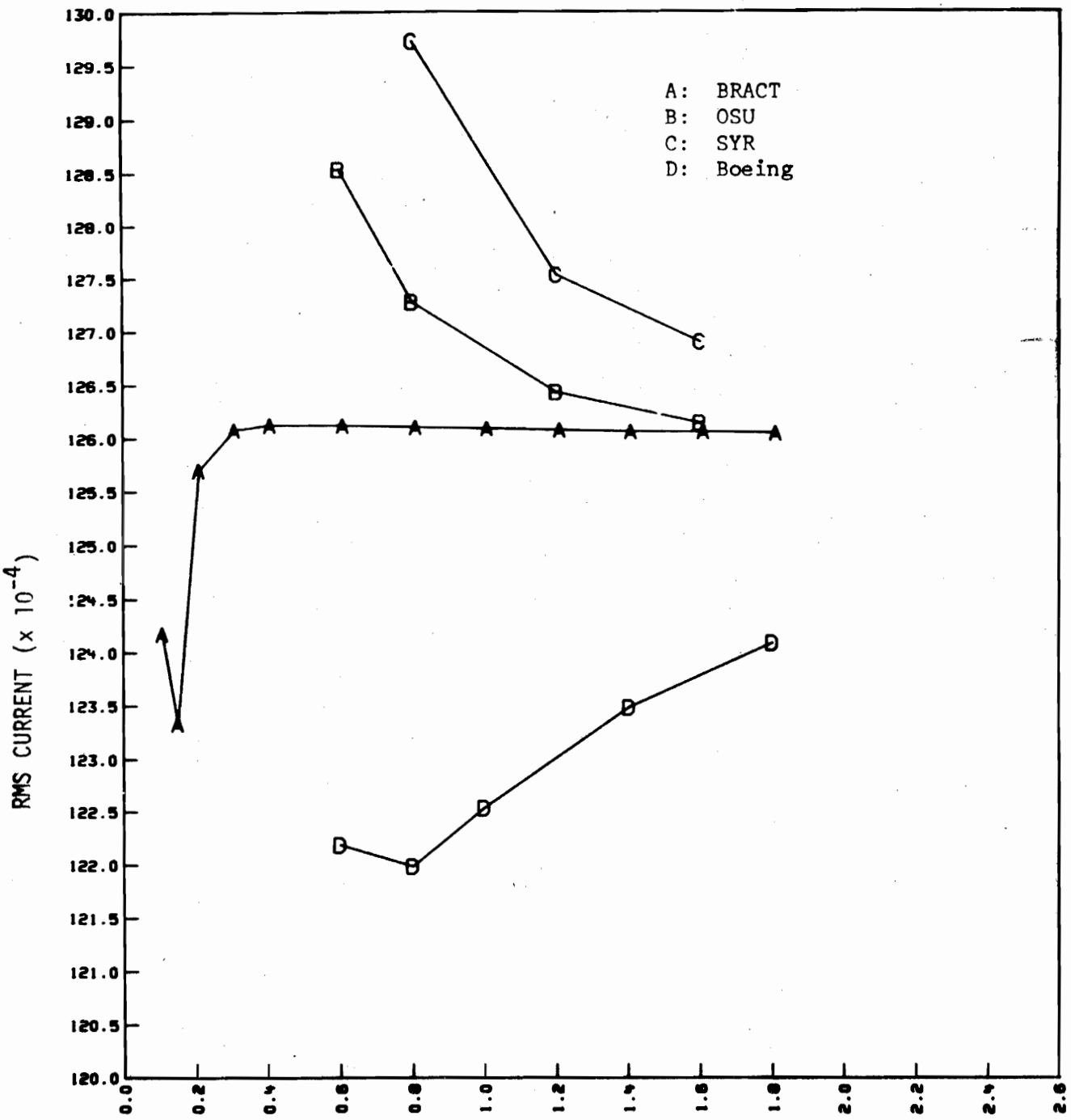

FIGURE 15. RMS CURRENT vs N_T FOR A STRAIGHT WIRE WITH 100X MULTIPLIER COMPUTED USING DIFFERENT PROGRAMS.

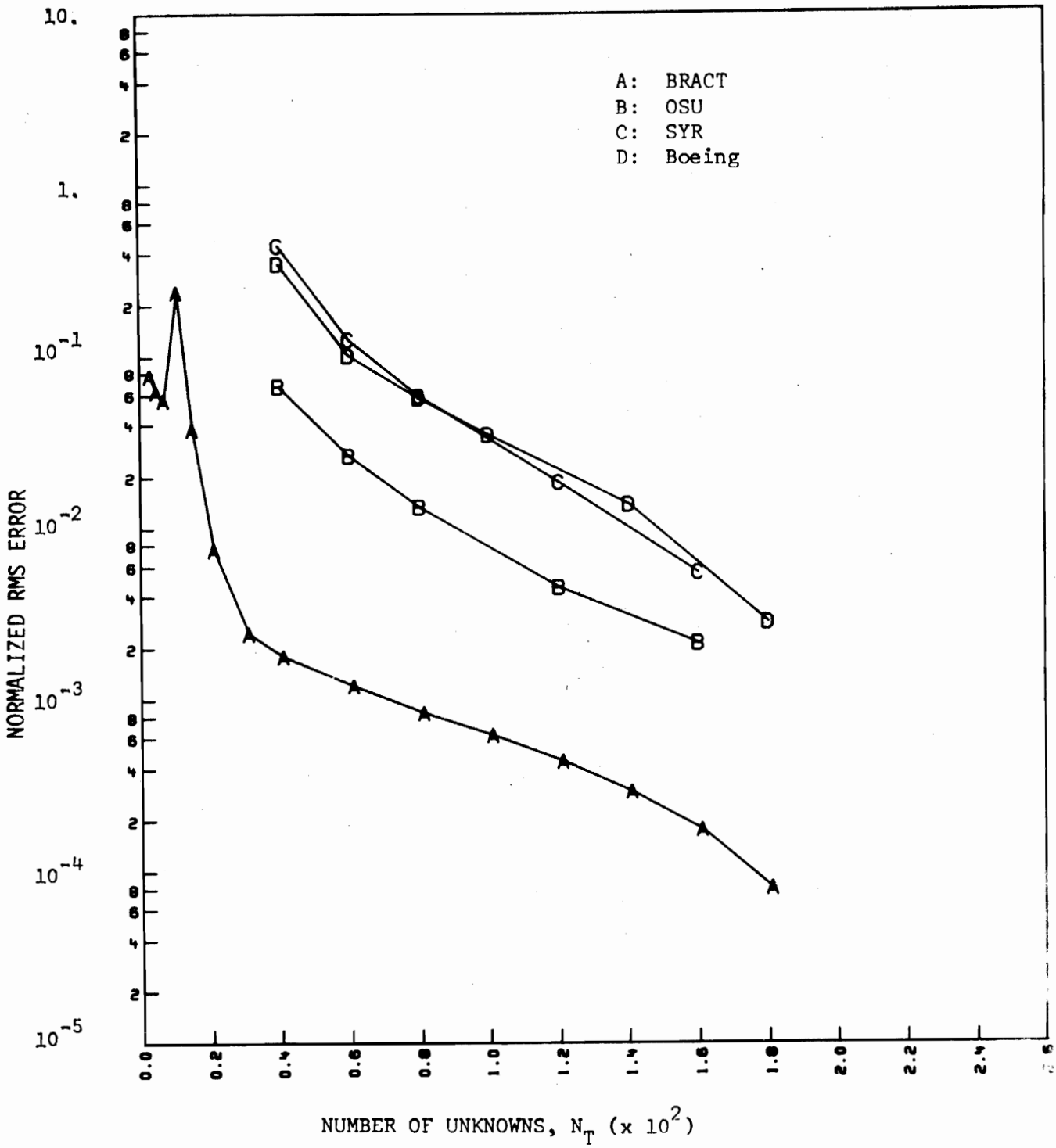

FIGURE 16. NORMALIZED RMS ERROR vs N_T FOR A STRAIGHT WIRE WITH 100X MULTIPLIER RESULTING FROM DIFFERENT PROGRAMS.

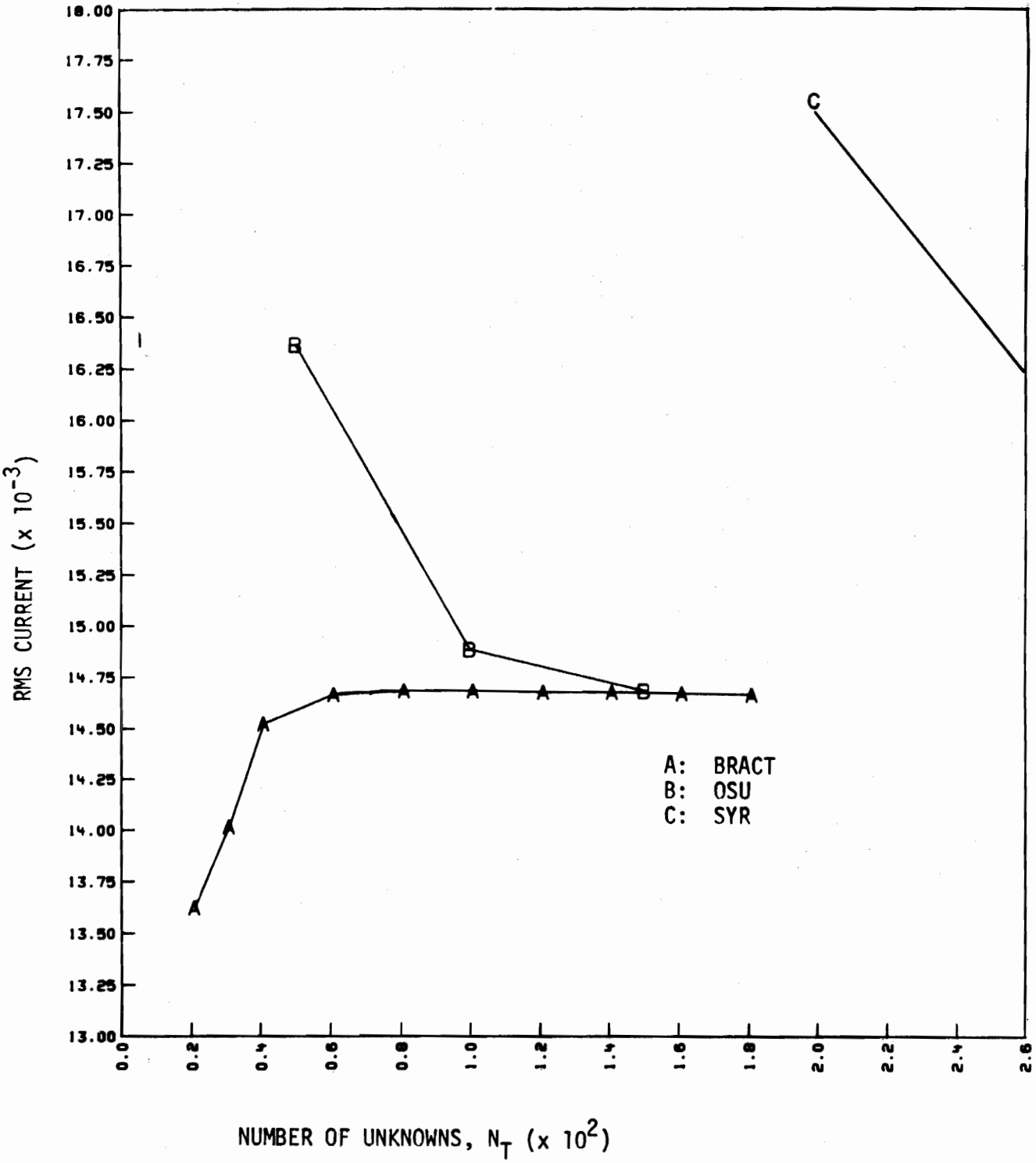

FIGURE 17: RMS CURRENT vs N_T FOR A STRAIGHT WIRE WITH 200X MULTIPLIER COMPUTED USING DIFFERENT PROGRAMS

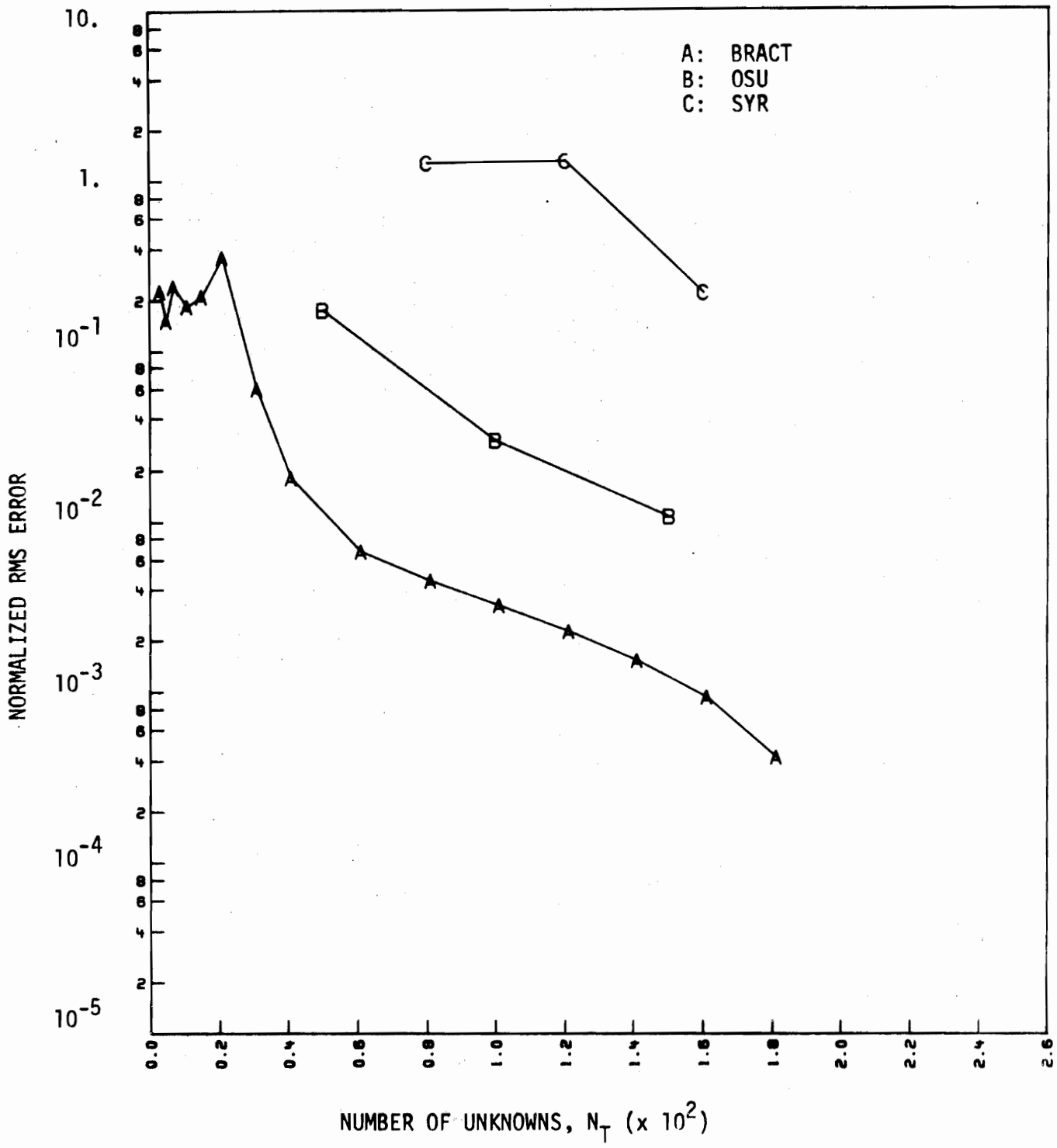

FIGURE 18: NORMALIZED RMS ERROR vs N_T FOR A STRAIGHT WIRE WITH 200X MULTIPLIER RESULTING FROM DIFFERENT PROGRAMS

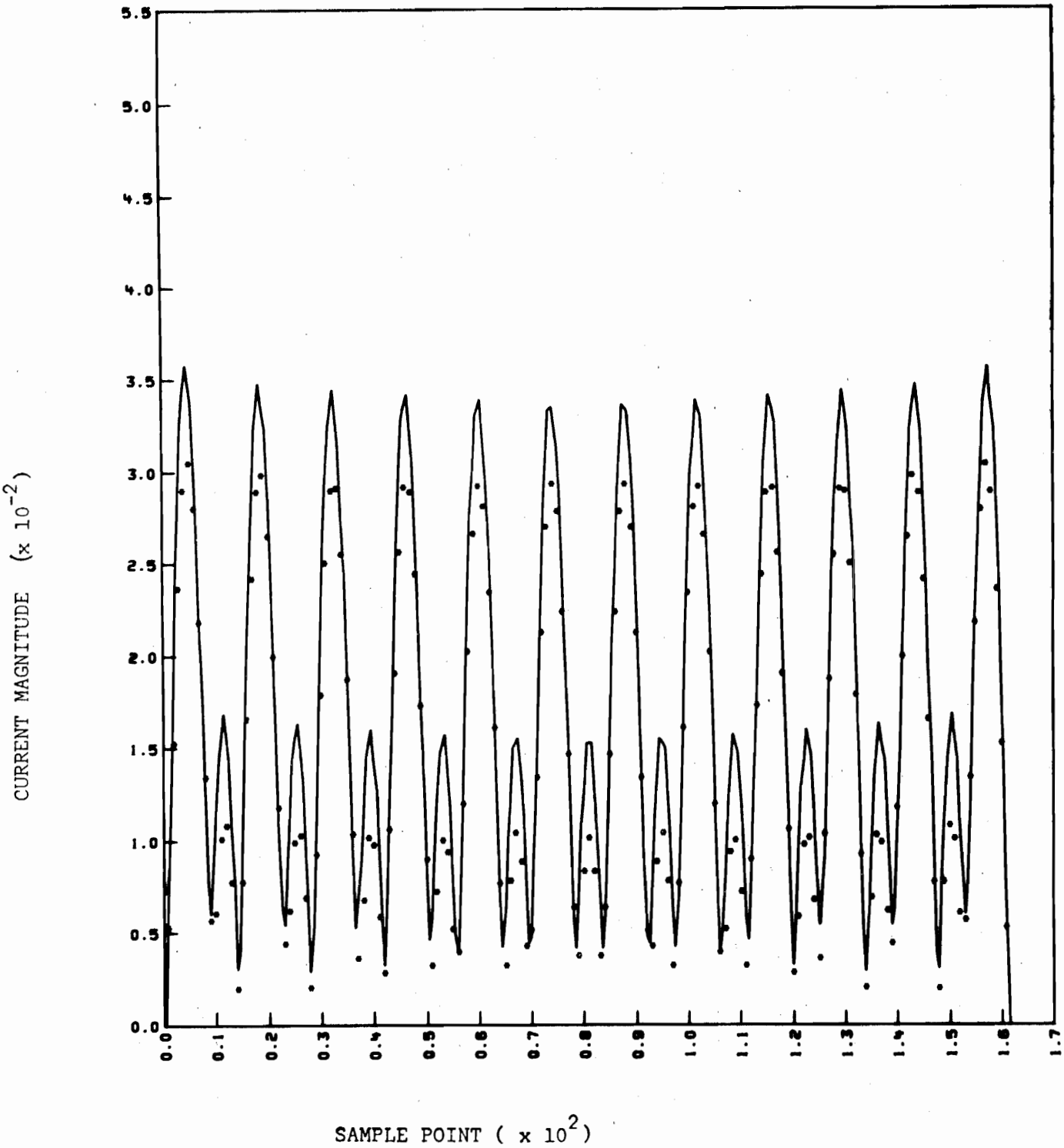

FIGURE 19a : CURRENT MAGNITUDE vs SAMPLE POINT FOR A STRAIGHT WIRE WITH A 200X MULTIPLIER COMPUTED USING SYR WITH N_T = 160. THE REFERENCE SOLUTION (*) USED N_R = 200.

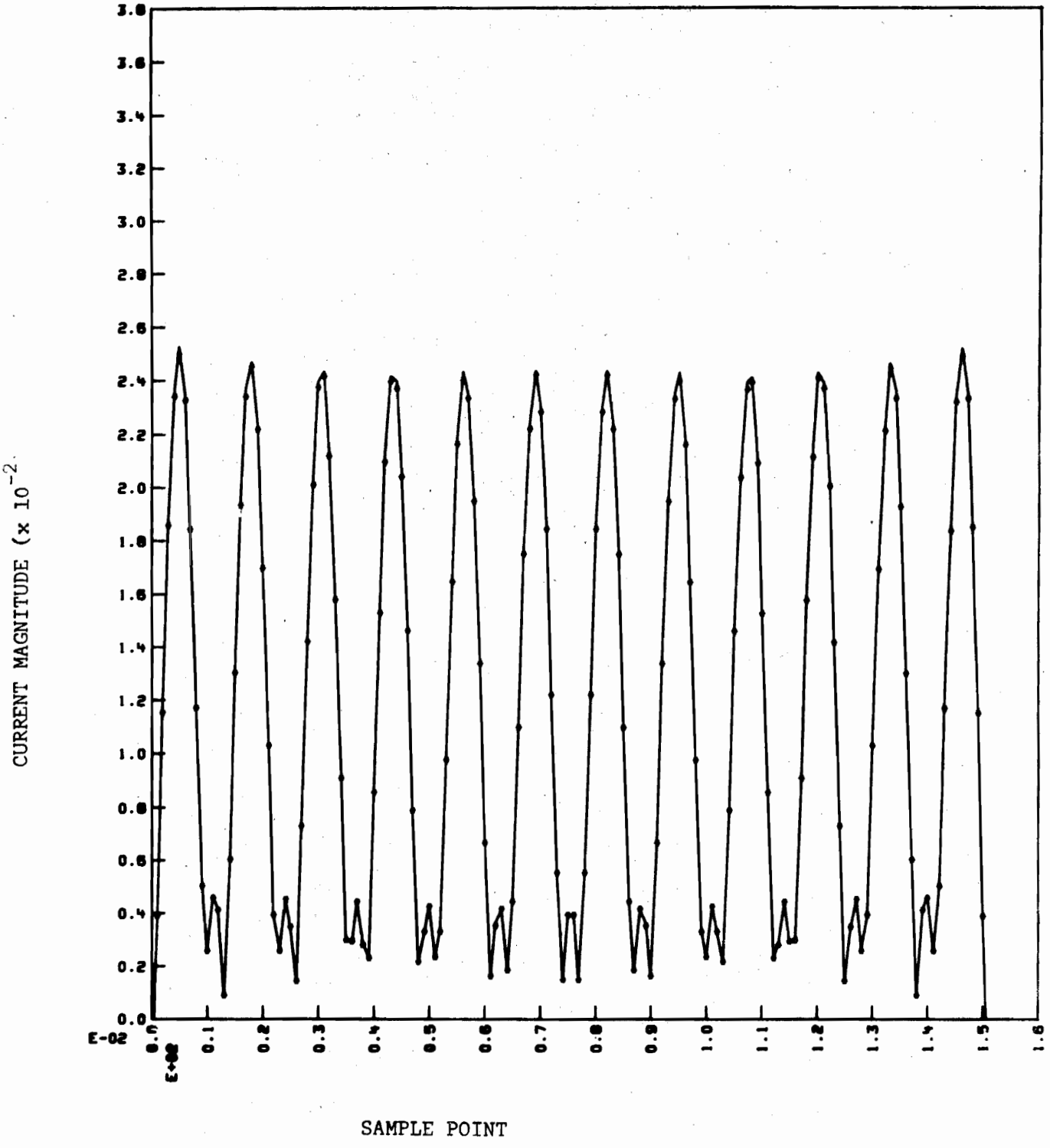

FIGURE 19b: CURRENT MAGNITUDE vs SAMPLE POINT FOR A STRAIGHT WIRE WITH A 200X MULTIPLIER COMPUTED USING OSU with N_T = 150. THE REFERENCE SOLUTION (*) USED N_R = 200.

b) L Wire Analysis

The summary data for the L wire structure lead to conclusions similar to those for the straight wire. The data for I_{RMS}, (figures 20 to 22) for which the Boeing results do not even fall within the same range, indicate that

1) the Boeing program (collocation, pulses, Potential) is inadequate from a convergence viewpoint.

2) the SYR program (Galerkin, piecewise linear, Potential) suffers from a poor convergence rate for structures large in terms of wavelength.

Based upon these observations, the Boeing and SYR programs are excluded from further consideration.

Once again, the summary data illustrate the near similarity of the OSU and BRACT programs. However, the OSU program does exhibit some advantages in convergence rate as evidenced by the I_{RMS} and $(\varepsilon_S)_{RMS}$ vs N_T plots of Figures 20 and 25.

For the 1X case (total wirelength 0.366λ), the OSU program converges somewhat more rapidly and exhibits a lower normalized root mean square error. For the 5X case (total wirelength 12.8λ), the differences are again small with the OSU program exhibiting the advantage.

As was mentioned previously, the plots of current magnitude for the OSU program were constructed by connecting the current amplitudes at segment centers with straight lines. This feature does not however enter into any of the summary data computations since only data computed by the source program was used.

Hence, in a plot of $|I|$ vs. N_T, the computed values for the test case are located at points where the piecewise linear curve exhibits slope discontinuities. On the other hand, the BRACT program plots were constructed using the computed data points and were interpolated using the BRACT interpolation formula. These source curves give a very accurate idea of the actual current being used in the source program for evaluating interactions although it is reiterated that the specific functional behavior does not enter into the summary data computations.

An investigation of the source data for the 1X and 5X cases leads to the discovery of a potential source of difficulty in the BRACT program. The scheme used for representing the current over a given segment on the structure (sinusoidal interpolation) allows for amplitude and derivative discontinuities in the current at segment edges, i.e., at the point of connection of one segment to another. Although this discontinuity is generally imperceptible, cases do occur where the discontinuity is significant. As an

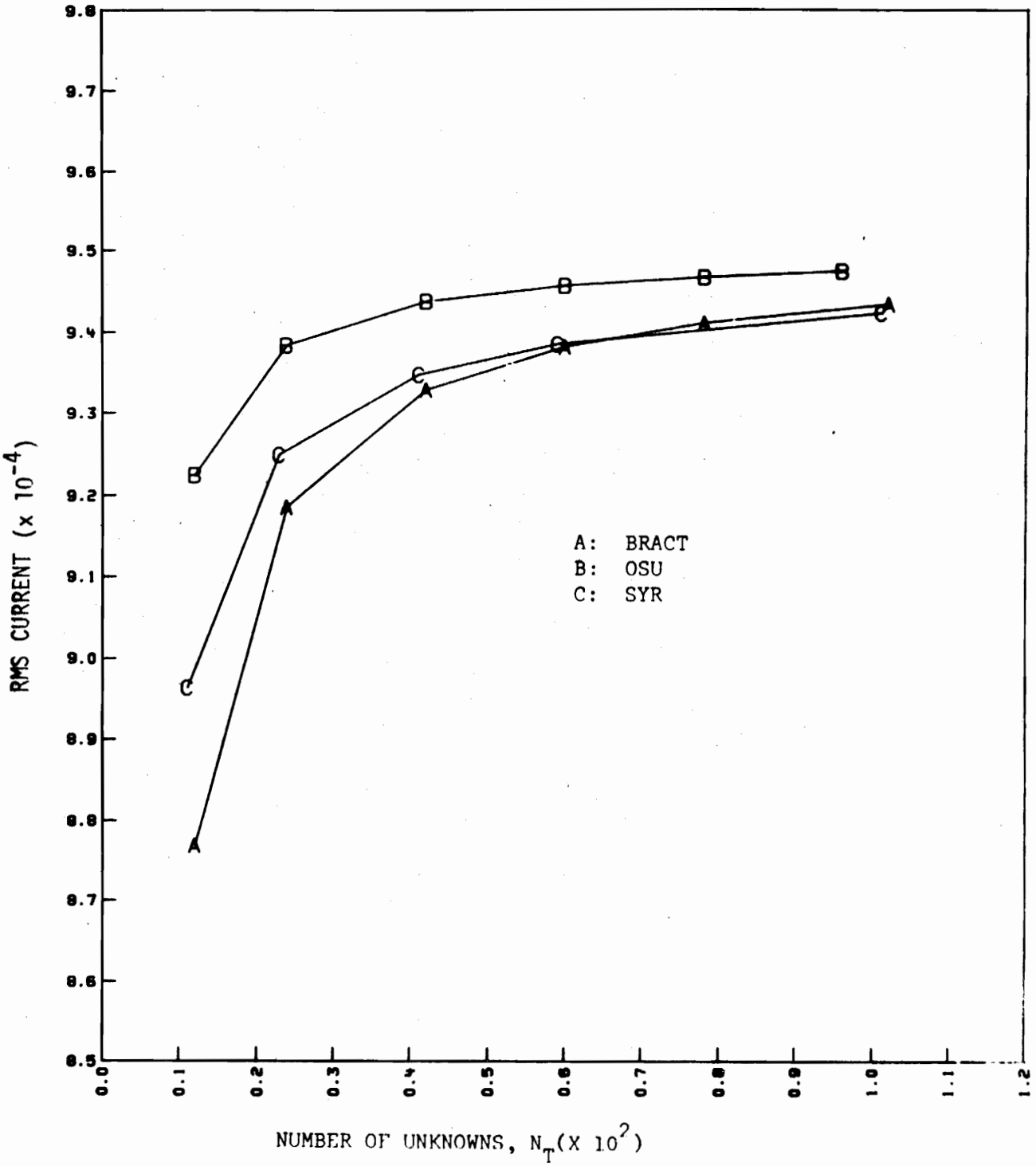

FIGURE 20: RMS CURRENT vs N_T FOR AN L WIRE WITH A 1X MULTIPLIER COMPUTED USING DIFFERENT PROGRAMS.

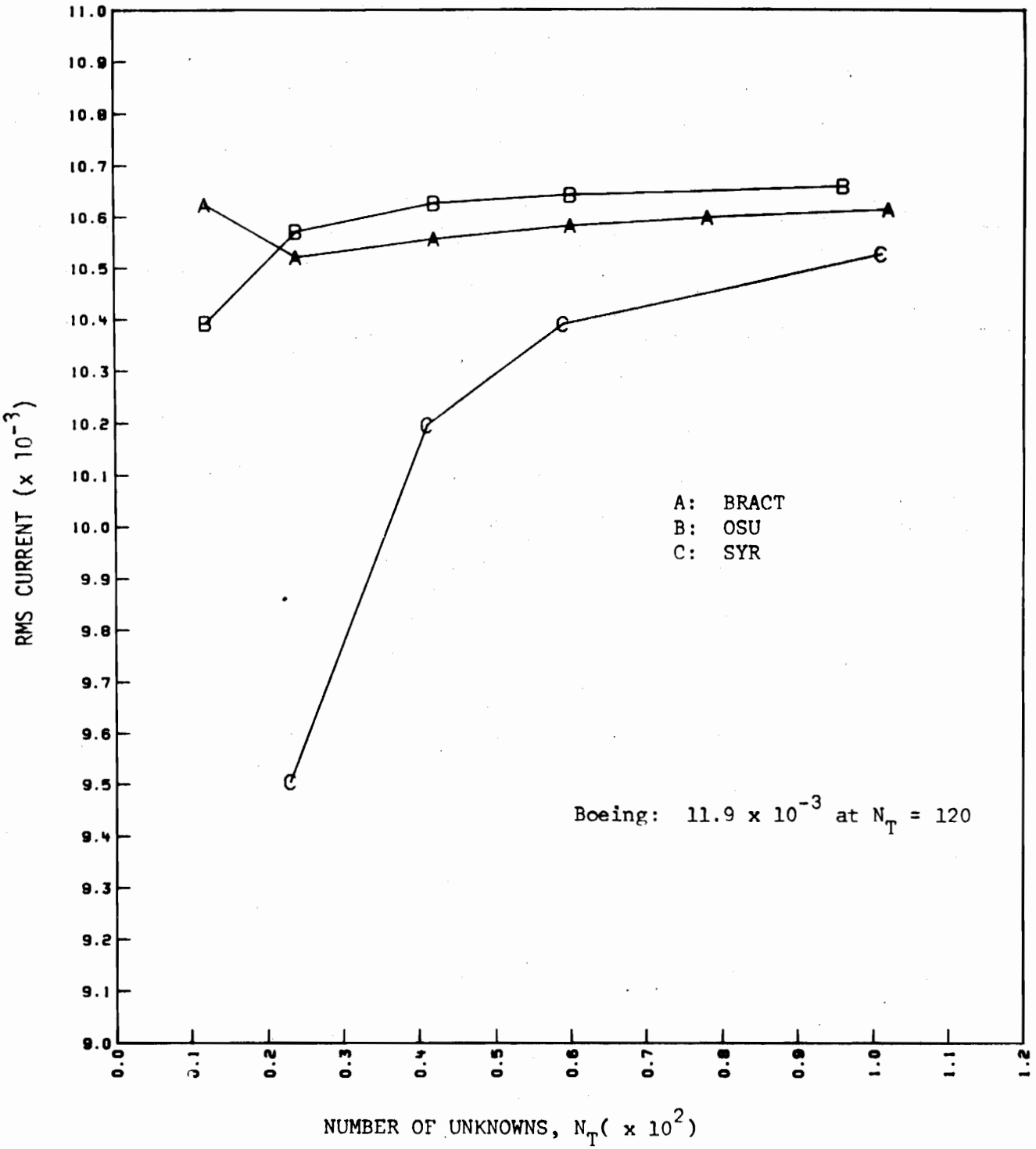

FIGURE 21: RMS CURRENT vs N_T FOR AN L WIRE WITH A 5X MULTIPLIER COMPUTED USING DIFFERENT PROGRAMS.

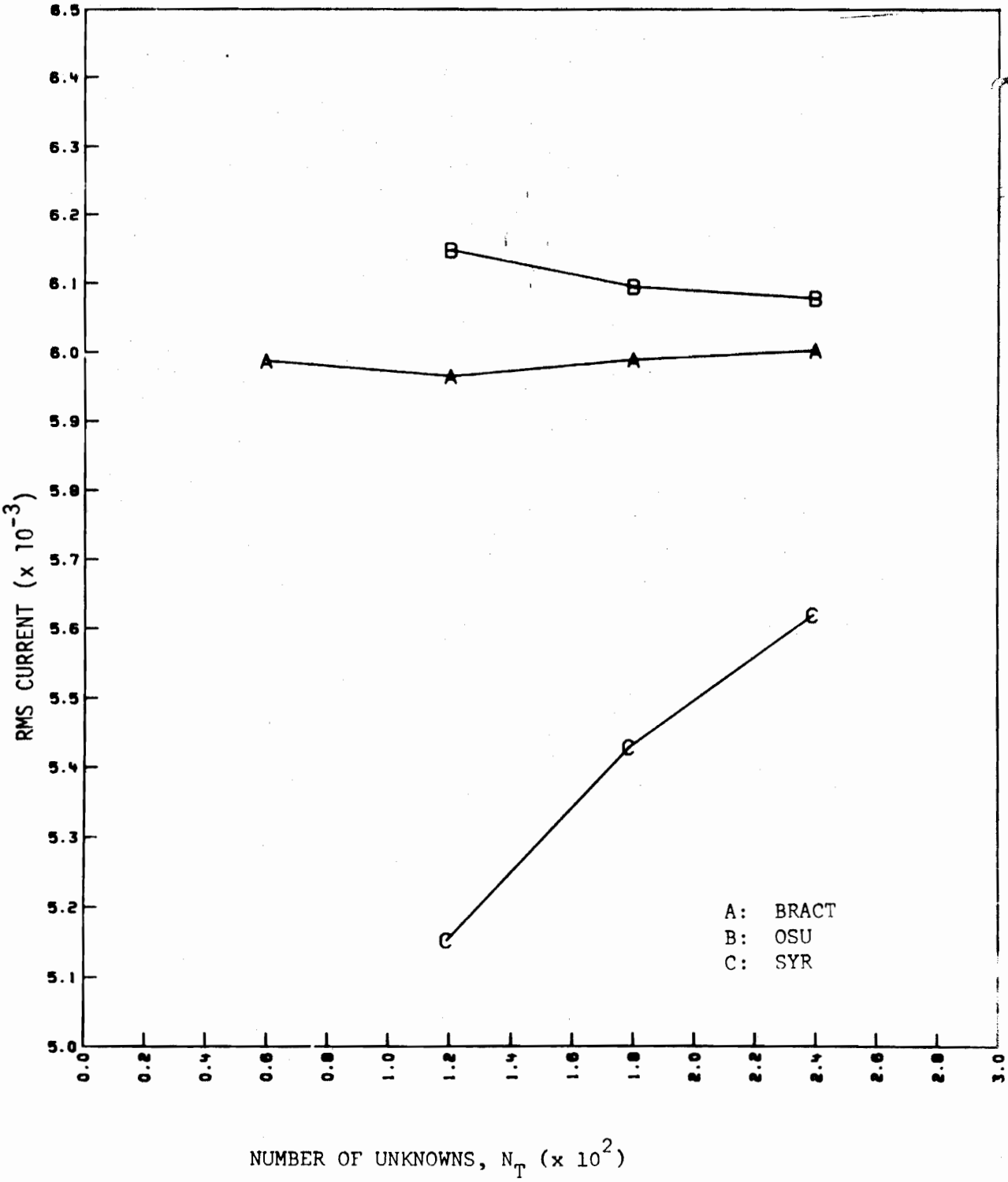

FIGURE 22: RMS CURRENT vs N_T FOR AN L WIRE WITH A 35X MULTIPLIER COMPUTED USING DIFFERENT PROGRAMS.

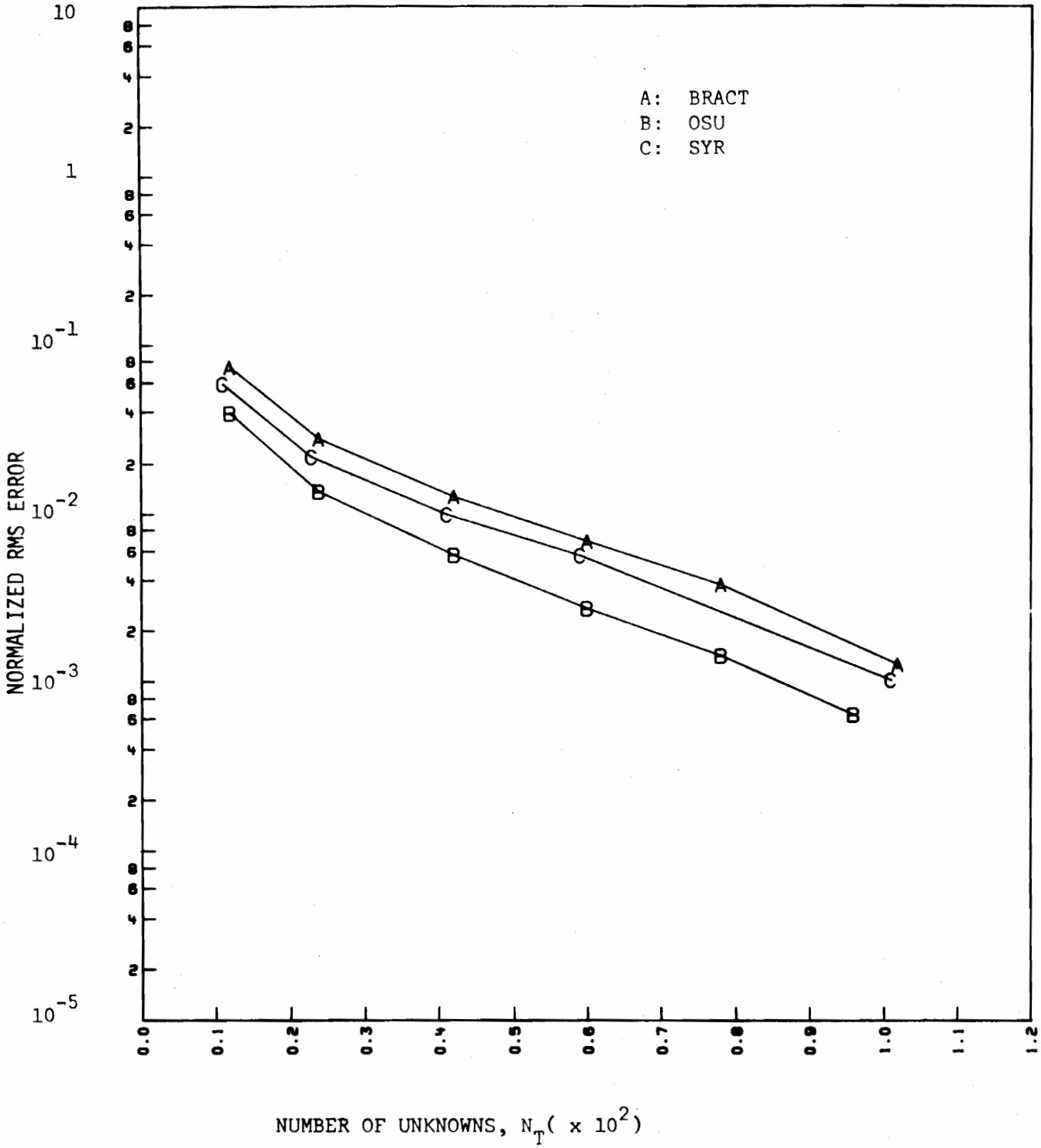

FIGURE 23: NORMALIZED RMS ERROR vs. N_T FOR AN L WIRE WITH A 1X MULTIPLIER RESULTING FROM DIFFERENT PROGRAMS.

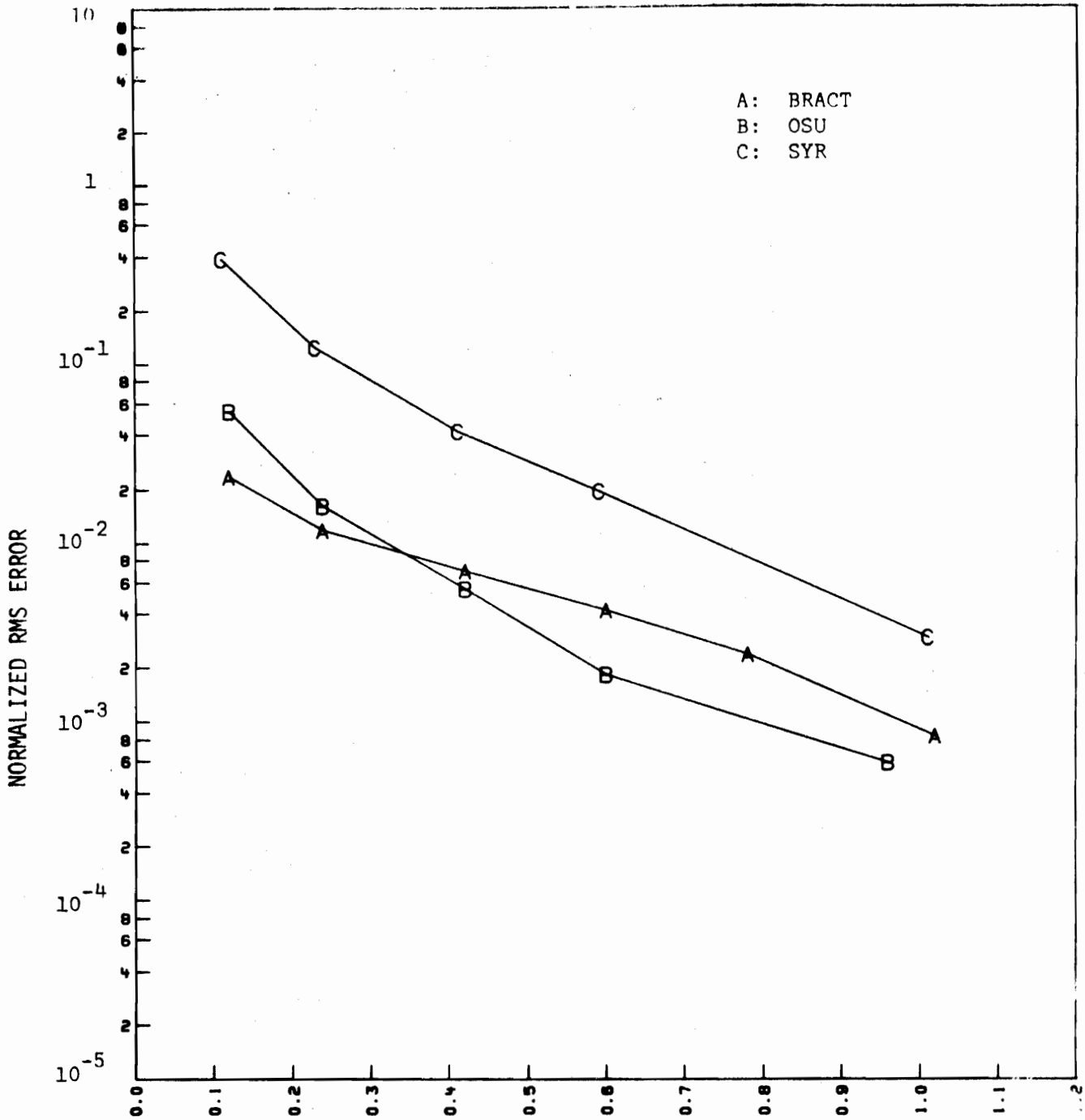

FIGURE 24: NORMALIZED RMS ERROR vs N_T FOR AN L WIRE WITH A 5X MULTIPLIER RESULTING FROM DIFFERENT PROGRAMS.

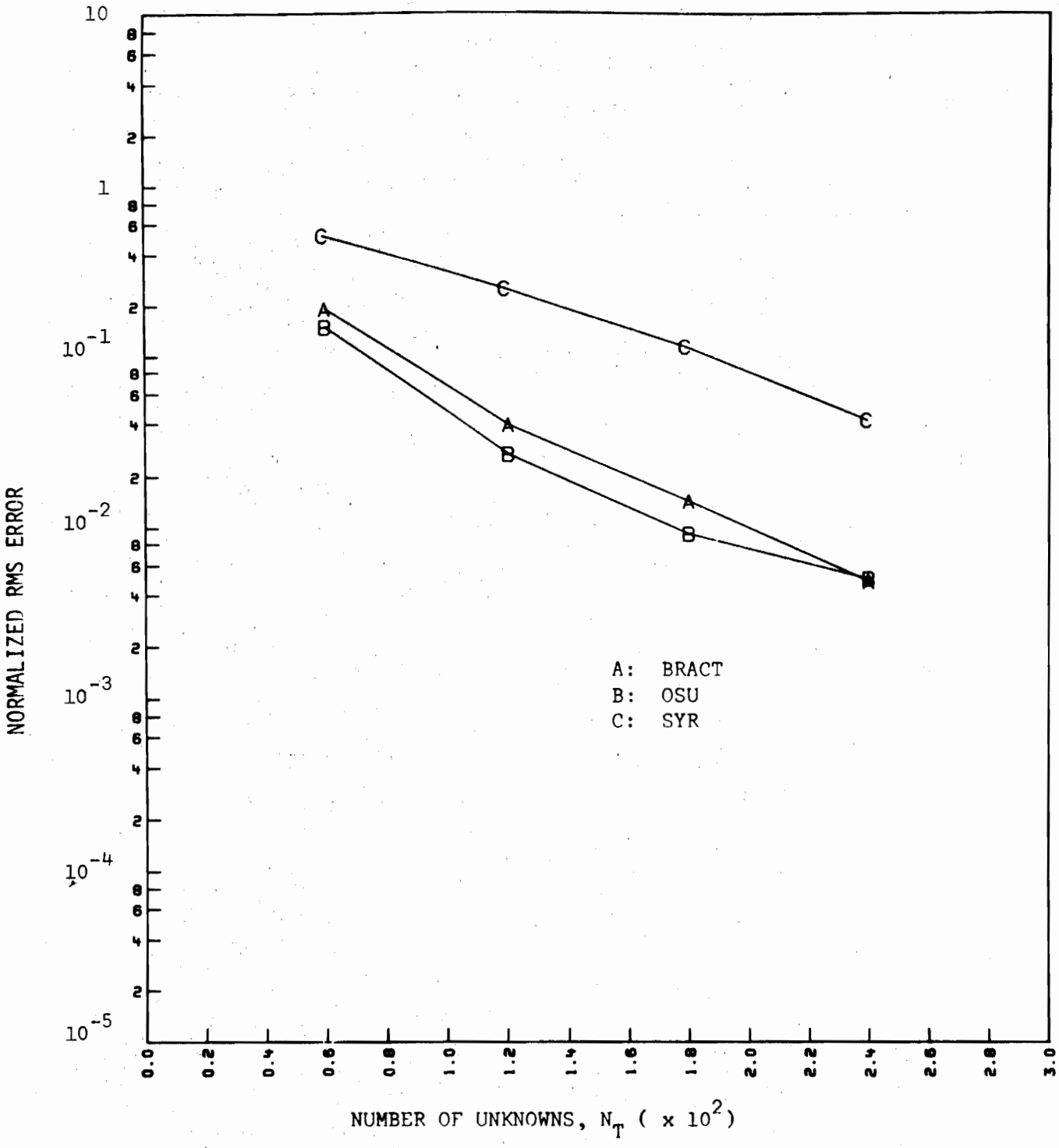

FIGURE 25: NORMALIZED RMS ERROR vs. N_T FOR AN L WIRE WITH A 35X MULTIPLIER RESULTING FROM DIFFERENT PROGRAMS.

example, the 1X case current magnitude plots for N_T = 12 and 24 are offered. Fig. 26 for N_T = 12 shows a sizable discontinuity in amplitude at the bend in the L wire and a smaller discontinuity at the adjacent edge on the short arm of the L wire. A similar phenomenon is observed for the N_T = 24 case in Figure 27. Obviously, the effects of the discontinuity can numerically propagate through the interpolating scheme to locations away from the point at which the discontinuity might be expected. Although this type of behavior is very evident only at low sampling densities, its effect on computations is probably felt for all N_T's. The OSU program also suffers from some difficulties at the wire junction although not as severe as in BRACT. Figure 28 is a plot of the current magnitude for the 1X case, N_T = 12 for the OSU program with the piecewise sinusoidal interpolation scheme used to construct the entire curve as the program would actually use it. In this particular case, only a derivative discontinuity, which the scheme allows, is evident at and near the bend. Also shown on this curve is the reference solution for comparison. A somewhat more striking example of this type of behavior is presented in Figure 29 for the 5X case. The difficulties near the bend are evident. Even though such problems can arise, the OSU program is superior to BRACT in this respect.

c) Cross-Wire Analysis

The cross wire analysis is meant to test a program's ability to handle a multiple wire junction while the L wire analysis merely tested the program's ability to model the interactions associated with an orthogonal intersection of two wires. At this point, the cross wire analysis is quite academic since the advantages of the OSU program have already been realized. Furthermore, the OSU program has, through its formulation, the implicit enforcement of the Kirchoff current law at junctions, while the BRACT program does not, in general, satisfy that law. For a further discussion of this point, the reader is referred to Appendix A.

Without making specific judgments regarding the capability of a given program to adequately model a junction, one can nonetheless form some opinions regarding the program's efficiency from the summary data. Figures 30 through 35 indicate a small advantage in favor of the OSU program. Since the source data for this case is more difficult to interpret than for the other cases, it will not be used here to support the summary data. Rather, it will suffice to state that the effects of having an effective charge accumulation at the junction in the BRACT program leads to a deterioration in its ability to model electromagnetic interactions for this type of structure.

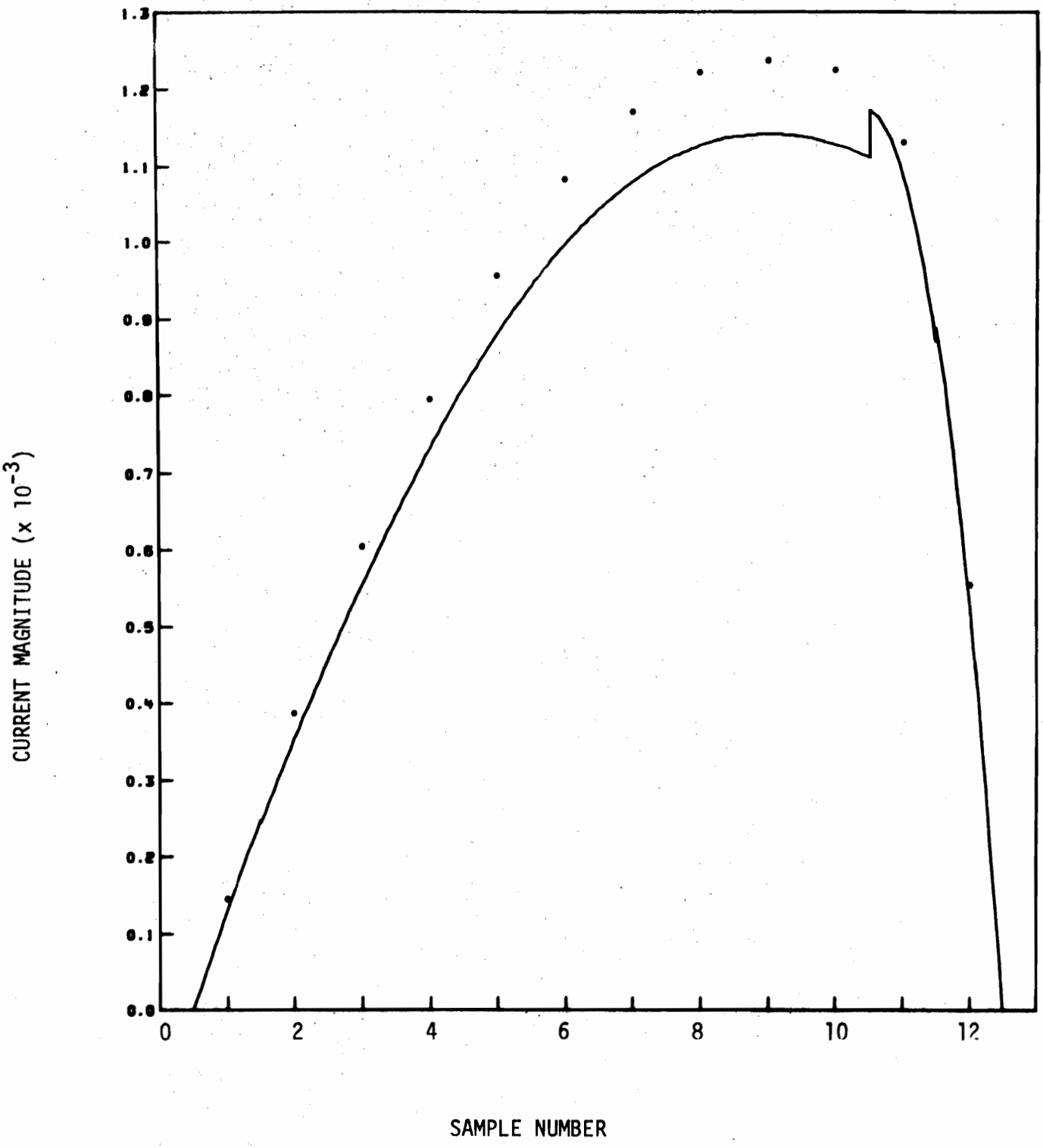

FIGURE 26: CURRENT MAGNITUDE vs SAMPLE POINT (LOCATION) FOR AN L WIRE WITH A 1X MULTIPLIER COMPUTED USING BRACT WITH N_T = 12. FOR THE REFERENCE SOLUTION (*) N_R = 120

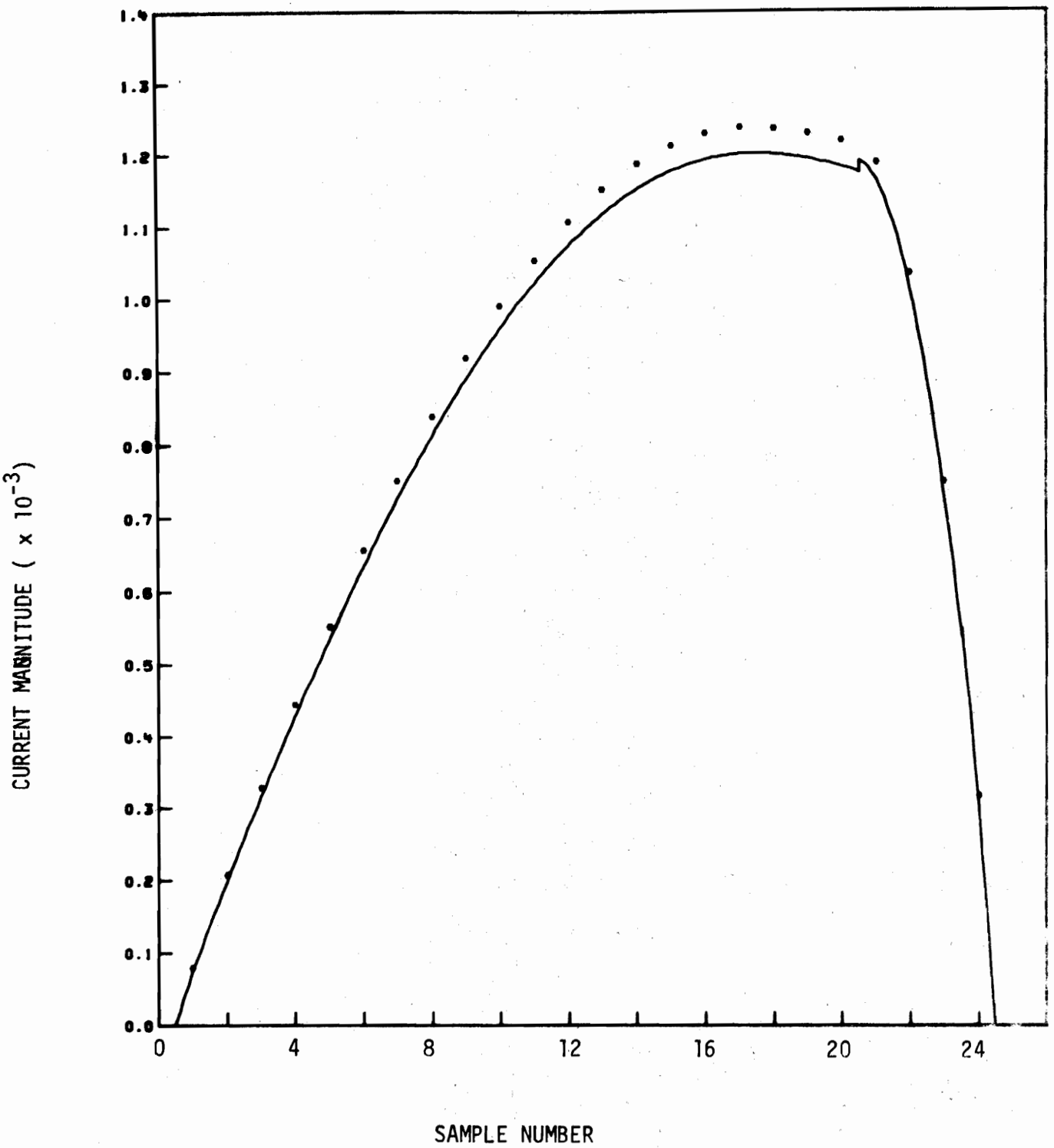

FIGURE 27: CURRENT MAGNITUDE vs SAMPLE POINT (LOCATION) FOR AN L WIRE WITH A 1X MULTIPLIER COMPUTED USING BRACT WITH N_T = 24. FOR THE REFERENCE SOLUTION (*) N_R = 120

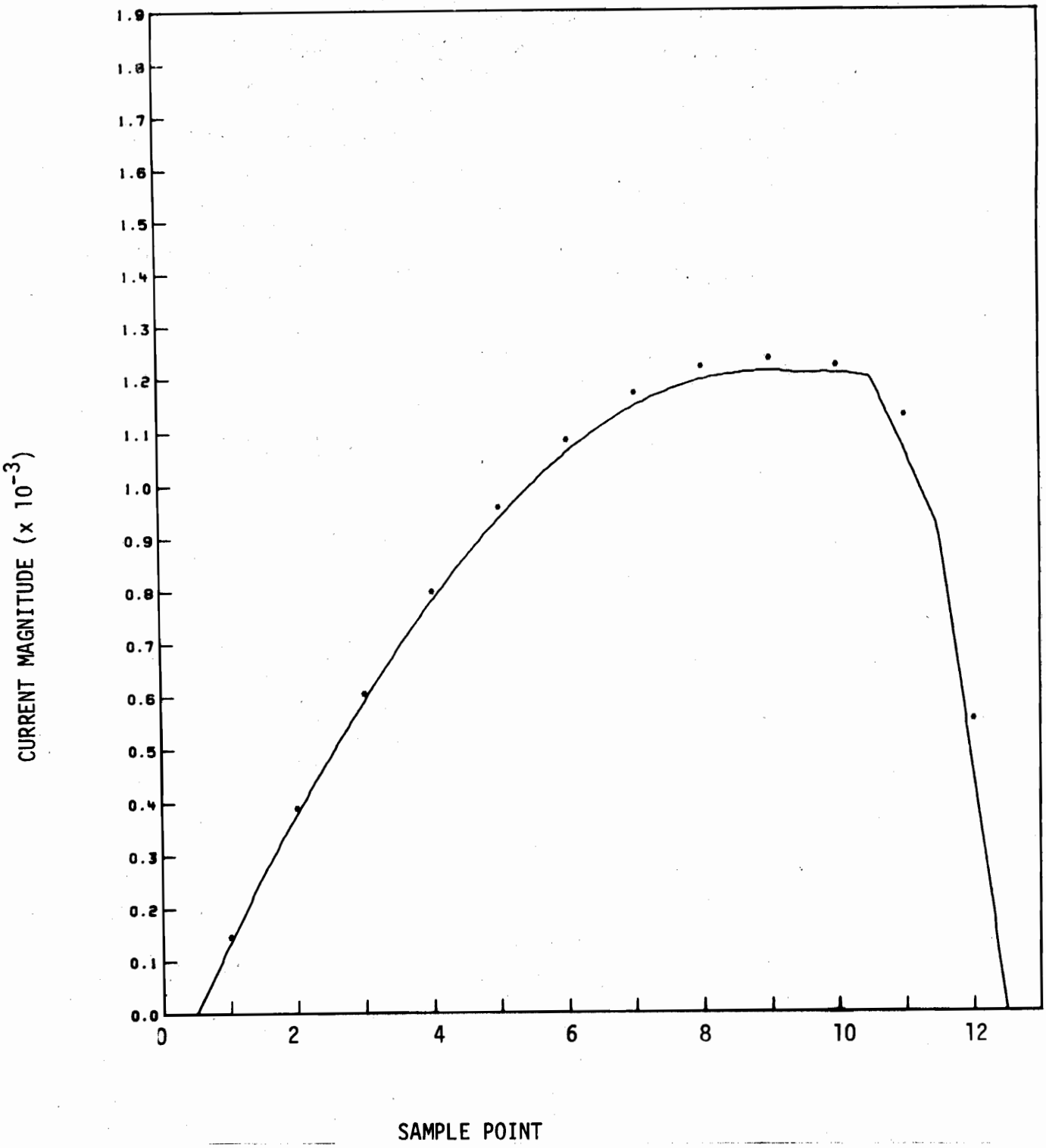

FIGURE 28: CURRENT MAGNITUDE vs. SAMPLE POINT (LOCATION) FOR AN L WIRE WITH A 1X MULTIPLIER COMPUTED USING OSU WITH N_T = 12. FOR THE REFERENCE SOLUTION (*) N_R = 120.

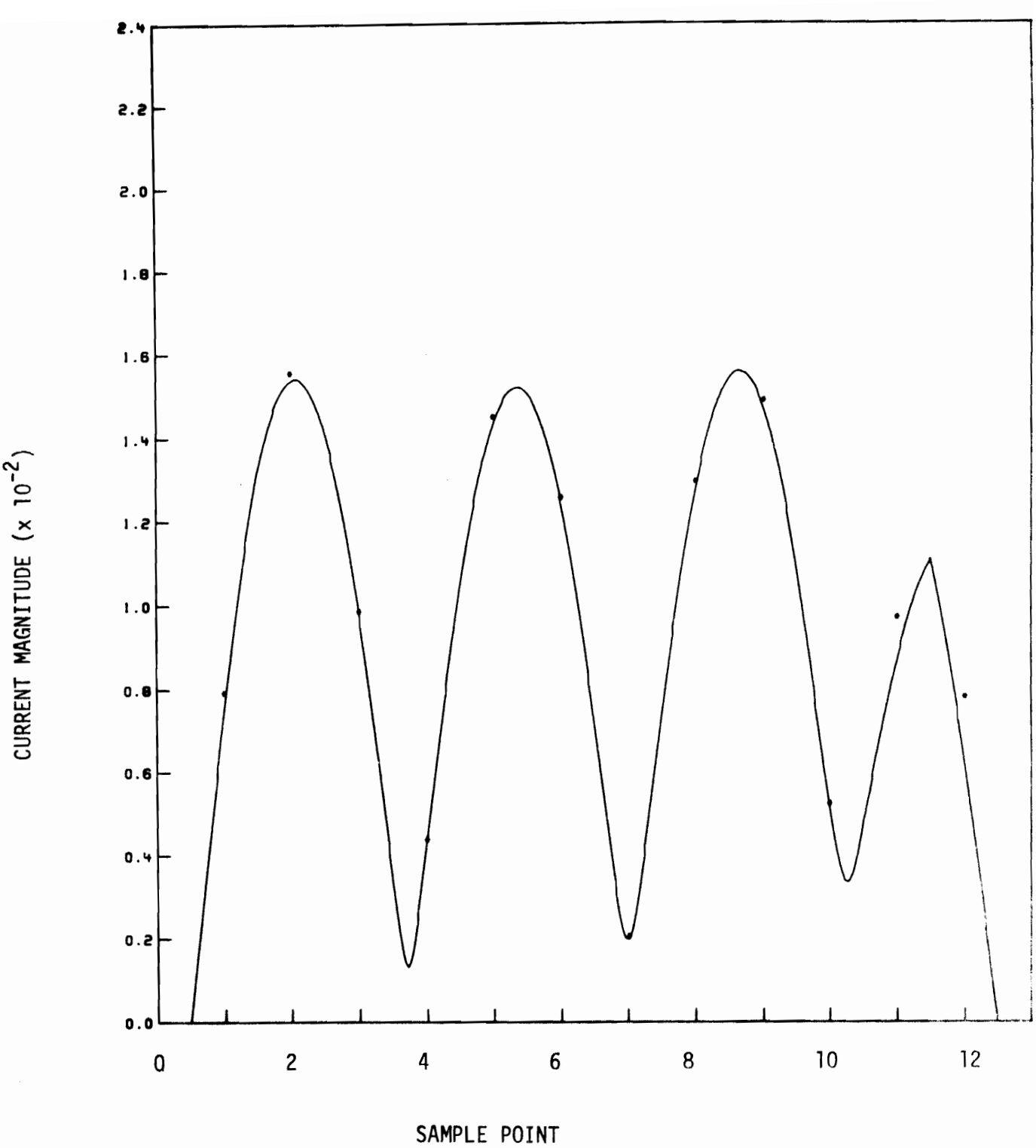

FIGURE 29. CURRENT MAGNITUDE vs SAMPLE POINT (LOCATION) FOR AN L WIRE WITH A 5X MULTIPLIER COMPUTED USING OSU WITH N_T = 12. FOR THE REFERENCE SOLUTION (*) N_R = 120

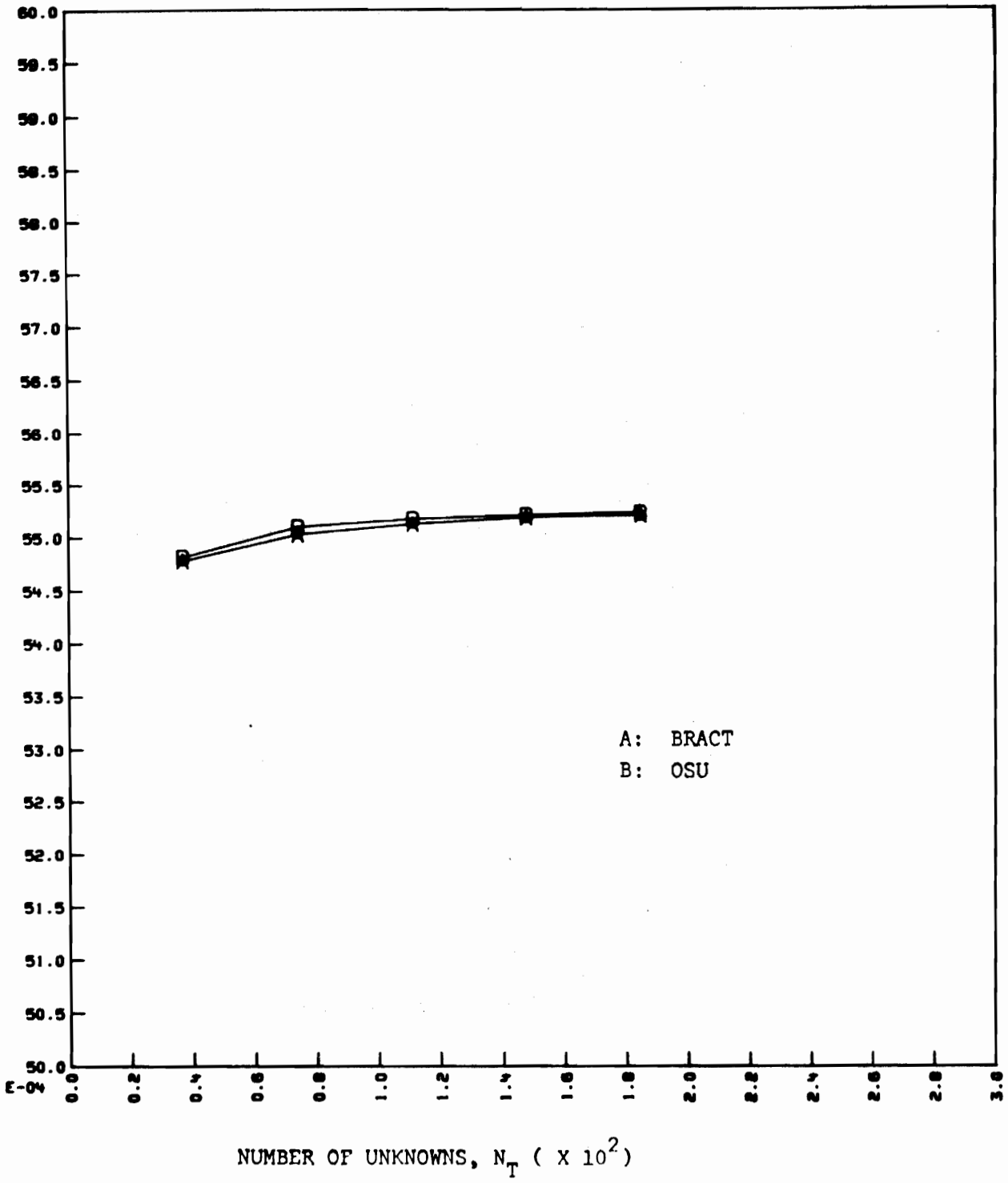

FIGURE 30: RMS CURRENT vs. N_T FOR A CROSSED WIRE WITH A 1X MULTIPLIER COMPUTED USING DIFFERENT PROGRAMS.

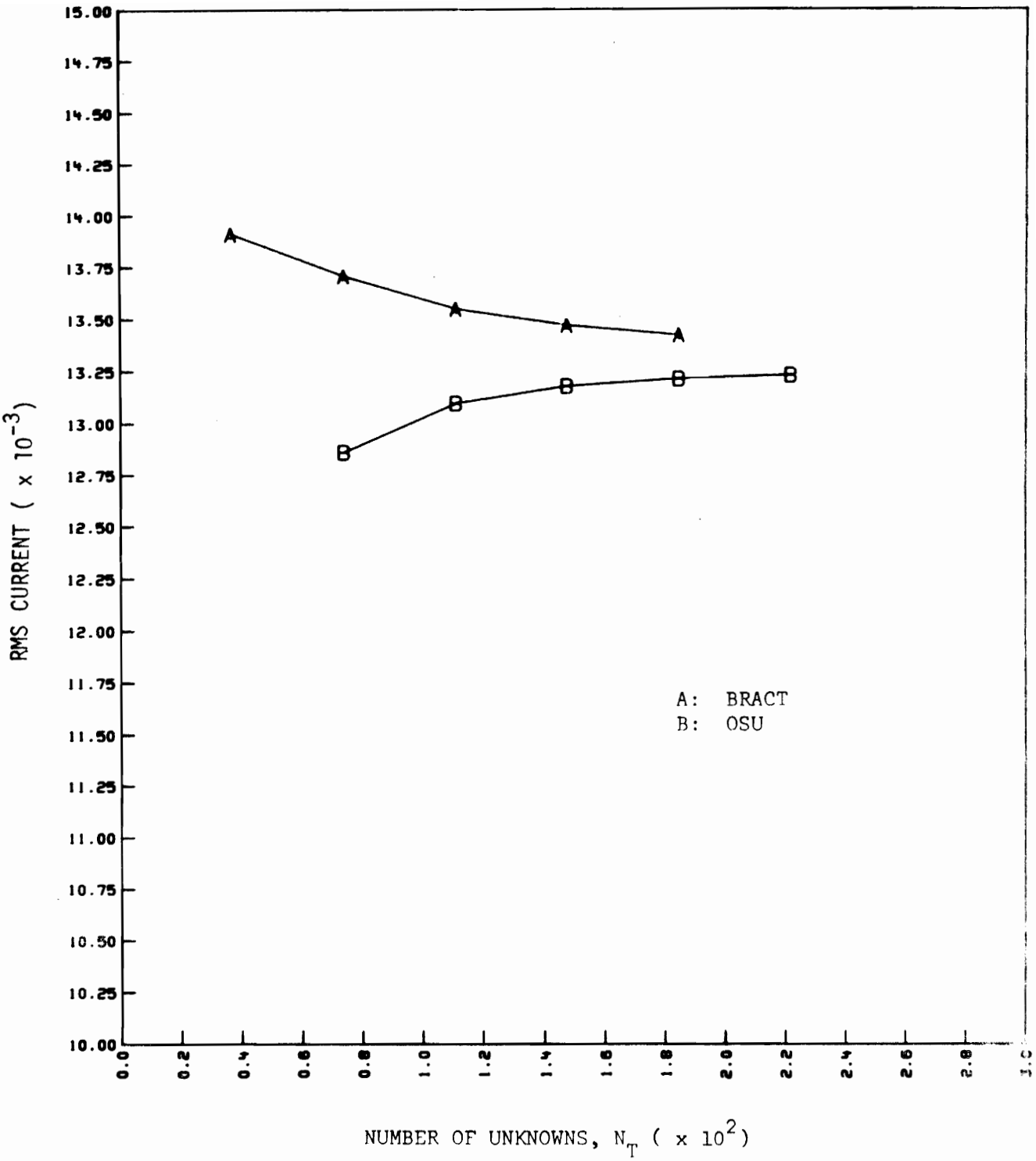

FIGURE 31: RMS CURRENT vs N_T FOR A CROSSED WIRE WITH A 10X MULTIPLIER USING DIFFERENT PROGRAMS.

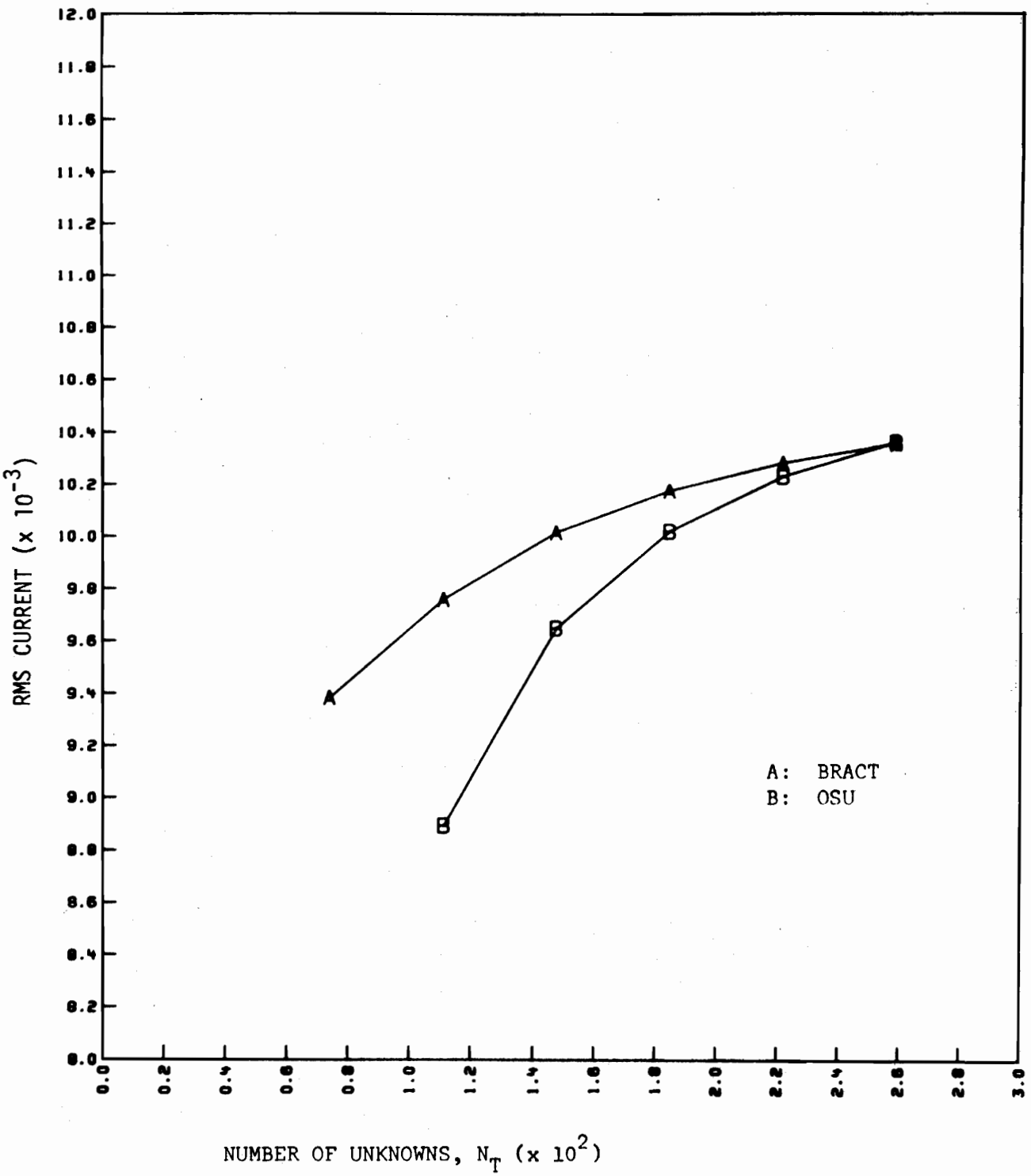

FIGURE 32: RMS CURRENT vs N_T FOR A CROSSED WIRE WITH A 35X MULTIPLIER COMPUTED USING DIFFERENT PROGRAMS.

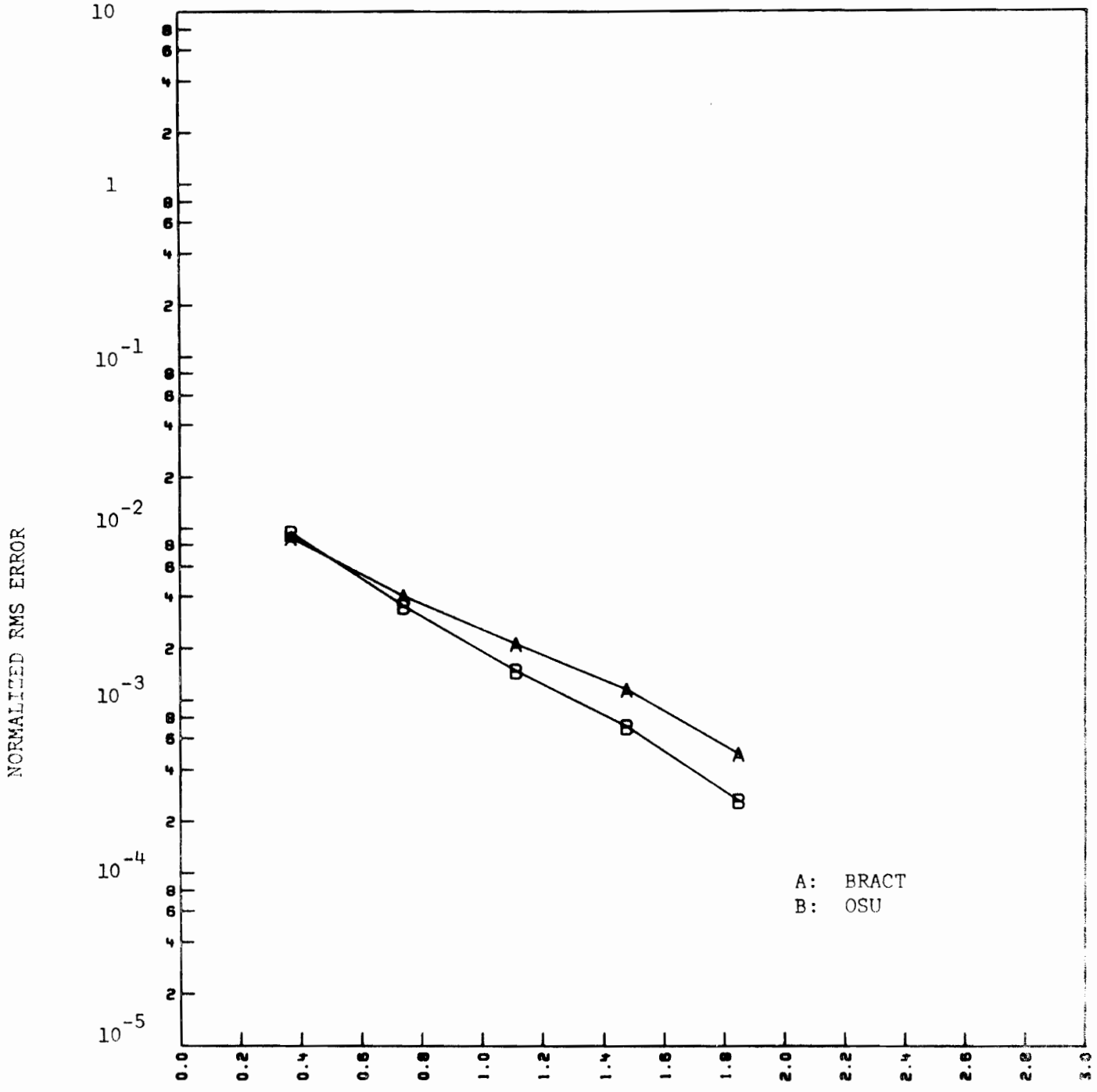

FIGURE 33: NORMALIZED RMS ERROR vs N_T FOR A CROSSED WIRE WITH A 1X MULTIPLIER RESULTING FROM DIFFERENT PROGRAMS

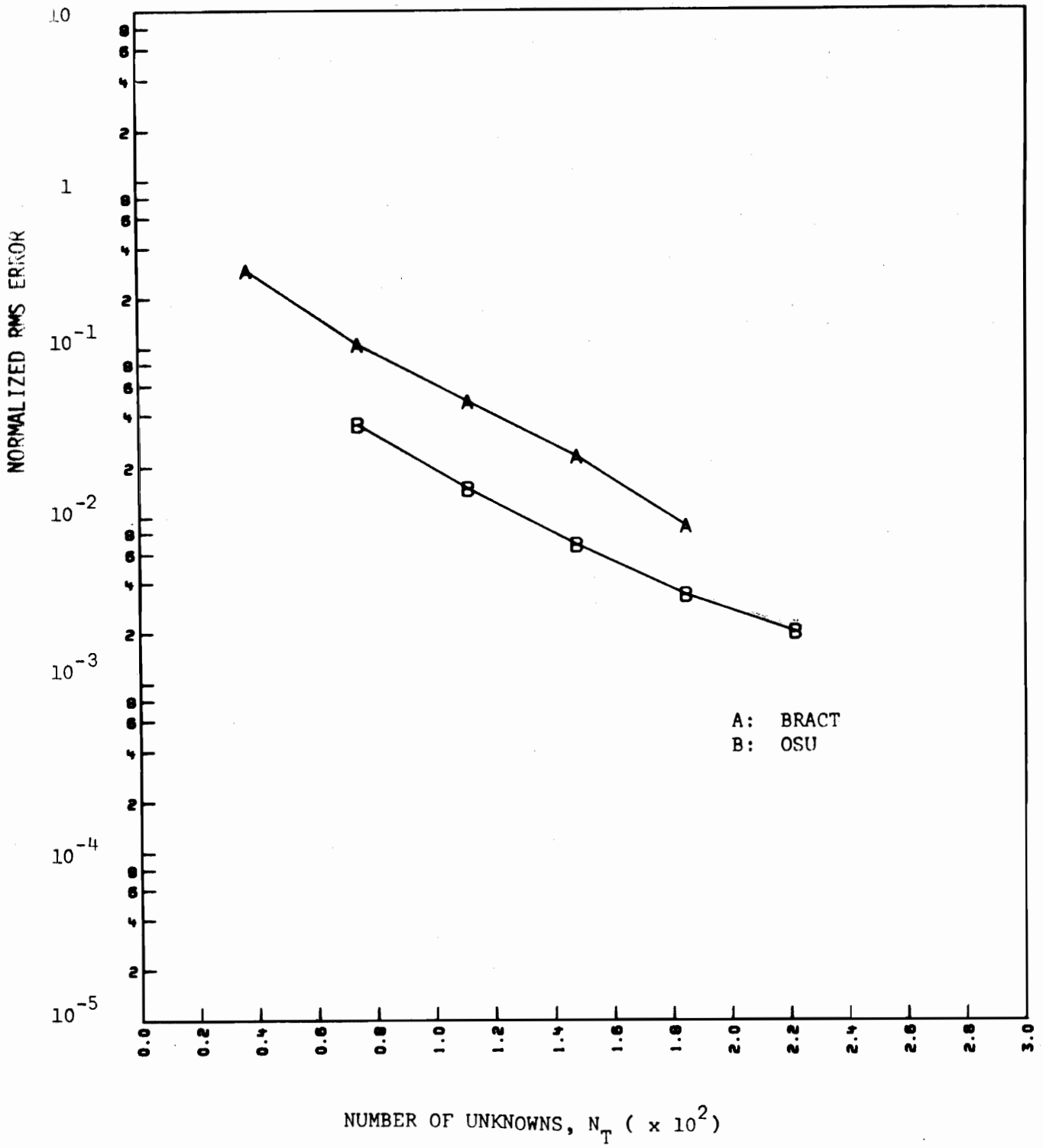

FIGURE 34: NORMALIZED RMS ERROR vs N_T FOR A CROSSED WIRE WITH A 10X MULTIPLIER RESULTING FROM DIFFERENT PROGRAMS

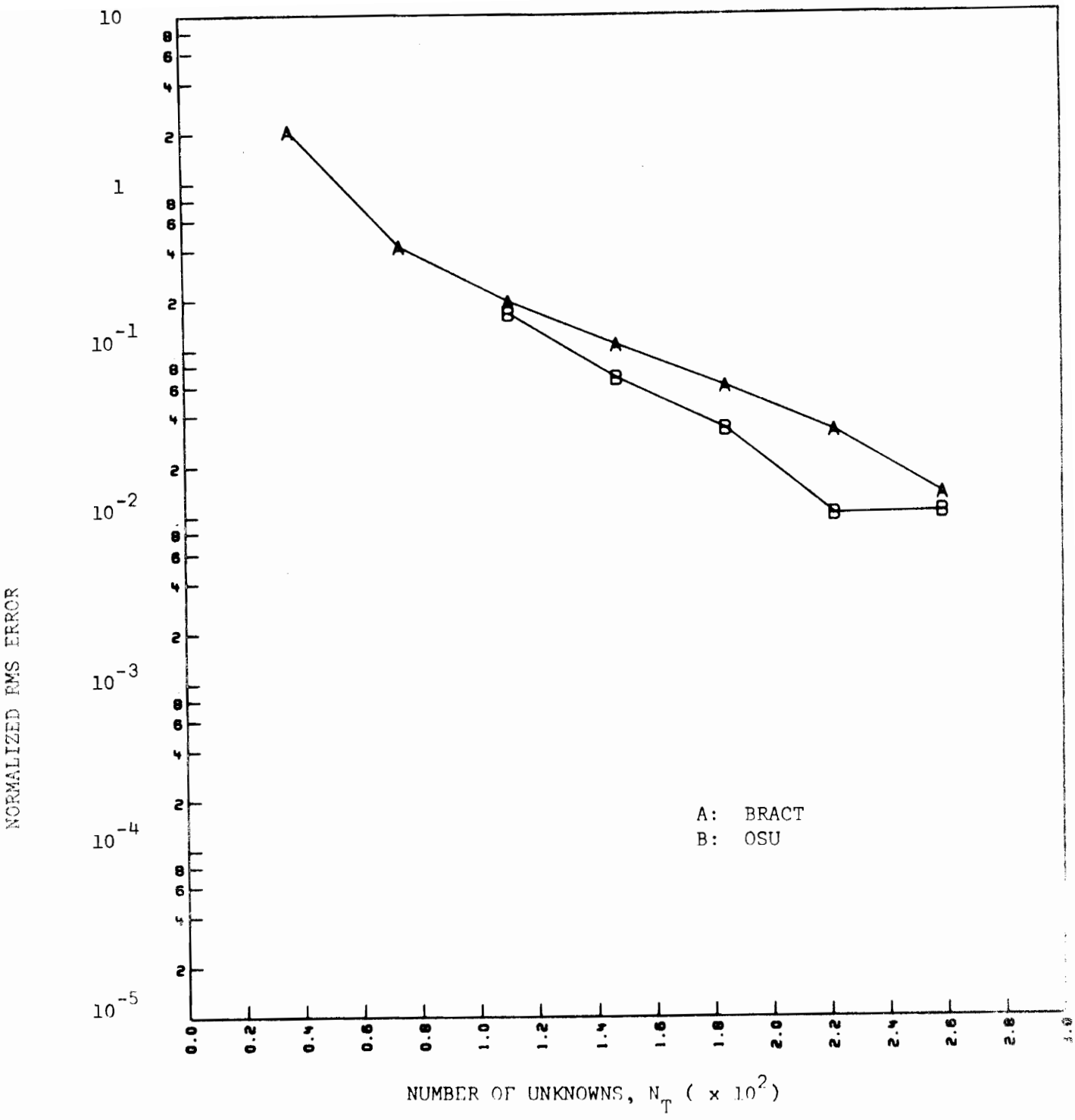

FIGURE 35: NORMALIZED RMS ERROR vs N_T FOR A CROSSED WIRE WITH A 35X MULTIPLIER RESULTING FROM DIFFERENT PROGRAMS

4) Computer Time Requirements

The typical computation time required is an important quantity in assessing the usefulness of a given program. To this end, an attempt was made to determine the time requirements of each program.

During the course of the numerical studies, average values of the coefficients A and B in the computer time expression

$$T(\text{sec}) = A\,N^2 + B\,N^3$$

where N is the total number of unknowns were determined. Using this form, one can identify that portion of the time which is characteristically associated with filling the coefficient matrix containing N^2 elements, and that portion associated with the matrix equation solution. Although other operations are performed in the program which might possess these behaviors, the ones above are certainly dominant.

Average values for the coefficients for several of the programs test evaluated using a CDC 7600 are given in the following table:

Program	A	B
OSU	3.5×10^{-4}	1.07×10^{-6}
SYR	2.6×10^{-4}	5.0×10^{-6}
BOEING	3.0×10^{-4}	5.36×10^{-6}
BRACT	4.2×10^{-4}	3.4×10^{-6}

As is evident from the table, the B coefficients are quite different. The reason for this is that some of the programs obtained a solution through an inversion procedure (SYR, BOEING) while the others did not obtain an inverse but merely solved the matrix equation. The B coefficient for OSU is also small because the square root method was used to solve the matrix equation for which the impedance matrix was necessarily symmetric. Naturally, the Boeing and BRACT programs could not use this technique because the impedance matrices in these programs are generally not symmetric. The SYR program does not explicitly make use of the matrix symmetry that arises in using Galerkin's method. In fact, due to numerical inaccuracies involved in calculating the entries, it is noted that the impedance matrix is not quite symmetric.

Figure 36 is a plot of the computation time varying as the square of the number of unknowns versus the number of unknowns. This time is referred to as fill time. The BRACT program, which uses an adaptive integration scheme guaranteeing a certain level of relative

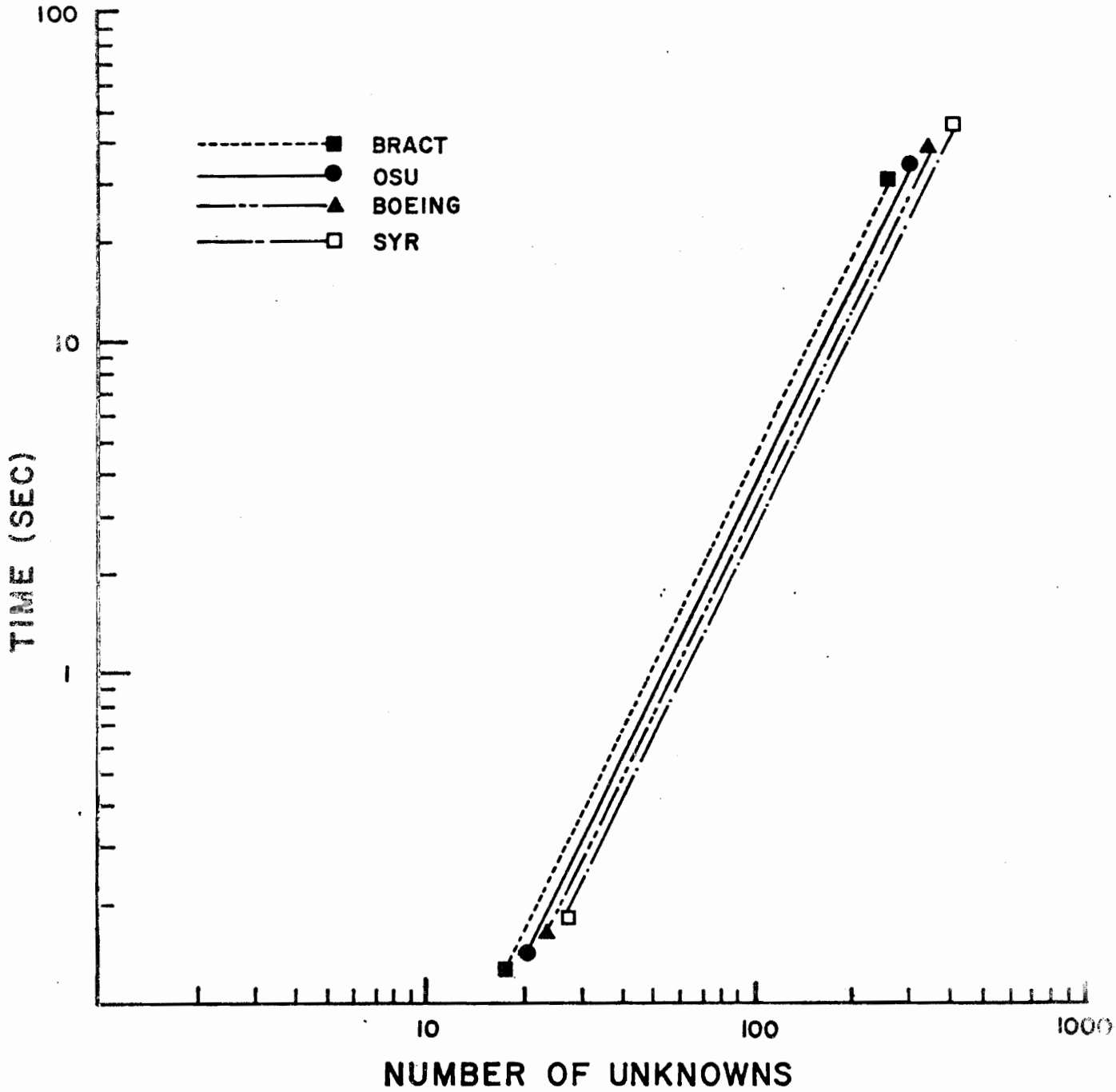

Figure 36 a: COMPUTER TIME PROPORTIONAL TO N^2 versus NUMBER OF UNKNOWNS

accuracy in the required integrations, is seen to be the slowest. Not only does this program use a very accurate numerical integration method, it must also evaluate six contributions for each entry in the impedance matrix (E_ϕ and E_ρ for sine, cosine, and constant portions of the segment current), a time consuming operation even though five of the six terms are evaluated analytically. On the other hand, the SYR program performs the required integration by using the approximation scheme shown in Figure 1, thereby allowing the indicated speed in the SYR program. The OSU program makes use of the analytical expressions for the fields due to the sinusoidal currents and then integrates the weighted results using either a numerical procedure or exponential integrals. This is also a time consuming operation as seen in the large A value in spite of the fact that only one half of the symmetric impedance matrix is filled.

It is beyond the scope of this effort to delve deeply into the fill schemes of the computer programs. Whether it is better to perform extremely accurate integrations and pay the time penalty or to perform cruder integrations for the sake of speed are interesting questions although somewhat task related.

Since the number of unknowns in a given computation affects both the solution accuracy and time requirement, it is useful to consider the behavior of normalized root mean square error with time. Figure 36b is a plot of normalized rms error versus time for a straight wire with 10X multiplier. The curves indicate the relative accuracy and efficiency with which each program can solve a given problem and in this particular case leads to the conclusion that OSU has a definite advantage. However, this conclusion cannot be drawn from similar plots for other cases since individual peculiarities in the codes and the likelihood that some programs are better suited to some problems and not others may change the relative positions of the curves. However, the overall consistency in the relative position of a particular curve can and does lead to a useful judgment.

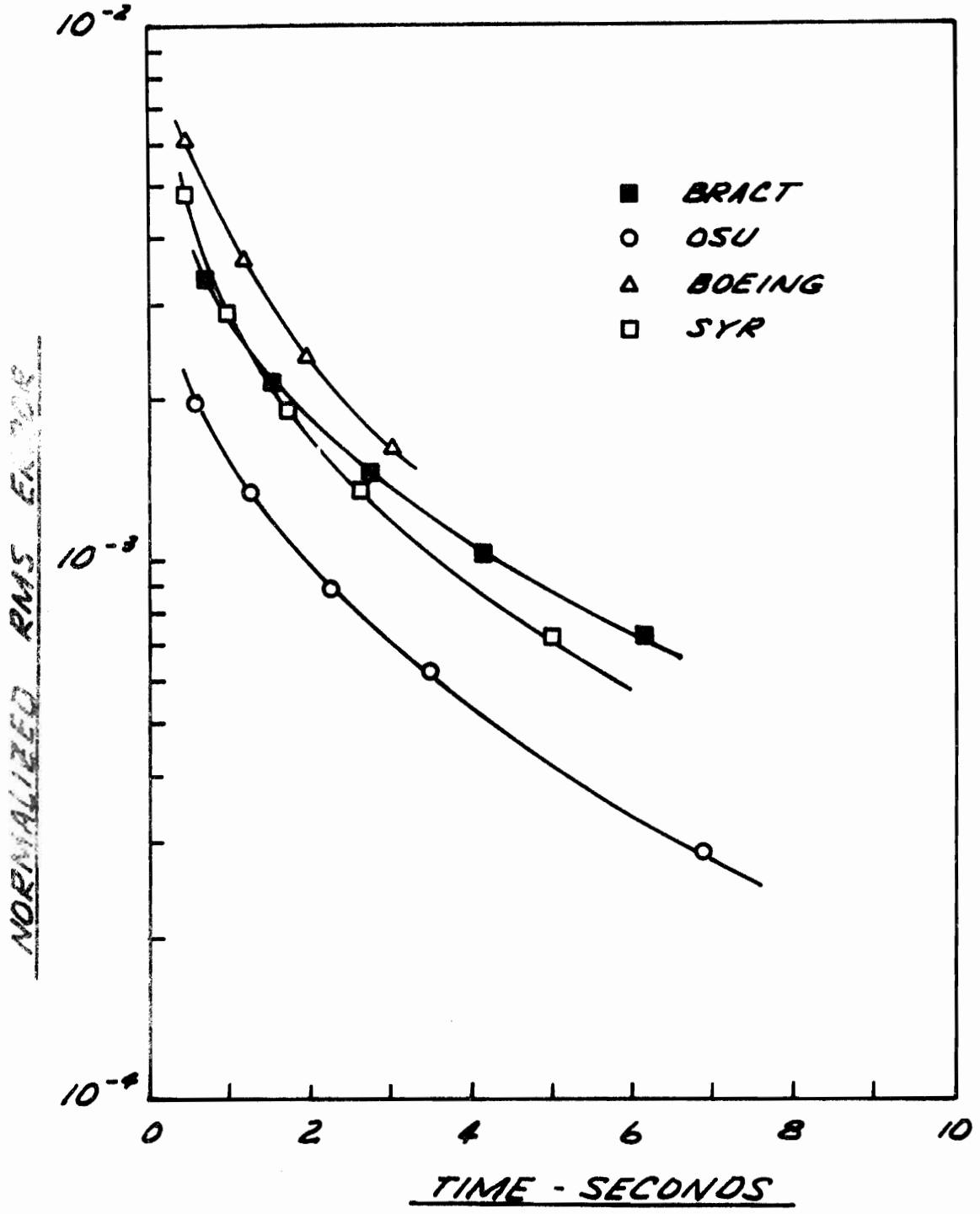

Figure 36b: NORMALIZED RMS ERROR vs. TIME FOR VARIOUS PROGRAMS.

VIII. Summary of Results and Recommendation

The results generated by the four computer programs

1) Collocation, sinusoidal interpolation, Pocklington (BRACT)
2) Collocation, pulses, Potential (Boeing)
3) Galerkin, piecewise linear, Potential (SYR)
4) Galerkin, piecewise sinusoidal, Pocklington (OSU)

have been carefully studied. Of prime usefulness have been summary results relating a scalar parameter obtained from a computed solution to the number of unknowns. The most widely used summary results, viz., the RMS current and the normalized RMS error have been used to estimate the overall quality of each computer program as well as to indicate possible deficiencies. These data were thus used as the key element with the indicated deficiencies subsequently studied in the source data, i.e., the actual current distributions. In essence then, the summary data relieved the evaluators of the burden of studying each individual piece of source data while at the same time allowing them the option of considering that data when deemed necessary.

One of the first important observations made during this study was that interpolation functions involving sinusoids were superior. As a result, later portions of the study were concentrated on programs using sinusoidal functions even though these functions generally increased the complexity of the programs. Hence, even though pulse and piecewise linear basis functions were simpler, their marked inferiority insofar as convergence rates were concerned led to their dismissal.

After delving into the investigation it became clear to the evaluators that as many questions were being uncovered as were being answered. For instance, the dismissal of the linear basis functions led to the termination of the consideration of the SYR program (Galerkin, piecewise linear, Potential). But a scheme using Galerkin's method, the Potential integral equation, and piecewise sinusoidal interpolation functions might be superior to the others tested.

Concerns of this type have plagued the investigators but due to time limitations the study had to be concentrated on the specific programs listed earlier, each program being treated as an entity unto itself with no significant attempt at modification.

The question of program simplicity was also continually in the minds of the evaluators. It was found that the simplest program (Boeing) could not however be considered to be of the quality of OSU or BRACT. The next more complicated program (SYR) could also not match the performance of OSU and BRACT with regard to convergence rates. Hence, based on these observations these two programs were excluded from serious

consideration at later stages in the investigation.

The OSU and BRACT programs exhibited a great deal of similarity in treating straight wire structures. However, a deficiency appeared in BRACT when the wire had a sharp bend as in the L wire case. The BRACT interpolation functions, which allow discontinuities in certain cases for the L wire. The deficiency in the BRACT program becomes even more pronounced when the currents near a multiple wire junction is considered. Since Kirchoff's current law is not, in general, satisfied at the junction, and since BRACT exhibited some difficulty at wire bends, the program could lead to unacceptable errors near junctions. On the other hand, the OSU program had a better performance record for these cases and possessed at worse a current slope discontinuity in the L wire and cross wire cases. That program leads to an inherent satisfaction of Kirchoff's current law by virtue of its junction treatment.

As a result of the preceeding observations, the evaluators have decided that among the programs tested (without any modifications) the OSU program was the most outstanding. However, certain qualifications are appended to this recommendation. For instance, the investigators fully anticipate the need for future modifications to some of the fundamental modules in the OSU program. These might be needed in order to allow the program to deal with thick wires or end caps. As in the case of a lossy ground interaction where Sommerfield integrals modify the kernel, the added complexities might enhance the desirability of a collocation solution over a Galerkin's formulation. The additional field evaluations and subsequent integration in the latter case could be burdensome. Hence, the evaluators are and will be studying methods of upgrading BRACT to the level of the OSU program in order to permit a choice between the Galerkin and collocation methods. At the present time, OSU is definitely superior.

IX. Related Topics

1. Time Domain Formulation - Application to Aircraft

Electromagnetic transient responses of bodies may be obtained through transformation of frequency domain characteristics, the singularity expansion method, or through solution of time dependent equations directly in the time domain. Until recently, however, few time domain calculations hav been performed for determining the electromagnetic characteristics of thin wire structures. In 1968, Bennett and Weeks presented time-domain solutions for several electromagnetic objects employing a time dependent integral equation based on the magnetic field. About the same time, Sayre and Harrington applied the thin wire approximation to a coupled set of equations based on the magnetic vector and electric scalar potentials and obtained results for the linear dipole and circular ring. Miller, et al. (1973) and Poggio, et al. (1973) applied the thin wire approximation to a time-dependent version of the frequency domain Pocklington electric field integral equation. While some aspects of their analysis is similar to the previously listed efforts, they included in addition a 9-point Lagrangian interpolation scheme which permitted efficient treatment of more complicated wire structures as demonstrated by the analysis of the zig-zag antenna.

Here, we consider the applications of the time domain formulation to calculate the current on aircraft when illuminated by EMP. The first step in assessing the EMP survivability/vulnerability of an aircraft system is to determine the electric current flowing on the outer skin of the aircraft when illuminated by EMP. With present state-of-the-art, however, it is not possible to calculate in detail these currents due to the extreme complexity of the aircraft surface geometry. Consequently, approximations are made of the surface geometry. The numerical solution begins by approximating the aircraft geometry by a set of cylinders, and subsequently calculating the currents of this set of cylinders.

The theory and the numerical approach used were presented in the latter two papers. A users manual, program listing, and sample output is given in Van Blaricum and Miller, (1972). This program is based on a moment method solution of the time dependent electric field integral equation

$$\hat{s}\cdot\bar{E}_{inc}(\bar{r},t) = \frac{\mu_o}{4\pi}\int_{C(\bar{r})}\left\{\frac{\hat{s}\cdot\hat{s}'}{R}\frac{\partial}{\partial t'}I(s',t') + C\frac{\hat{s}\cdot\bar{R}}{R^2}\frac{\partial}{\partial s'}I(s',t') - C^2\frac{\hat{s}\cdot\bar{R}}{R^3}q(s',t')\right\}ds' \qquad (63)$$

where $\bar{E}_{inc}(\bar{r},t)$ is the incident field at observation point $\bar{r}$ at time t, $\hat{s}$ and $\hat{s}'$ are unit vectors parallel to $C(\bar{r})$ at $\bar{r}$ and $\bar{r}'$, c is the velocity of light, μ_o the permeability of free space, $I(s',t')$ and $q(s',t')$ are the current and charge at source point s', retarded time $t' = (t - R/C)$ where $R = |\bar{r}-\bar{r}'|$, and $C(\bar{r})$ is the structure contour. The moment method solution proceeds by approximating the object by a set of straight wire segments and using a subsectional bases function expression in space and time in the form of a 9-point Lagrangian interpolation scheme to describe the current on each segment. The integral equation is reduced to a matrix form

$$\underline{E}_{sca} + \underline{E}_{inc} = \underline{\underline{Z}}\,\underline{I} \tag{64}$$

where $\underline{E}_{inc}$ is the value of $\bar{E}_{inc}(\bar{r}_o,t_o)\cdot\hat{s}_o$ at time t_o and for $\bar{r}_o$ a wire radius away from $C(\bar{r})$ at the observation point, and where $\underline{E}_{sca}$ is the electric field tangent to the wire segment at $\bar{r} = \bar{r}_o$ and $t = t_o$, due to earlier charges and currents.

The solution is obtained by finding $\underline{\underline{Y}} = \underline{\underline{Z}}^{-1}$ once (since $\underline{\underline{Z}}$ is independent of time) and then calculating $\underline{I}$ by solving (64) sequentially at each time step. As a consequence of this time stepping procedure, the computation time is controlled mainly by the number of time steps desired in the solution for a given number of segments. Once the currents are obtained, other aspects of the electromagnetic behavior of the structure may be found. The radiated far fields may be computed, thus providing radar cross-section. Near fields may also be computed for use in coupling and interaction studies.

For wide-band calculations, this time-domain method has several advantages over more commonly used frequency-domain solutions. In general, the time-domain method is much more efficient than frequency-domain methods for obtaining the transient behavior for a given excitation. Further, non-linear loading is more tractable in this time-domain formulation which permits evaluation of the transient behavior of devices such as a spark gap attached to an antenna. Finally, the dynamic electromagnetic behavior of the structure is generated directly in the time domain which permits the natural development of the response to be followed and allows ready identification of peak currents and structure resonances.

A typical result is shown in Figures 37 and 38. For this example, a set of 0.8m diameter cylinders were arranged to approximate the geometry of a 747 aircraft. The EMP wave used here is a 4 term exponential with a rise time of 20 nsec, zero crossing at 1.5 usec and with a peak field strength of 5×10^4 V/m. The EMP wave arrives from the front and left of the aircraft, the angle away from nose-on incidence was chosen so that the entire left wing was illuminated simultaneously, and the electric field of the EMP wave was chosen parallel to the left wing. Figure 37 shows the axial current on the fuselage immediately behind the wings, and Figure 38 plots the magnitude of the current at various positions along the aircraft at select times. These currents are plotted perpendicular to the aircraft, and are shown in an isometric view taken from behind and above the aircraft.

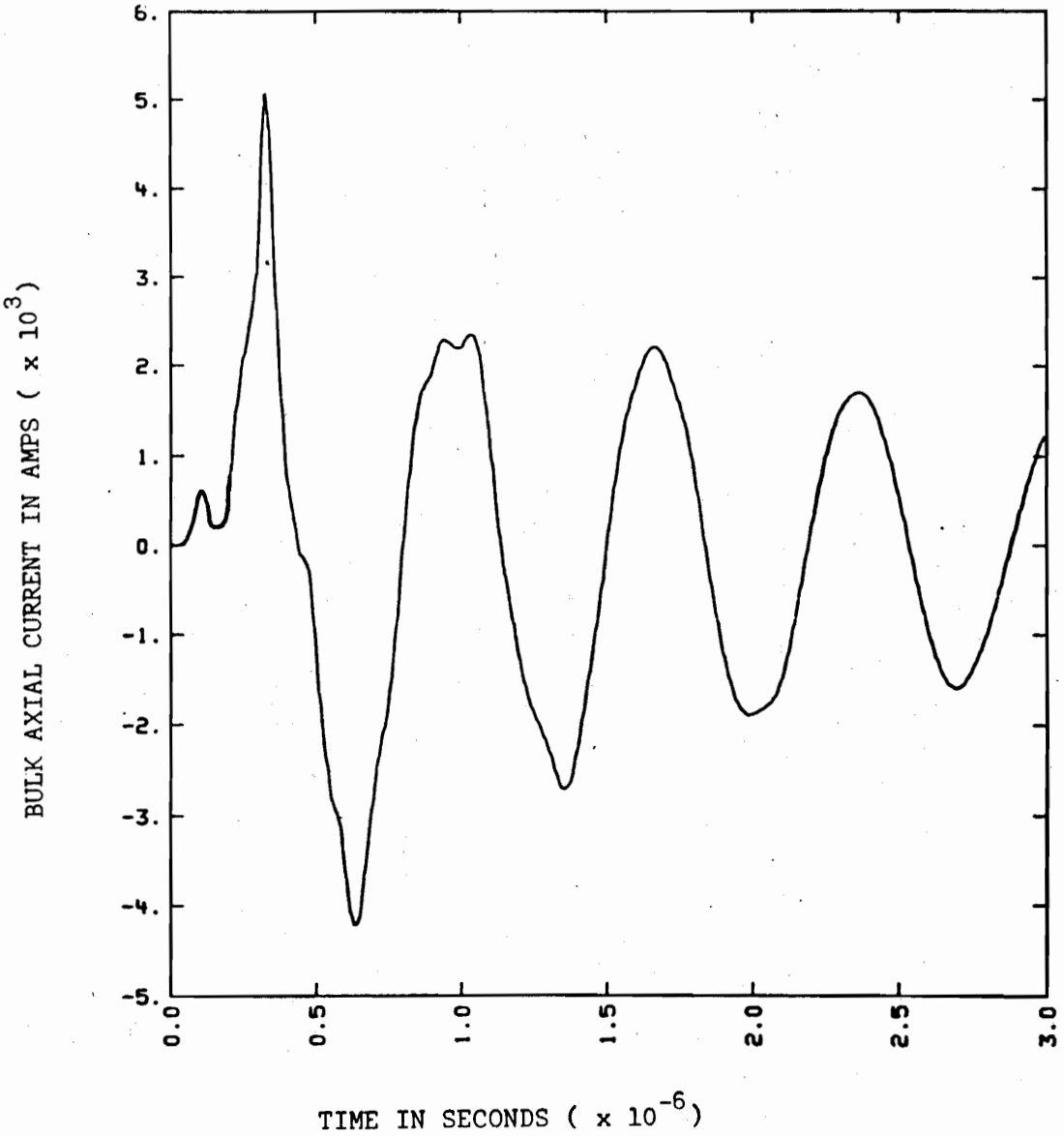

FIGURE 37: CURRENT ON FUSELAGE BEHIND WINGS OF A 747 AIRCRAFT.

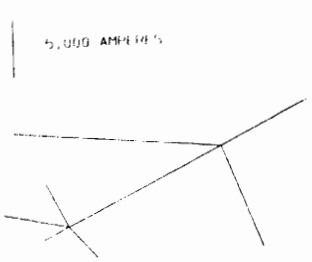

TIME = 0.
747 - EMP INCIDENT - 90 34 90

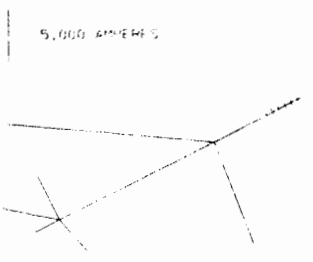

TIME = 4.000E-08
747 - EMP INCIDENT - 90 34 90

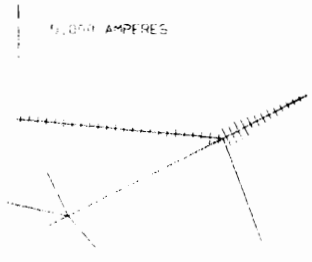

TIME = 8.000E-08
747 - EMP INCIDENT - 90 34 90

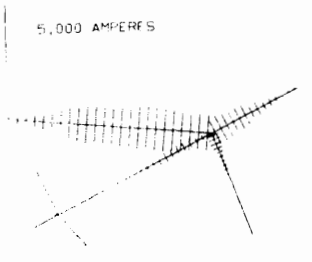

TIME = 1.200E-07
747 - EMP INCIDENT - 90 34 90

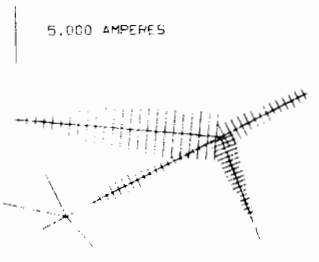

TIME = 1.600E-07
747 - EMP INCIDENT - 90 34 90

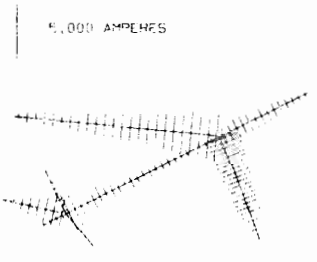

TIME = 2.000E-07
747 - EMP INCIDENT - 90 34 90

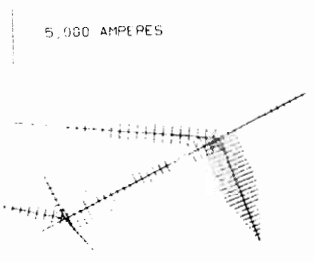

TIME = 2.400E-07
747 - EMP INCIDENT - 90 34 90

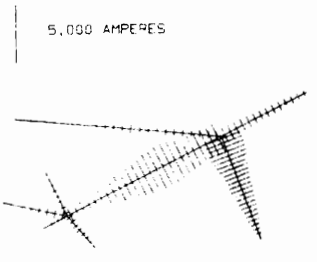

TIME = 2.800E-07
747 - EMP INCIDENT - 90 34 90

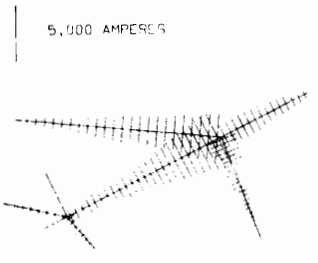

TIME = 3.200E-07
747 - EMP INCIDENT - 90 34 90

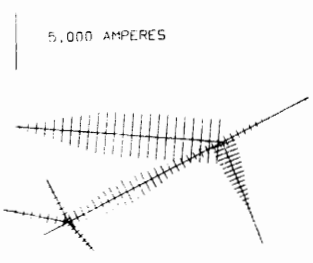

TIME = 4.000E-07
747 - EMP INCIDENT - 90 34 90

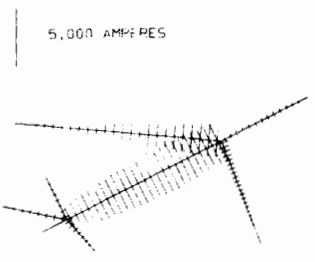

TIME = 6.000E-07
747 - EMP INCIDENT - 90 34 90

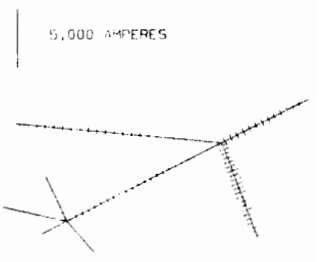

TIME = 8.000E-07
747 - EMP INCIDENT - 90 34 90

Figure 38 Development of current on a 747 aircraft. (t = 0 is the time just prior to the instant that the wave illuminates any portion of the aircraft.)

2. Numerical Study of Segmentation and Junction Effects

Some of the junction treatments discussed above have been applied to a simple structure whose segmentation was systematically varied to test their capability to handle segment length variations at or near a junction. Our interest in this particular aspect of the junction treatment stems from experience with the MB Associates approach which did appear to produce incorrect results primarily when unequal length junction segments were employed. As demonstrated above, that particular junction approach can be incorrect even when all segments at the junction have the source length. In spite of that, it is useful to examine the sensitivity of computed results to this particular factor.

i) V-Dipole Antenna

Results obtained for vee-dipole antenna study are shown in Figures 39 and 40 and Table 2. The data summarized in the table are for the antenna input properties at 100 kHz, a frequency slightly less than the resonance frequency, and include both admittance and impedance values. Plots of the impedance variation in the vicinity of the resonance are shown in Figures 39 and 40. Again, generally good agreement is exhibited by these various methods. It should be noted that in addition to the programs mentioned above, data obtained for the vee-dipole problem from a time-domain calculation is also shown. It too agrees well with the other calculations. Generally speaking, the divergence of the numerical results for input impedance is less than ±20%, indicating the degree of reliability which these numerical procedures apparently possess.

The effect of varying the structure numerical description in such a way as to determine the effects of unequal segment lengths at the vee-junction are shown in Figure 41. There results for the input reactance as a function of the number of current samples on the center of the antenna are shown relative to the nominal configuration case, where all segments which meet at the multiple junction are equal (or nearly so). The data obtained from the MK-I program exhibits a considerable degree of variation as the junction geometry varied, as does also that computed by

*All vee-dipole results presented here except those labeled Boeing and Arens were obtained at least partially from codes run on LLL computers. The Boeing data was furnished through the courtesy of Mr. Walter Curtis of Boeing, and the Arens data through the courtesy of Mr. Virgil Arens of Arens Applied Electromagnetics, Gaithersburg, MD. Regarding the Arens results on Figure 41, Mr. Arens feels the reactance variation with M may be due to the use of too short segments. Some of the OSU data was kindly supplied by Prof. Jack Richmond of Ohio State University, and some of the Syracuse data by Prof. Bradley Strait of Syracuse University.

TABLE 2

V-DIPOLE RESULTS AT 100 kHz

		BRACT							TIME
		MK I	MK I'	MK III	SYRACUSE	OHIO STATE	BOEING	ARENS	DOMAIN
RESISTANCE	(OHMS)	36.7	40.1	33.4	38.5	38.9	39.1	36.0	40.8
REACTANCE		-22.7	-38.0	-38.3	-41.9	-38.6	-40.9	-28.1	-47.6
CONDUCTANCE	(MILLIMHOS)	19.7	13.1	12.9	11.9	13.0	12.2	17.3	10.4
SUSCEPTANCE		12.2	12.5	14.8	12.9	12.9	12.8	13.5	12.1

MK I' is identical to MK I except the tangential field is integrated to define the driving voltage.

MK III is BRACT with the charge redistribution (Boeing) junction treatment.

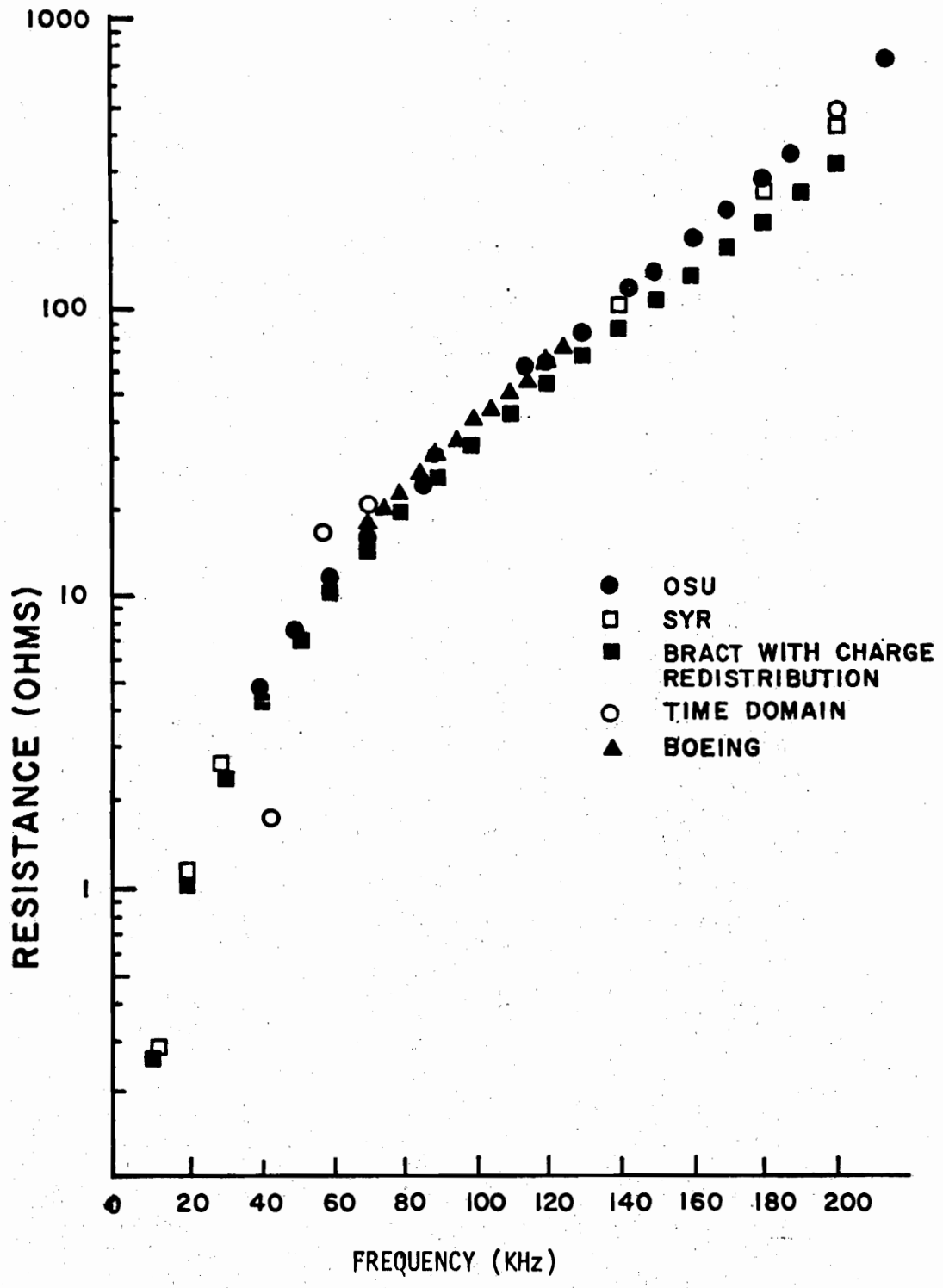

Figure 39 Resistance vs. Frequency for a V Dipole Antenna (see Figure 41) as Computed Using Different Programs

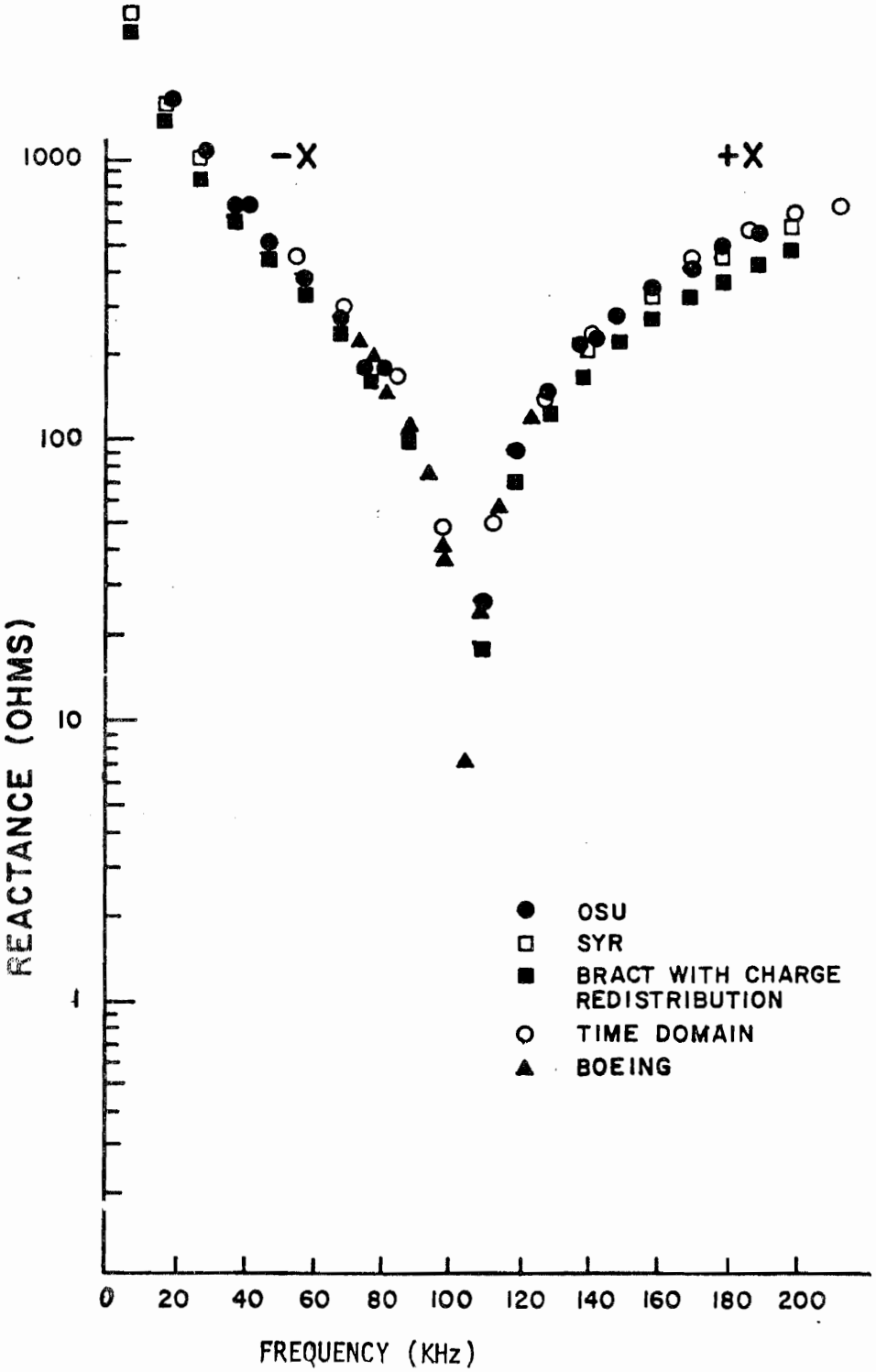

Figure 40 Reactance vs. Frequency for a V Dipole Antenna (see Figure 41) as Computed Using Different Programs

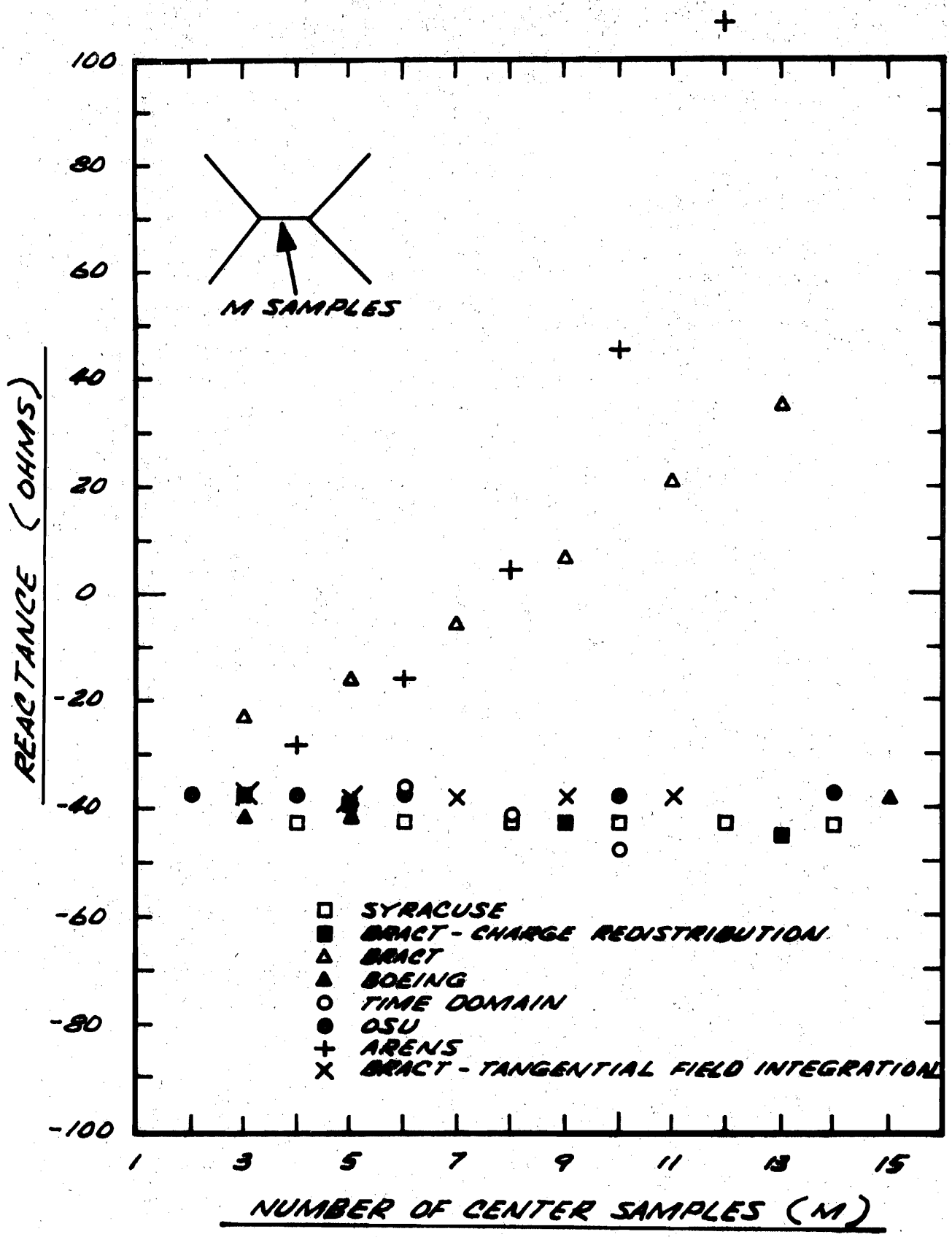

FIGURE 41. REACTANCE vs. NUMBER OF CENTER SAMPLES FOR A V-DIPOLE ANTENNA AS COMPUTED USING DIFFERENT PROGRAMS.

Arens(+).However, the other results are stable with little sensitivity to the structure geometry. It should be noted that the MK I results can be shown to remain stable as well if the input admittance is redefined in terms of the current at the antenna feed point divided by the integral of the tangential electric field along the antenna in the vicinity of the source (the MK I' results).

Somewhat unexpectedly, the scattering results also were found to be sensitive to the junction treatment. Computed results for the transfer admittance of the V-dipole at 100 kHz are shown in Table 3. We observe that the MK I junction treatment yields transfer admittance which are also dependent upon the junction segmentation. This is not true of the other procedures used.

ii) Aircraft Stick-Model Calculations

The comparisons presented above are useful in determining the relative merits of the different computer codes. They are limited however, to test cases which do not very closely resemble the actual aircraft geometry of immediate concern. Even the crossed wire model, which may be viewed as a crude attempt to model an aircraft, is not as accurate in this sense as one might reasonably expect of computer codes having the flexibility and generality of those considered. In order to demonstrate the application of these codes to the aircraft problem, we present some comparative results in this section for a stick model of the 747 using the model parameters given by Boeing (1972).

a) Frequency Domain Results

The 747 numerical model has the dimensions shown on Figure 42. While details of the specific segmentation used for the various codes are slightly different, they involved on the order of unknowns.

Calculated current distributions from the Boeing, Syracuse, and MBA codes are shown in Figures 43 and 44 for the excitation geometry indicated and for frequencies of 1.8 and 6.0 MHz. Note that the current magnitudes, plotted as lines perpendicular to the structure segment to which they apply, are not spatially coincident for all codes due to the slight differences in their segmentation as mentioned above. The agreement between the codes used is seen to be quite good, within 10% or so referred to the maximum values.

TABLE 3

MAGNITUDE OF TRANSFER ADMITTANCE (millimhos)

# Segments on Center	GIANT	MK IIIA	BRACT	OSU
3	11.5	11.4	14.7	11.5
5	11.7	11.6	15.9	11.5
9	11.6	11.5	16.8	11.5
13	11.5	11.4	11.0	

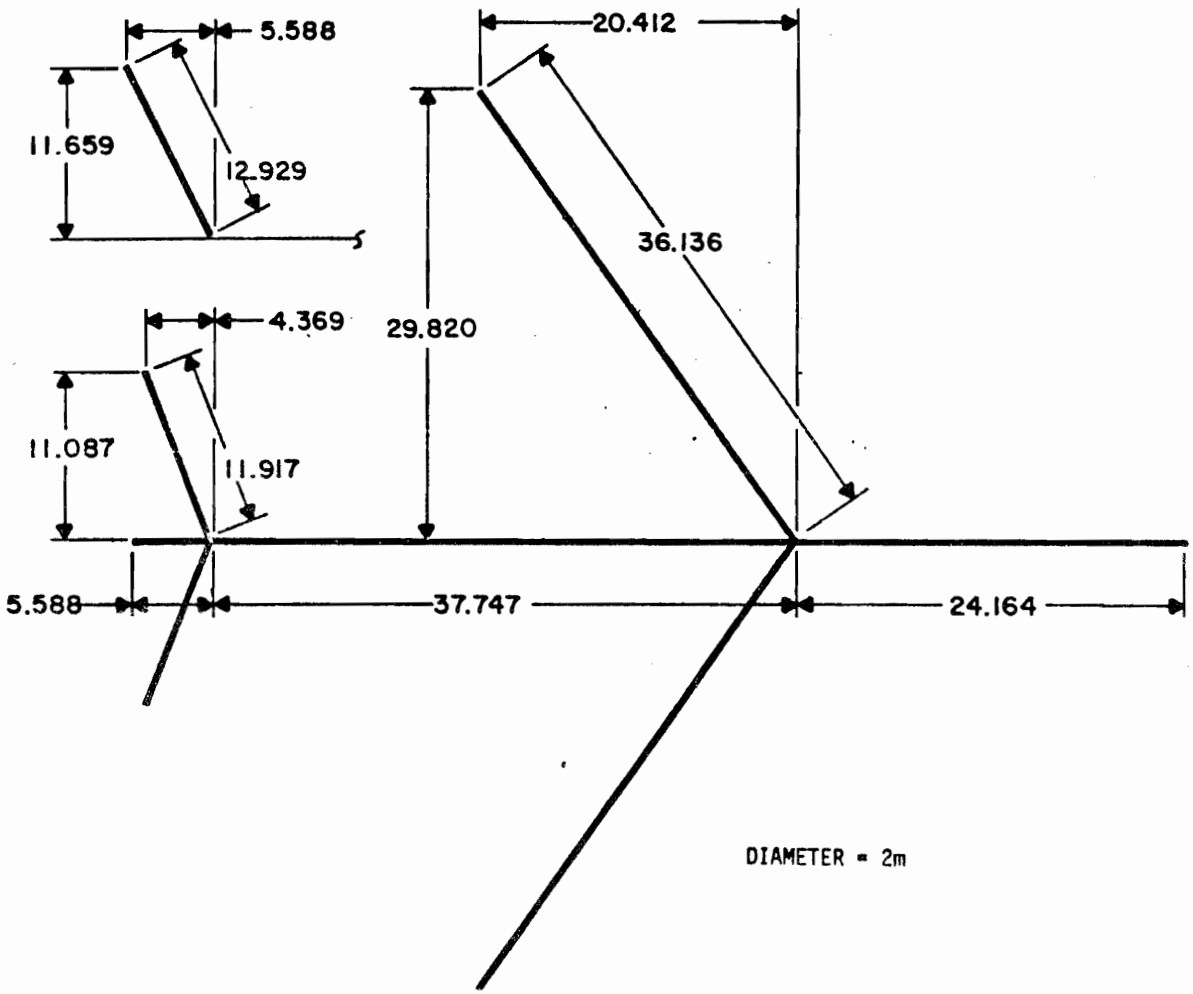

FIGURE 42 DIMENSIONS IN METERS USED FOR 747 MODEL

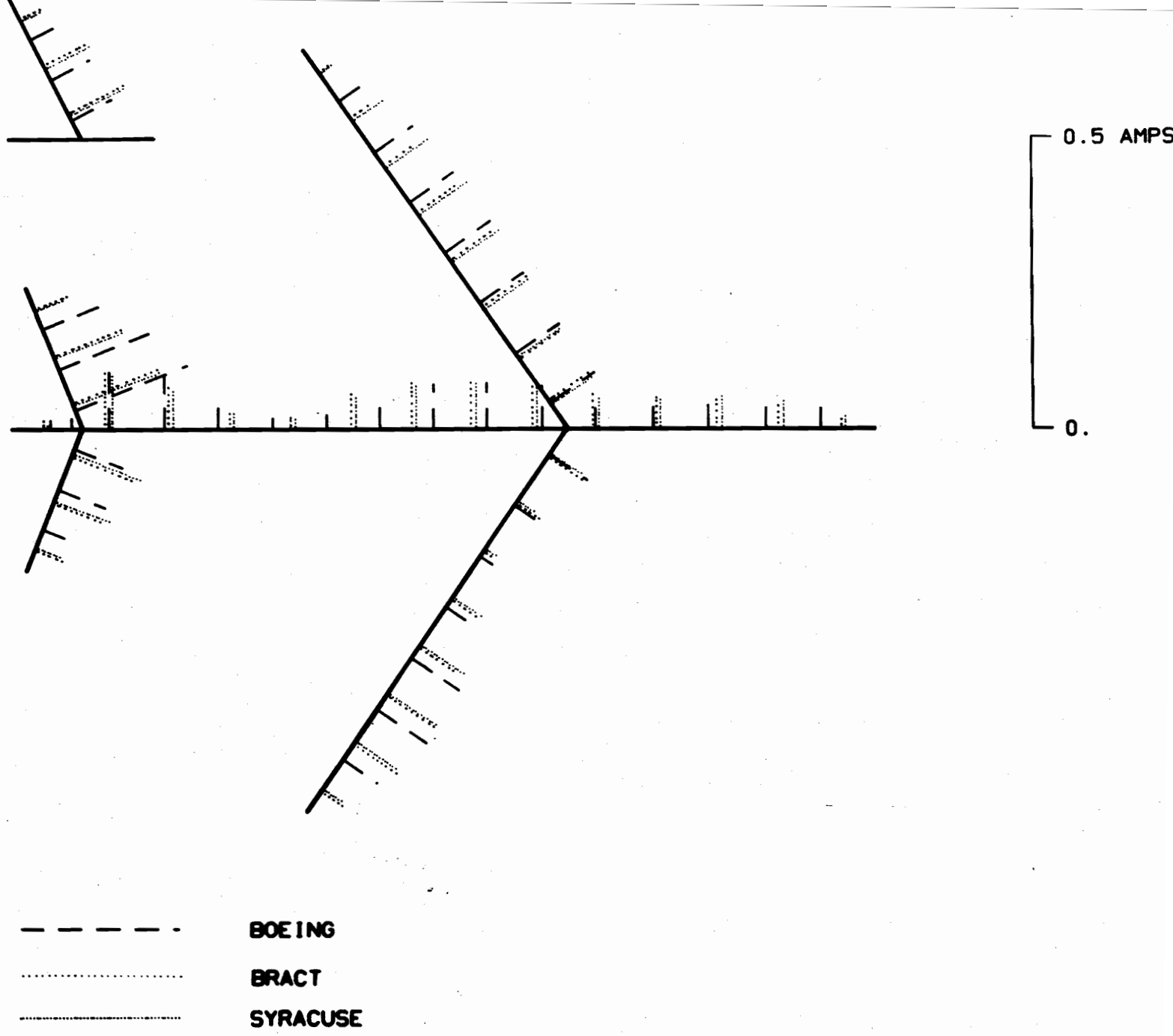

Figure 42. Calculated Current Distributions at 1.8 MHz on Stick Model of Boeing 747 Using Different Programs.

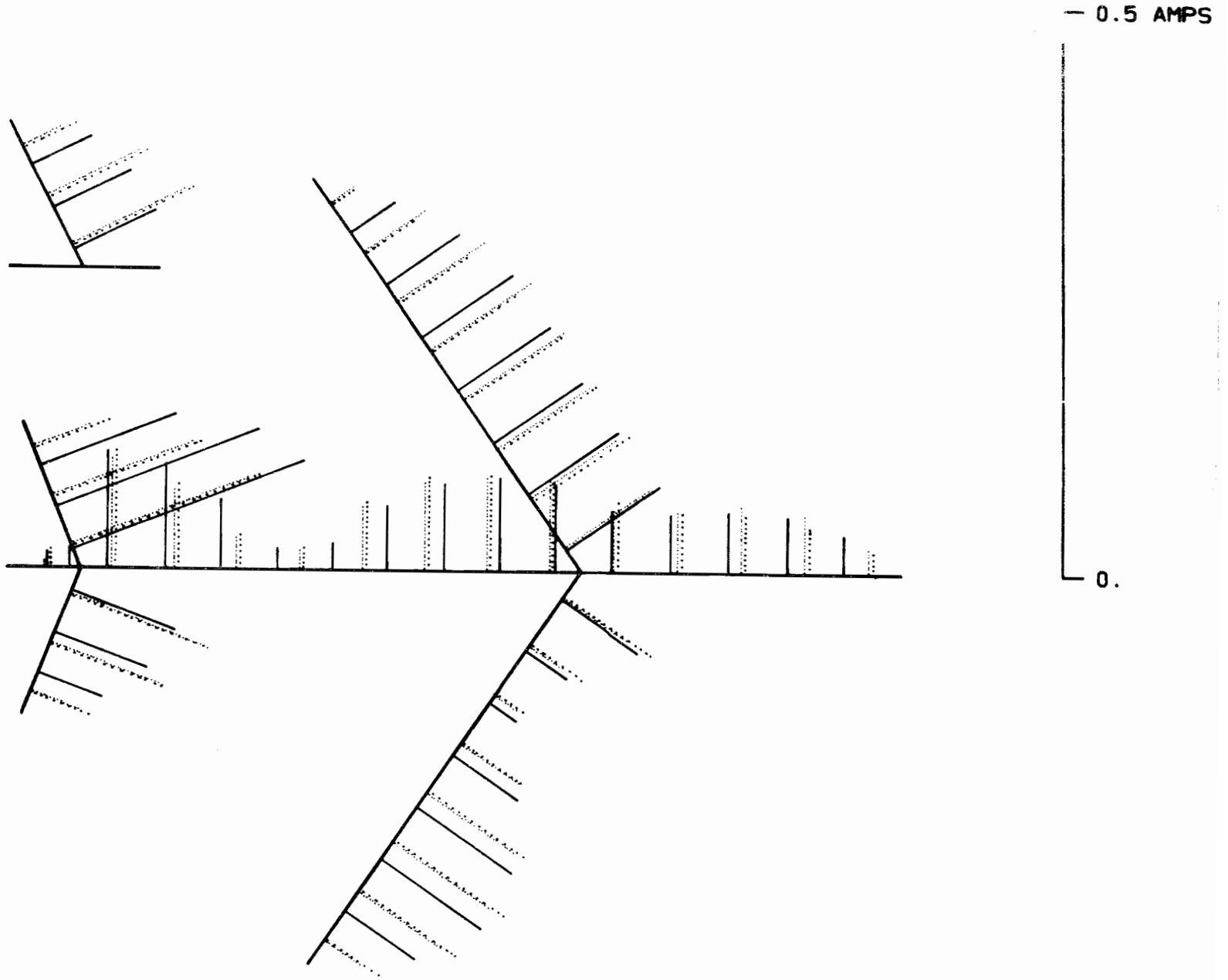

Figure 43. Calculated Current Distributions at 6.0 MHz on Stick Model of Boeing 747 Using Different Programs.

3. Recommendations for Future Work

Questions Originating During the Reported Effort

During the course of this study several questions arose which need clarification. A number of these questions result from detailed consideration of the junction problem. The suggested areas of investigation are:

I) study of local phenomena at wire intersections

i) detailed local current distribution
ii) validity of assumptions in thin wire approximation
iii) effects of radii discontinuities
iv) effects of sharp angle bends

II) study of end effects

i) end cap corrections
ii) effects of different end cap shapes

Another area requiring investigation is the extension of the techniques described in this report to cylinders of larger radii. This might involve studies into the probable effects of introducing careful surface integrations in the thin wire code, the use of higher order modes of circumferential variation than the constant mode of the thin wire approximation, and/or the extension of the thin wire approximation. The study should also include investigations of non-circular cylinders.

Previously Recognized Extensions

The above studies have been suggested during the present, ongoing effort. It is also felt that studies of wire grid modeling, and solid surface modeling using their respective integral equations are required. Also, the implementation of necessary high frequency techniques is deemed advantageous.

In order to validate many of the results reported herein (and to be generated in the future), an experimental investigation is needed. This effort should involve the determination of the surface current distribution (or bulk current distribution) on straight wires, L wires, crossed wires, wire models of the Boeing 747, and on a scale model of the Boeing 747. Naturally, these experiments should be performed in the frequency regime where the thin wire approximation is valid and perhaps slightly beyond where cross sectional diameters are an appreciable portion of the wavelength.

The prinicpal investigators recognize that the OSU program employing Galerkin's method, piecewise sinusoids, and Pocklington's integral equation is superior to BRACT (collocation, sinusoidal interpolation, Pocklington) in its present form. However, since BRACT does not require a separate weight integral to be performed, and since modifications and extensions as proposed previously would further complicate field expressions, it is felt that the circumvention of the weight integral may be important. To this end, it is recommended that

some of the shortcomings of BRACT be studied so that the program can be upgraded to perhaps provide the accuracy and efficiency of the OSU program.

4. Assumptions, Approximations, and Recommendations for Wire Computer Program Users

Mathematical Model

1. Perfect conductivity.
2. Wire sections long compared to diameter ($\frac{L}{D} \geq 10$).
3. Wire circumference less than 0.5λ.
4. Circumferential current negligible.
5. No circumferential variation of axial current.
6. Thin wire approximation valid.

Physical Model

1. Model is a piecewise linear representation (e.g., polygon for circle).
2. An equivalent circular cylinder is used to model non-circular cross-sections.

Computer Model

1. Segment length (Δ) : $\Delta/\lambda \leq 1/6$
2. Segment length (Δ) : $\Delta/D \geq 3$
3. Segment length (Δ) relationship to total structure length is structure dependent.
4. Avoid abrupt diameter changes.
5. Avoid abrupt changes in segment length (not too restrictive except perhaps at junctions).
6. Develop wire model to resemble physical body as much as practicable.

Validation of Results

1. As an initial step, check a program against test results, e.g., those in this report.
2. Check reciprocity.
3. Check near fields at several points.
4. Check smoothness of results.
5. Check continuity of current at junctions.
6. Check convergence (run for several values of N).
7. Run two different programs for same problem, if possible.
8. Check for non-physical oscillations near wire ends or bends.

Troubleshooting

1. Check geometry definition - consistency.
2. Check excitation definition.
3. Check code dimension statements.
   - word size
   - routine functions
   - heirarchy of declarations
   - complex functions
   - variable initialization

Appendix A - Junction Treatments and Related Topics

Introduction

Brief consideration has been devoted to the multiple junction problem, i.e., the treatment of intersections of more than two wires. Left unanswered were questions concerning accuracy and adaptability.

One of the first and most fundamental questions associated with multiple wire junctions is whether the thin wire approximation, with its attendant assumptions regarding negligible circumferential currents and circumferential invariance of axial current density, is valid near a junction. Clearly the assumptions are quite well adapted to thin wires when interactions with neighboring conducting elements are very weak or almost symmetrical with respect to location on the wire cross section. For example, a straight wire or a straight wire perpendicular to a conducting plane satisfied the symmetry conditions. However, an intersection of two wires such that the union is not a straight line certainly destroys the symmetry as would intersections of more than two wires. The question that must be asked is whether the assumptions relating to the thin wire approximation can lead to erroneous results when it is known that the current density does not possess the required characteristics. At present there does not seem to be a definitive answer to this question. Nonetheless, one might infer from physical reasoning that although an overall solution might be quite adequate, the local behavior near junctions might be suspect. Indeed, the fields very near junctions may not be reliable due to the non-uniform distribution of current density imposed by the non-symmetrical nature of the junction. Further investigation of phenomena near junctions is required if one is interested in fields or currents close to that junction. It has been found through experimental observations (though somewhat gross) that the thin wire approximation with its concommitant assumptions is adequate for most applications such as the investigation of bulk currents induced by impinging fields although results very near junctions may be questionable. Hence the thin wire approximation has been retained and junctions have been treated as if the assumptions are valid. In the following we therefore address ourselves to a determination of accuracies available through different treatments, each of which uses the thin wire approximation. In fact, we start immediately with a discussion of basis functions and their effects on junction treatments.

The essential reason for whatever difficulty may be posed by the multiple junction is that any numerical development which employs current derivatives or multiterm current bases will ultimately involve a relationship between the current on a given segment and those on its adjacent neighbors. Consider for example using the potential integral equation, which contains an explicit current derivative (or charge) term (Harrington, 1968) for single wire. If a pulse current basis is used, a finite difference approximation for the derivative must then lead to a pulse charge basis which spans the neighboring halves of two connected segments and which involves at a minimum their associated current samples. The use instead of a 2-term linear basis does not significantly alter this situation since upon requiring current

continuity at segment junctions, the current and its slope within a segment will be given in terms of the current values at its ends. These cases are illustrated below.

A similar situation holds for other integral equations which may not have explicit current derivatives but which are used with multi-term bases. The two-term sinusoidal basis is treated in precisely the manner as the two-term linear basis illustrated above, with the important exception that the former has a sinusoidal charge basis as well. This results in a more efficient solution for long structures compared with that obtained from pulse or linear bases. Note that two term bases guarantee a continuous current but can result in discontinuous derivatives or charges.

Three term expansions (constant, sine, and cosine or constant, linear, and quadratic) have been handled in different ways. The most convenient to use, but least accurate, extrapolates the current from segment i to the centers of segments i - 1 and i + 1 (Yeh and Mei, 1967). This permits the i'th segment current to be expressed in terms of the center currents on the i - 1, i and i + 1 segments, but does not guarantee either current amplitude or slope continuity at the junctions. An alternative approach is to match both slope and amplitude at each junction. This gives rise to the same total number of equations as the first method, and thus also allows the final set of unknowns to be the center current values. However, the equations for a sequence of connected segments are coupled.

Error Studies

Considering then that even simple junctions require handling in such a way as to relate the current amplitudes of adjacent segments, it is no surprise that multiple junctions can make this procedure more involved. We will examine here several multiple junction treatments from the viewpoint of assessing their possible errors and their compatability with the basis and weight functions which are used. For simplicity, attention will be confined to a junction at which the linearly varying current on the main branch will be assumed to divide into M-1 equal branch currents. The geometry is sketched below for the M=3 case with all currents positive into the junction,

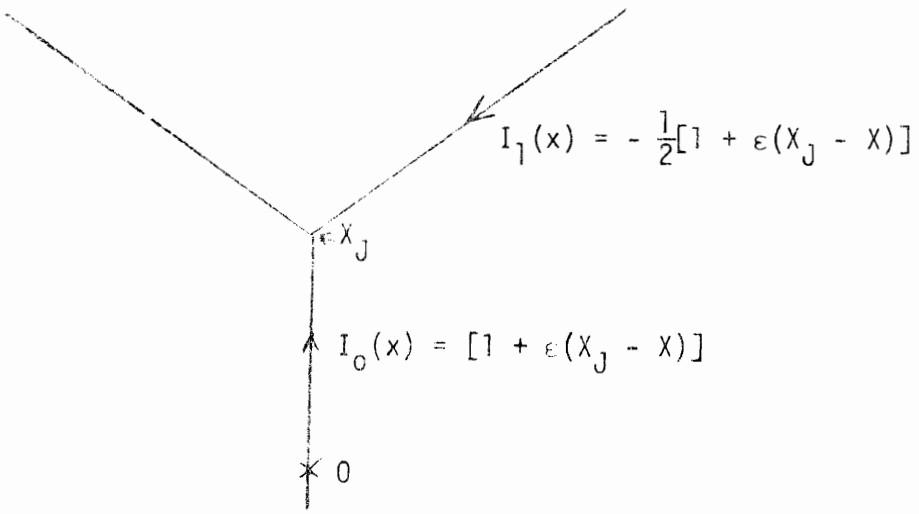

the distance x measured as positive along all wires from point o on main branch, I_1 represents the secondary branch currents on segments of length Δ, and Δ_0 represents the segment length on main branch.

1) MB Associates

This treatment, developed for the three term expansion, (Maxum, et al., 1969) uses

$$\sum_{j=0}^{M-1}{}' \; I_j = \tilde{I}_{ie}(x_i + \Delta_i/2 + \bar{\Delta}/2)$$

where the subscript e denotes an extrapolated current, the prime on the summation indicates the j=i term is not included, I_j is the current at the segment center and

$$\Delta_i = \frac{1}{M-1} \sum_{j=0}^{M-1}{}' \; \Delta_j$$

Evaluating the summation we have

$$\tilde{I}_{0e} = -[1 - \varepsilon\Delta_1/2]$$

and

$$\tilde{I}_{1e} = [1 + \varepsilon\Delta_0/2] - \frac{M-2}{M-1}[1 - \varepsilon\Delta_1/2]$$

But the actual extrapolated values of I_0 and I_1 ought to be (with a sign change to convert an incoming current to an outgoing current)

$$I_{0e} = I_0(X_0 + \Delta_0/2 + \bar{\Delta}/2) = -[1 - \varepsilon\Delta_1/2]$$

and

$$I_{1e} = I_{1e}(x_1 - \Delta_1/2 - \bar{\Delta}/2) = \frac{1}{M-1}\left[1 + \varepsilon\bar{\Delta}/2\right]$$

$$= \frac{1}{M-1}\left\{1 + \frac{1}{M-1}\left[\Delta_0 + \Delta_1\ (M-2)\right]\frac{\varepsilon}{2}\right\}$$

The error in the $\tilde{I}_{ie}$ values, E_{ie}, can be determined to be

$$E_{0e} = |I_{0e} - \tilde{I}_{0e}| = 0$$

and

$$E_{1e} = |\varepsilon|\ \frac{M-2}{(M-1)^2}\left\{\frac{\Delta_1}{2}(M-2) + \frac{\Delta_0}{2}M\right\}$$

For equal segment lengths $\Delta_0 = \Delta_1 = \Delta$

$$E_{1e} = \Delta\left|\ \frac{\varepsilon}{M-1}\left[2 - M\right]\right| = \frac{M-2}{M-1}\,|\varepsilon|\Delta$$

We see that although E_{0e} is zero for the case considered, E_{1e} is not, approaching the value $|\varepsilon|\Delta$ as $M\to\infty$. The fractional error e_{1e} is

$$e_{1e} = E_{1e}/I_{1e} = \frac{(M-2)|\varepsilon|\Delta}{\left|1 + \frac{\Delta\varepsilon}{2}\right|} \quad \text{for } \Delta_0 = \Delta_1$$

and grows without limit as $M \to \infty$. Only when the current slope is zero, i.e., $\varepsilon = 0$, does this method work without error, or when $M = 2$ (a simple junction), with the latter strictly true only for a linear current variation.

2) Charge Redistribution

Curtis has developed a junction treatment (Boeing, 1972) for use with a pulse basis and the potential integral equation. It involves computing the total charge on the junction wires from the sampled current values and then assuming the charge divides among the various segments according to the ratios of their individual surface areas to the total surface area. Proceeding as above, we compute from this procedure an approximate value for the junction current, denoted by I_{ij}, for comparison with the actual junction currents I_{iJ}.

From Equation (39), we have for the total charge Q_M

$$Q_M = \frac{1}{i\omega} \sum_{j=0}^{M-1} I_j$$

with I_j the inwardly directed sampled current values on the M intersecting wires. The total charge on an individual wire q_i which is given by

$$q_i = \frac{1}{i\omega} (I_i - I_{iJ})$$

is assumed to be related to Q_M as

$$q_i = R_i Q_M$$

where

$$R_i = a_i \Delta_i / \sum_{j=0}^{M-1} a_j \Delta_j$$

Thus

$$\tilde{I}_{ij} = I_i - i\omega q_i = I_i(1 - R_i) - R_i \sum_{j=0}^{M-1}{}' I_j$$

Returning to our test case, we have

$$I_{0J} = 1$$

$$I_{1J} = -\frac{1}{M-1}$$

For the approximated values of I_{iJ} we find,

$$\tilde{I}_{0J} = (1 + \varepsilon\Delta_0/2)(1 - R_0) - R_0[-(1 - \varepsilon\Delta_1/2)]$$

and

$$\tilde{I}_{1J} = -\frac{1}{M-1}(1 - \varepsilon\Delta_1/2)(1 - R_1) - R_1[1 + \varepsilon\Delta_0/2)$$

$$-\frac{M-2}{M-1}(1 - \varepsilon\Delta_1/2)]$$

Upon collecting terms, with all radii equal,

$$\tilde{I}_{0J} = 1 + \frac{1}{\Delta_0 + (M-1)\Delta_1}\varepsilon\Delta_0\Delta_1(M-2)/2$$

$$\tilde{I}_{1J} = -\frac{1}{M-1} - \frac{1}{\Delta_0 + (M-1)\Delta_1}\left(\frac{M-2}{M-1}\right)\varepsilon\frac{\Delta_0\Delta_1}{2}$$

The absolute errors are thus

$$E_{0J} = |I_{0J} - \tilde{I}_{0J}| = \frac{1}{\Delta_0 + (M-1)\Delta_1} \frac{|\varepsilon|\Delta_0\Delta_1(M-2)}{2}$$

$$E_{1J} = \frac{1}{\Delta_0 + (M-1)\Delta_1} \frac{M-2}{M-1} |\varepsilon| \frac{\Delta_0\Delta_1}{2}$$

while the fractional errors are

$$e_{0J} = E_{0J}$$

$$e_{1J} = E_{1J}(M-1) = E_{0J}$$

In contrast to the previous case, the error in E_{0J} is zero only when $\varepsilon = 0$ or $M = 2$. However, contrary to the finding before that $e_{1e} \to \infty$ as $M \to \infty$, here we find instead that $\varepsilon_{1J} \to \frac{|\varepsilon|\Delta_0}{2}$.

3) Segment Overlap

This approach, employed by Syracuse (Chao & Strait, 1970), and in an equivalent form by Richmond (1969), essentially decomposes the bases on a junction segment into two parts, one corresponding to the given segment and another to a neighboring segment. This is done for every segment pair so that there will be M-1 (or M, see below) such relationships for an M-wire junction. Note that M-2 of the wires will be overlapped with two adjacent wires, while the other two will be overlapped only once. (For a description see Logan (1973)).

In the context of our present test case we could have, using the overlap scheme shown, and denoting the overlapped bases with primes

$$I_0^{(1)} = I_0^{(1)'}$$

$$I_1^{(2)} = I_0^{(1)'} + I_1^{(2)'}$$

$$I_1^{(3)} = I_1^{(2)'} + I_1^{(3)'}$$

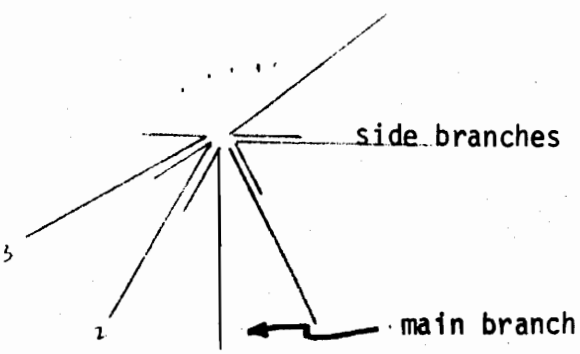

$$I_1^{(M)} = I^{(M-1)'} + I_1^{(M)'}$$

where the superscript refers to the wire number.

Now we have

$$I_0^{(1)} = -\left(1 - \frac{X - X_J}{\Delta_1}\right)$$

where it overlaps the first side branch, noting that the overlap length is Δ_1 and taking into account the current reference directions. Also, for all $I_1^{(J)}$, $J = 2, \ldots, M$

$$I_1^{(j)} = -\frac{1}{M - 1}\left[1 + \varepsilon(X_J - X)\right]$$

thus

$$I_1^{(2)'} = I_1^{(2)} - I_0^{(1)} = \frac{(M - 2)\Delta_1 + (X_J - X)(M - 1 - \varepsilon\Delta_1)}{(M - 1)\Delta_1}$$

Continuing

$$I_1^{(3)'} = I_1^{(3)} - I_1^{(2)'} = I_0^{(1)} = -\left(\frac{\Delta_1 - X - X_J}{\Delta_1}\right)$$

so that

$$I_1^{(2j)'} = \frac{(M - 2)\Delta_1 + (X_J - X)(M - 1 - \varepsilon\Delta_1)}{(M - 1)\Delta_1} \qquad j = 1, \ldots, M/2$$

$$I_1^{(2j + 1)'} = -\left(\frac{\Delta_1 - X - X_J}{\Delta_1}\right) = I_0^{(1)} \qquad j = 1, \ldots, M/2 - 1$$

It may be seen that the actual (unprimed) currents are given exactly by this decomposition into a two component (primed) basis on each segment. The method would be essentially error free for the sample current variation considered and a piece-wise linear basis. The essential limitation on accuracy in this regard is the amenability of the basis to represent the actual current. This factor also applies to the other junction treatments of course. It does however exhibit a characteristic that could degrade the solution accuracy ultimately available, where, as in the present case, the total current is given as the difference between two nearly equal component currents.

Two questions deserve consideration regarding this particular junction approach. They are: (1) can the method be implemented without the artifice of using overlapping wires at the junction; and (2) for what kinds of current bases is this junction treatment best suited? We attempt to answer these in order below.

For the purpose of developing the discussion let us first consider using a two term current basis applied to a simple V-dipole as shown below.

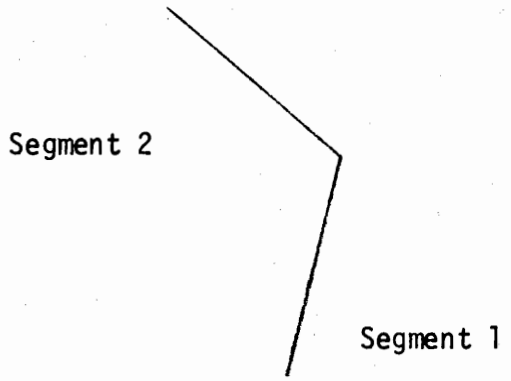

For simplicity and since there is no loss of generality, we employ only two segments to model the dipole. This leads to 4 unknowns and a requirement for a total of 4 equations for their determination. This set of equations can involve almost any combination of field boundary conditions and current conditions, the only constraint being that at least one (in this case) field value is required for a non-trivial solution. Two obvious current conditions are for zero current at each open end of the V-dipole. An additional condition that the currents on segments 1 and 2 match at their junction reduces to one the number of unknowns and remaining equations required, which also equals the number of junctions involved. It will be true in general that the number of unknowns will equal the number of simple junctions when a 2-term basis is employed together with current amplitude matching at the junctions.

It is thus natural when using a 2-term basis to view it as a junction-oriented expansion with the unknowns being the current values at the junctions. This is of course equivalent to using as the unknowns the current values at the segment centers, a procedure more natural to

pulse and 3-term expansion which may be viewed as segment-oriented expansions. The essential difference which holds when using a 2-term basis as a segment oriented expansion is that any one of the segment center current samples can be eliminated in terms of the other unknown current values. This leads to some ambiguity as to the current samples which will be used as unknowns. The piecewise linear (triangle) and piecewise sinusoidal 2-term bases have thus been used almost entirely as junction-oriented expansions which span two segments and which insure current continuity at their common junction.

To return to the V-dipole being considered, we now examine the boundary condition treatment. One additional equation is required to complete the development. Point matching, which is not suitable for 2-term bases (see above), could evidently be implemented by matching the field on either arm of the V. There is again an ambiguity involved as to which arm to use. Another possibility is to use the field at the junction, but the field behavior near junctions is so erratic that this also is not recommended. In order to sample the field on every segment it is perhaps best to combine the individual field values from connected segments a pair at a time, which amounts to using a junction oriented weight function.

For Galerkin's method, weight functions are used having the same functional form as the current expansion. The development of the explicit form for a multi-term weight function follows in exactly the same way used for the current expansion, and can be used for either a segment or junction oriented current basis. The weight functions can be matched at junctions, etc., the principal difference from the current treatment being that the values assigned to the weight function at the match points are arbitrary. As specific examples, the piecewise linear and sinusoidal weight functions are employed with equal junction values throughout although a variation of these values along the structure could be incorporated if desired. For the V-dipole case, a 2-term Galerkin's method would employ integration of the fields along the length of the 2 segments to obtain one field equation. This would complete the V-dipole equations.

Now let us examine the problem encountered when a third wire is added to the V-dipole. With 6 unknowns and 3 open-wire end conditions, 3 unknowns remain for a 2-term expansion. The equivalent of matching the current amplitude at a 2-wire junction would be zero net current flow (Kirkhoff's Law) into the multiple junction. This provides an additional equation leaving then 2 unknowns and 2 required field equations. In the general case of M wires, M-1 unknowns and M-1 field equations would result, a situation analogous to M wires connected in series.

By treating the 3-wire junction as described above, 2 unknowns might be associated with the junction, and 2 field equations would be encountered as shown below, using a junction oriented basis.

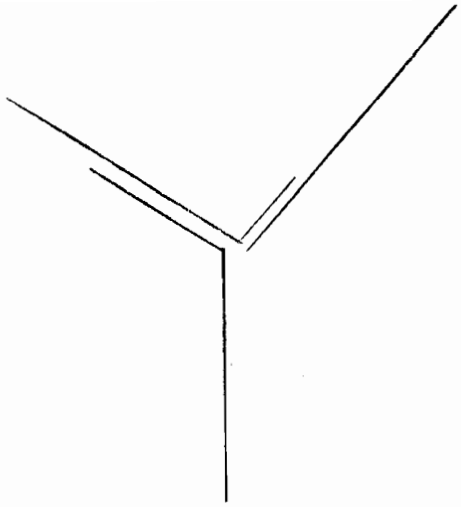

M - 1 Overlaps

But an equivalent representation would be simply

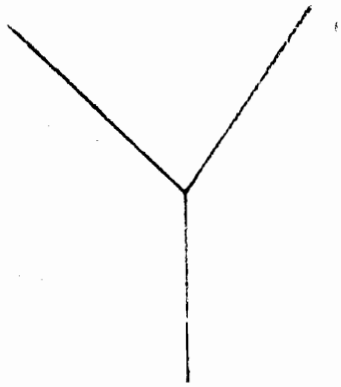

using a segment oriented basis. In either case the total current at the junction would be zero. As shown in the latter case, it is unnecessary to use overlapped segments. Their employment comes from using a junction oriented basis, a situation alleviated by using the segment oriented expansion. In the latter case however, the combination of field equations to be used is not unique, although the same can be said of the former since the overlap geometry also has the same degree of variability when M-1 overlaps are used. The essential thing is that the fields of all segments are sampled and possibly combined, if overlapping is used, in a non-redundant way. If M overlaps are used for the current representation, there are still only M-1 independent overlap field equations which can be generated. Further the M junction currents are reduced to M-1 by the auxiliary condition that their sum be zero. At any rate, we thus conclude that the use of overlapped segments to model a multiple junction is brought about by the use of a junction oriented basis.

As to the use of this junction treatment for other current bases, it is clear that it can not be employed without modification with a basis having more than 2 terms. This is due to the fact that ~M junction conditions would be needed for a 3-term expansion compared with the ~ single condition necessary for the 2-term basis. The additional conditions involved would require other, not necessarily

obvious, current relationships to be established.

4) The TCI Treatment

A multiple junction approach for the 3-term sinusoidal basis and point matching has been described by Andreason (1968). It involves the use of current extrapolation at simple junctions and the derivation of an end current value for a wire connected to a multiple junction. The steps in this procedure are:

1) Express the current on the j^{th} junction wire as (the positive current direction is inward)

$$I_j(s) = I_j^i e^{-iks} + I_j^0 \cos ks + P\, I_j^1\, ks\, J_0(ks)$$

where the first term represents an outward propagating spherical TEM wave, caused by an emf applied to one of the junction wires. The sum

$$\sum_{j=1}^{M} I_j^i = 0.$$

The second term represents a standing spherical TEM wave whose sum is also zero, while the third term represents a standing spherical TM wave of order 1. It is associated with junction charge and is described by a Bessel function of generally non-integer order j. Note that the first two terms above are equivalent to the sine and cosine terms in the 3-term expansion.

2) Solve for I_j^0 in terms of the sampled current I_j at the center of the segment to obtain

$$I_j^0 = \frac{I_j - I_j^i e^{-iks_j} - P\, I_j^1\, ks_j\, J_0(ks_j)}{\cos ks_j}$$

3) Form the sum $\sum_{j=1}^{M} I_j^0$ which equals zero to obtain for P

$$P = \frac{\sum_{}^{M} \frac{I_j}{\cos ks_j} + \sum_{}^{M} I_j^i \tan ks_j}{\sum_{}^{M} I_j^1 \frac{ks_j\, J_\nu(ks_j)}{\cos ks_j}}$$

4) Introduce a scalar potential A_j for each wire in the directions θ_j, ϕ_j which has a singularity in the direction of the wire, assume $A_j = \mu I_j/4\pi$, and obtain for the potential $V = rA\sqrt{\mu\varepsilon}$

$$V = -\frac{\eta}{4\pi} \sum_{j=1}^{M} I_j \log \left[\tan^2\left(\frac{\theta}{2}\right) + \tan^2\left(\frac{\theta_j}{2}\right) - 2 \tan\left(\frac{\theta}{2}\right) \tan\left(\frac{\theta_j}{2}\right) \cos\left(\phi-\phi_j\right)\right]$$

5) Obtain a relationship between the junction currents and voltages as

$$V_{jJ} = \frac{\eta}{2\pi} I_{jJ} \log \left[\frac{2 \cos^2\left(\frac{\theta_j}{2}\right)}{\theta_{o_j}}\right]$$

$$- \frac{\eta}{4\pi} \sum_{k=1}^{M}{}' I_{kJ} \log \left[\frac{\sin^2\left(\frac{V_{jk}}{2}\right)}{\cos^2\left(\frac{\theta_j}{2}\right) \cos^2\left(\frac{\theta_k}{2}\right)}\right]$$

with θ_j the cone angle of the j^{th} wire and V_{jk} the angle between the j^{th} and k'^{th} wires. Note that if there are no source voltages, the above expression provides a relationship between the junction currents.

6) The TM-wave current is similarly handled by writing the magnetic potential A_m for a single wire

$$A_m = J_V(ks)[A_1 P_V(\cos\theta) + A_2 P_U(-\cos\theta)]$$

which from $A_m = 0$ at $\theta = \theta_0$ and finite at $\theta = \pi$ gives for small core angles θ_0

$$\sum_{j=1}^{M} \left[1 + 2V \log \sin\left(\frac{V_{jk}}{2}\right)\right] T_j = 0; \quad k = 1, 2, \ldots, M$$

and has a non-trivial solution for the individual mode amplitudes T_j only for discrete values of V, the smallest value of which will be used.

7) Return now to the original current expression. Values for P and V have been found and I_j^Q is given in terms of the sampled current I_j and the TEM and TM currents I_j^i and I_j^l. But the junction current relationship and extrapolations to the next segment away from the junction enable the latter two currents to be eliminated as unknowns, arriving finally then at a single unknown I_j for each junction segment.

The complexity of this approach make it difficult to analytically assess as has been done with the previous cases. In addition, numerical results are currently not available for comparison with other approaches. It may be worthwhile to examine this procedure further to obtain a more definitive evaluation of its relative advantages.

ACKNOWLEDGMENT

The authors are grateful to the following individuals for their aid and cooperation during the course of this investigation:

V. Arens, Arens Applied Electromagnetics

C. E. Baum, AFWL

G. J. Burke, MBAssociates

C. Butler, University of Mississippi

J. P. Castillo, AFWL

T. Crow, Mississippi State University

W. Curtis, Boeing

M. Harrison, AFWL

W. Imbriale, TRW, Incorporated

J. Matuych, Rockwell International

K. K. Mei, University of California, Berkeley

J. Richmond, Ohio State University

B. Strait, Syracuse University

C. D. Taylor, Mississippi State University

F. Tesche, SAI, Berkeley

The authors are indebted to the Air Force Weapons Laboratory for the support of this study under Projects Orders 74-066 and 73-165.

REFERENCES

1. Andreasen, M. G. (1968), Analysis of Wire Antennas of Arbitrary Configuration by Precise Theoretical Numerical Techniques Semi Annual Report, ECOM Contract DAAB07-67-0631.

2. Bennett, C. L. and W. L. Weeks (1968), Electromagnetic Pulse Response of Cylindrical Scatterers, G-AP Symposium, Boston, Mass. See also "A Technique for Computing Approximate Electromagnetic Impulse Response of Conducting Bodies", Purdue University Report TR-EE69-11.

3. Boeing, AABNCP Preliminary EMP Hardening Concepts, July, 1972 (Confidential), Contract F29601-72-C-0028 (AFWL).

4. Chao, H. H. and B. J. Strait (1970), "Computer Programs for Radiation and Scattering by Arbitrary Configurations of Bent Wires", Scientific Report No. 7 on contract no F19628-68-C-0180; AFCRL-70-0374: Syracuse University, Syracuse, N.Y., Sept. 1970.

5. Crow, T. T. and T. H. Shumpert (1972), Electromagnetic Scattering from Configurations of Thin Wires with Multiple Junctions, Interaction Note 99, EMP Interaction Notes, AFWL.

6. Curtis (1972) See report (3) above.

7. Fenlon, F. H. (1969), Calculation of the Acoustic Radiation Field at the Surface of a Finite Cylinder by the Method of Weighted Residuals, Proc. IEEE, 57, p. 291.

8. Harrington, R. F. (1968), Field Computation by Moment Methods, MacMillan, New York.

9. Knepp, D. L. (1971), Numerical Analysis of Electromagnetic Radiation Properties of Smooth Conducting Bodies of Arbitrary Shape in the Presence of Known External Sources, Ph.D. Dissertation, University of Pennsylvania.

10. Logan, J. C. (1973), A Comparison of Techniques for Treating Radiation and Scattering by Wire Configurations with Junctions, Syracuse University Technical Report TR-73-10, August 1973.

11. Maxum, B. J., E. K. Miller, J. B. Morton and G. M. Pierrou (1969), "Mathematical Modeling of Aircraft Antennas and Supporting Structures", Interim Report, Contract DAAB07-68-C-0456, U. S. Army Electronics Command, Fort Monmouth, N. J.

12. Mei, K. K. (1965), On the Integral Equation of Thin Wire Antennas, IEEE Trans. Ant. and Prop., AP-13, p. 374

13. Miller, E. K. (1970), A Variable Internal Width Quadrature Technique Based on Romberg's Method, Journal of Computational Physics, v5, n2.

14. Miller, E. K. and F. J. Deadrick (1973), Some Computational Aspects of Thin Wire Modeling, UCRL-74818; also Interaction Note 153, AFWL.

15. Miller, E. K., A. J. Poggio and G. J. Burke (1973), "An Integro-Differential Equation Technique for the Time Domain Analysis of Thin Wire Structures, Part I. The Numerical Method", J. of Computat. Physics, 12, No. 1, pp.24-48.

16. Mittra, R. (ed.) (1973), Computer Techniques in Electromagnetics, Pergamon Press.

17. Pearson, L. W. and C. M. Butler, (1973), Some Weaknesses of Delta Function Testing in Method of Moments Solutions to Pocklington Type Models of Thin Wire Structures, IEEE GAP Int'l. Symposium, Boulder, Colorado.

18. Poggio, A. J., E. K. Miller and G. J. Burke (1973), "An Integro-Differential Equation Technique for the Time-Domain Analysis of Thin Wire Structures. II. Numerical Results", J. of Computat. Physics, 12, No. 2, pp. 210-233.

19. Richmond, J. H. (1973), "Radiation and Scattering by Thin-Wire Structures in the Complex Frequency Domain", Rept. 2902-10, The Ohio State U., Electroscience Lab, Dept. of E.E.

20. Richmond, J. H. (1969),"Computer Analysis of Three Dimensional Wire Antennas", Ohio State University, Electroscience Lab, Tech. Rept. 2708-4.

21. Sayre, E. P. and R. F. Harrington (1968), Transient Response of Straight Wire Scatterers and Antennas, Proc. 1968 Int'l Ant. Prop. Symposium, Boston, Mass., p. 160.

22. Strait, B. J., T. Sarkar and D. C. Kuo (1973), Special Programs for Analysis of Radiation by Wire Antennas, Dept. of Elect. Eng., Syracuse University, Scientific Report No 1, Contract F19628-73-C-0047.

23. Taylor, C. D. and T. T. Crow (1971), Induced Electric Currents on Some Configurations of Wires, Part I. Perpendicular Crossed Wires, Interaction Note 85, EMP Interaction Notes, AFWL.

24. Taylor, C. D. and D. R. Wilton (1972), The Extended Boundary Condition Solution of the Dipole Antenna of Revolution, Interaction Note 113, EMP Interaction Notes, AFWL.

25. Thiele, G. A. (1973), "An Introduction to Low Frequency Numerical Methods", Ohio State Short Course on Application of GTD and Numerical Techniques to the Analysis of Electromagnetic and Acoustic Radiation and Scattering, Columbus.

26. Thiele, G. A. (1970), "Wire Antennas", Chapt. 2 in Computer Techniques for Electromagnetics, ed. Raj Mittra, Pergamon Press.

27. Van Blaricum, M. and E. K. Miller (1972), "TWTD: A Computer Program for the Time-Domain Analysis of Thin-Wire Structures", Lawrence Livermore Laboratory, Rept. UCRL-51277.

28. Yeh, Y. S. and K. K. Mei (1967), Theory of Conical Equiangular Spiral Antennas: Part I - Numerical Techniques, IEEE Trans. Ant. and Prop., AP-15, p. 634.